universität wien

CHRISTIAN DOPPLER LABORATORY FOR
MID-IR SPECTROSCOPY &
SEMICONDUCTOR OPTICS

High Finesse Mirror Design, Fabrication and Characterization

Oliver Heckl

Mirror and Optical Coating Technical Overview

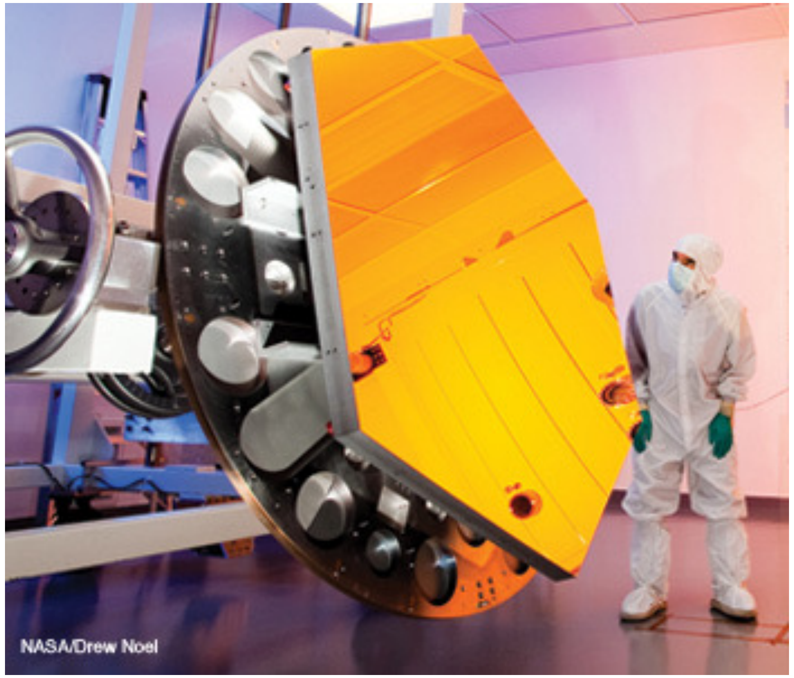
NASA/Drew Noel

Two main classes of thin-film reflective optical coatings:

simple metallic mirrors	single or protected Ag, Al, or Au layer	broadband, but high losses
interference coatings	alternating transparent dielectric films	very versatile, low losses

Reflectivity for prevalent metal mirrors

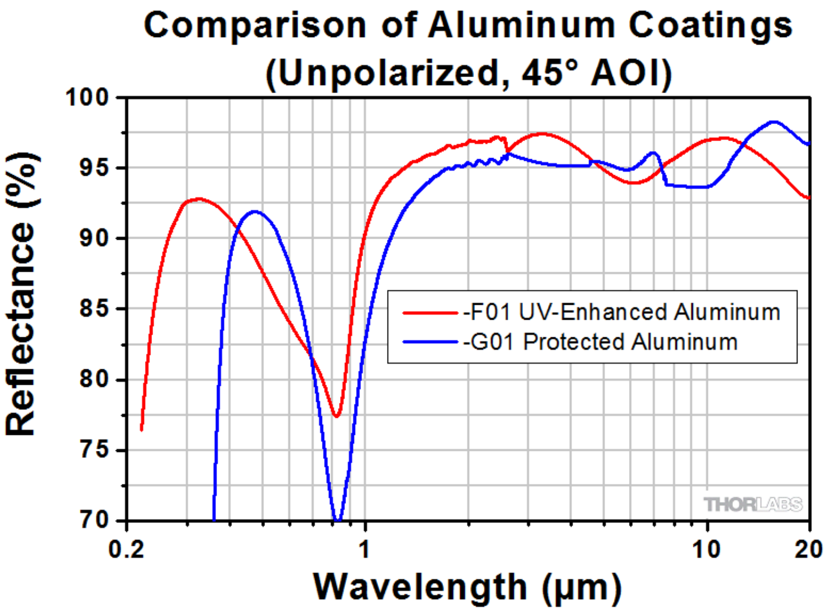

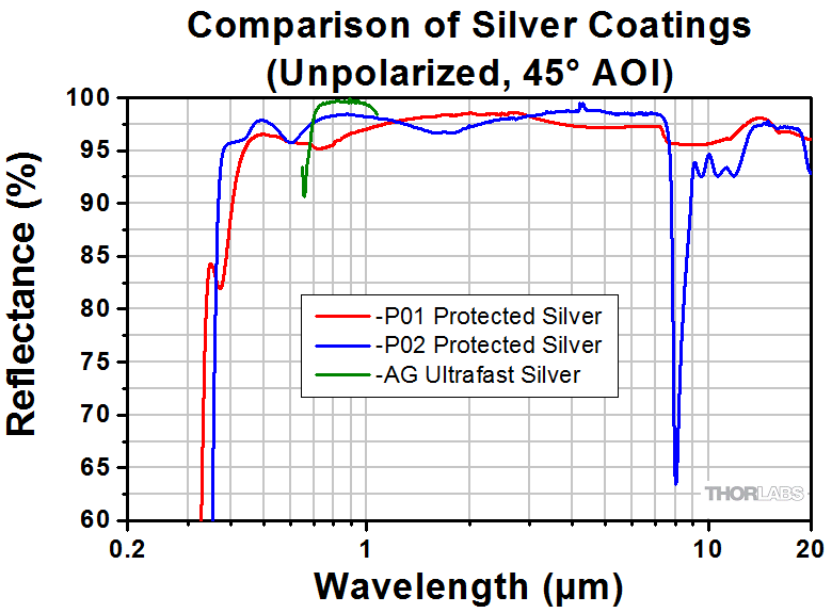

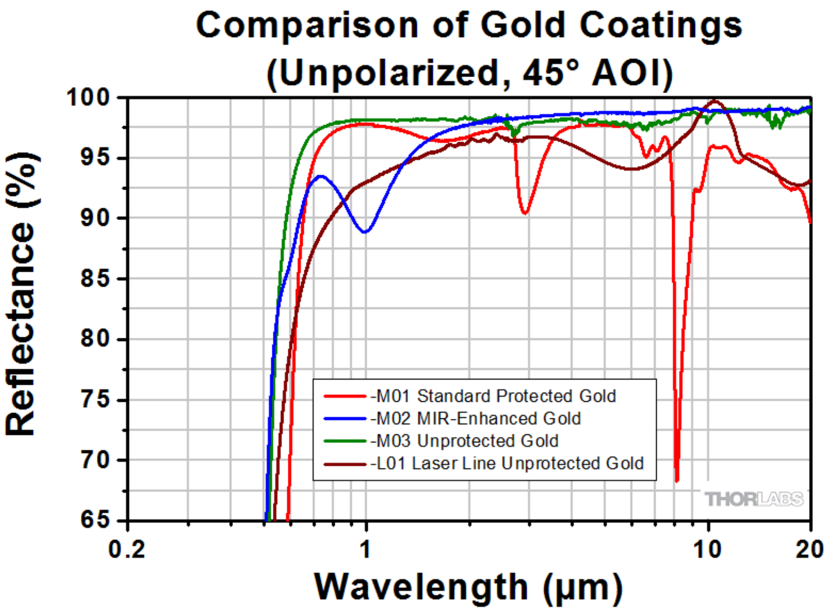

- Very broadband reflection for ranging from VUV/VIS to mid-IR wavelengths
- Percent-level losses at best → bad candidates for high-Finesse mirrors

Thorlabs webpage

How to do better – optical interference coatings

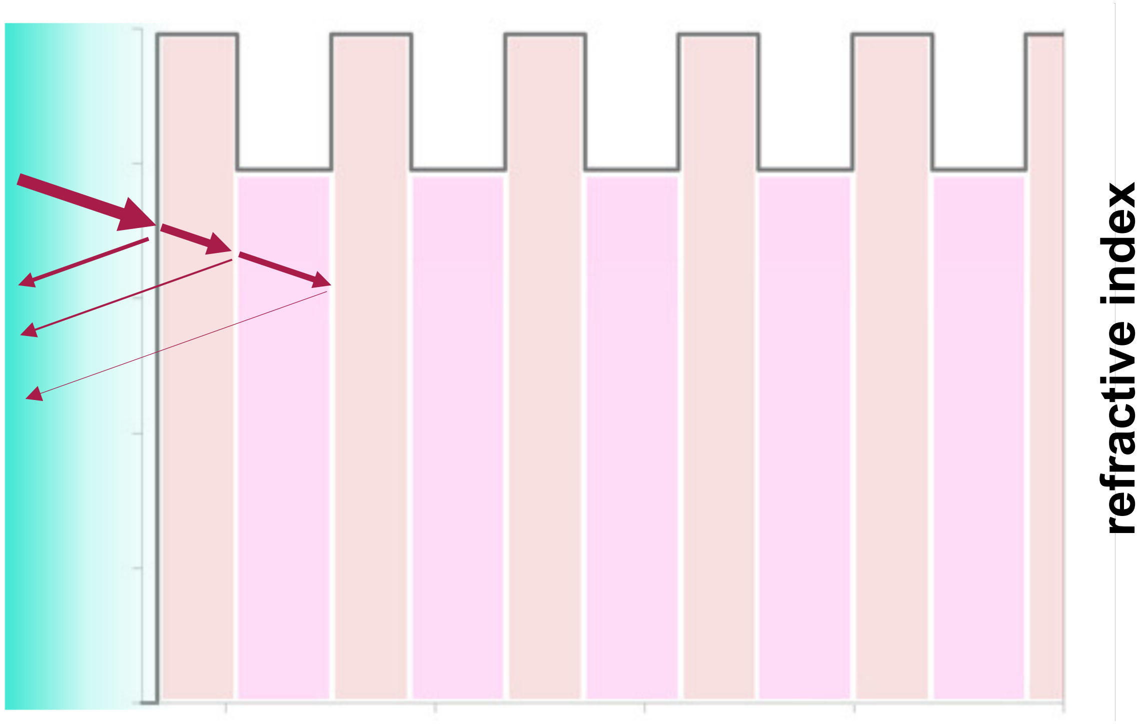

- Alternating layers of high / low index (quarter-wave thickness) thin films
  - at Bragg wavelength internal reflections add in phase, max. reflectivity

Reflection and Refraction

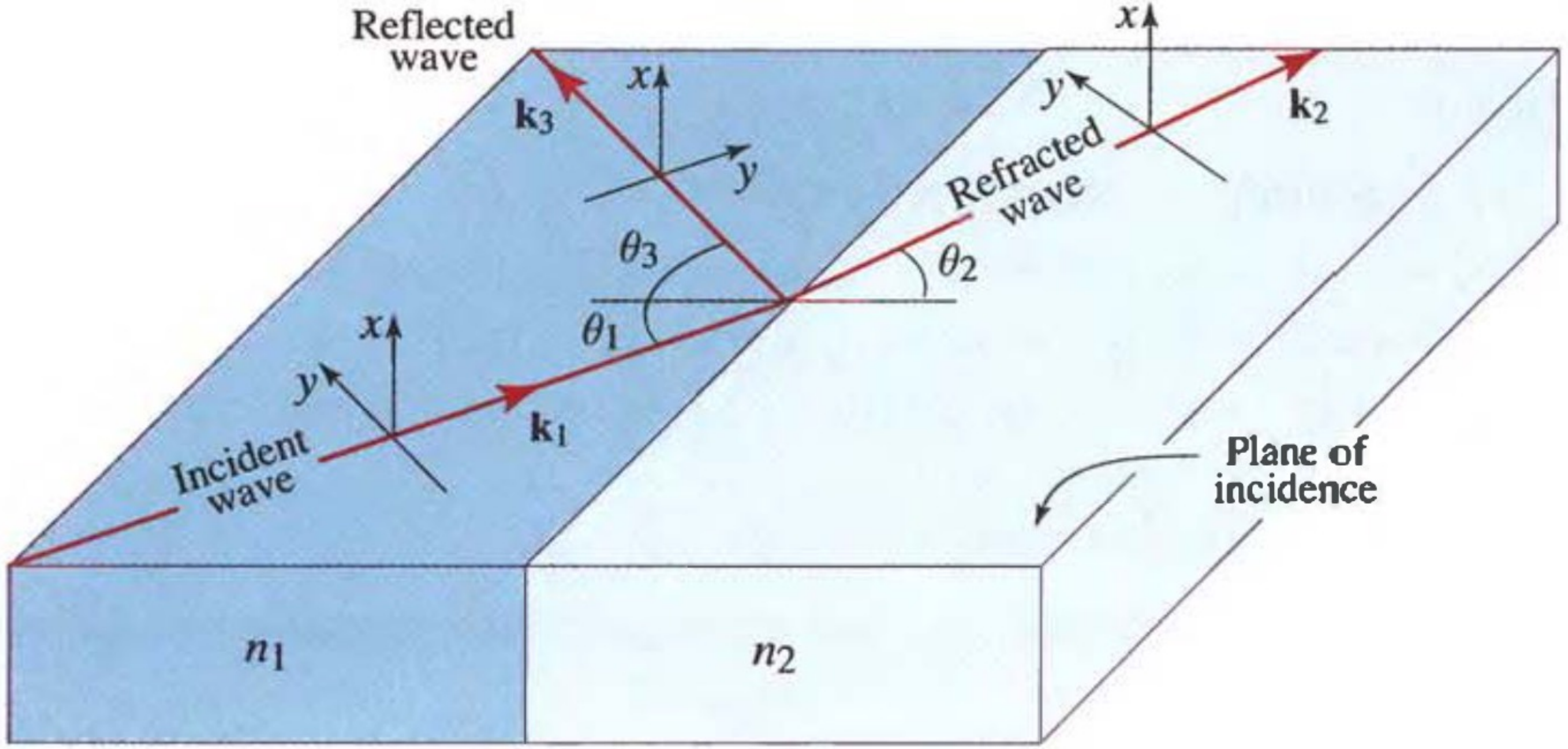

Figure 6.2-1 Reflection and refraction at the boundary between two dielectric media.

Saleh and Teich

Fresnel Equations

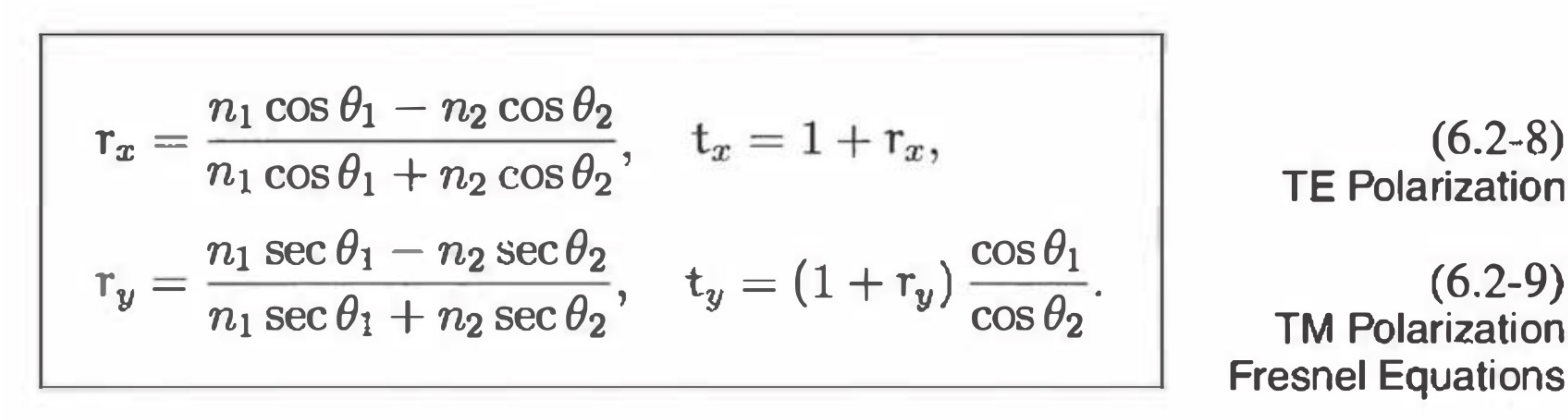

$$\mathrm{r}_x = \frac{n_1 \cos\theta_1 - n_2 \cos\theta_2}{n_1 \cos\theta_1 + n_2 \cos\theta_2}, \qquad \mathrm{t}_x = 1 + \mathrm{r}_x, \tag{6.2-8}$$

TE Polarization

$$\mathrm{r}_y = \frac{n_1 \sec\theta_1 - n_2 \sec\theta_2}{n_1 \sec\theta_1 + n_2 \sec\theta_2}, \qquad \mathrm{t}_y = (1 + \mathrm{r}_y)\frac{\cos\theta_1}{\cos\theta_2}. \tag{6.2-9}$$

TM Polarization
Fresnel Equations

With Snell’s law: $\cos\theta_2 = \sqrt{1 - \sin^2\theta_2} = \sqrt{1 - (n_1/n_2)^2 \sin^2\theta_1}$

Saleh and Teich

TE Polarization / s-Polarization: External Reflection; $n_1 < n_2$

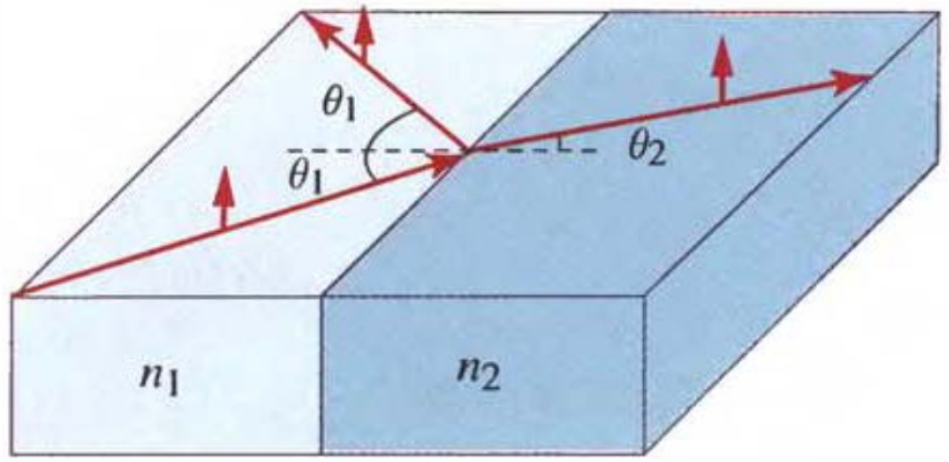

Figure 6.2-2 Magnitude and phase of the reflection coefficient as a function of the angle of incidence for *external reflection* of the *TE-polarized* wave ($n_2/n_1 = 1.5$).

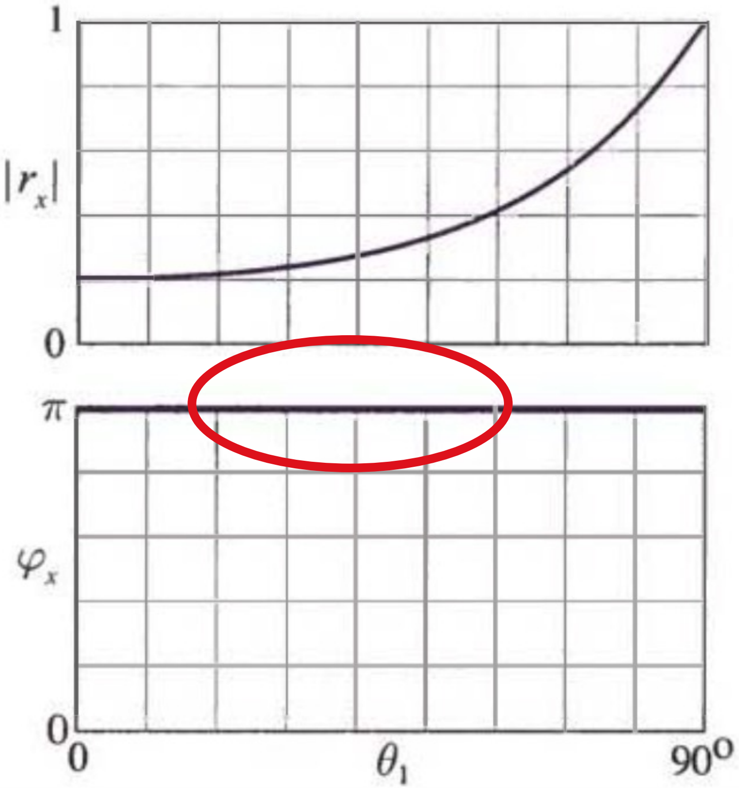

Note: reflection on optically denser medium introduces a π phase shift

Saleh and Teich

TE Polarization / s-Polarization: Internal Reflection; $n_1 > n_2$

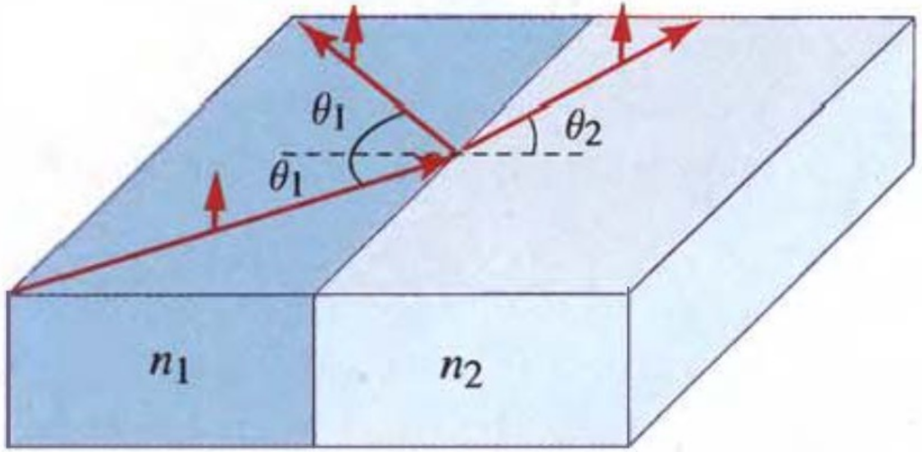

Figure 6.2-3 Magnitude and phase of the reflection coefficient as a function of the angle of incidence for *internal reflection* of the *TE-polarized* wave ($n_1/n_2 = 1.5$).

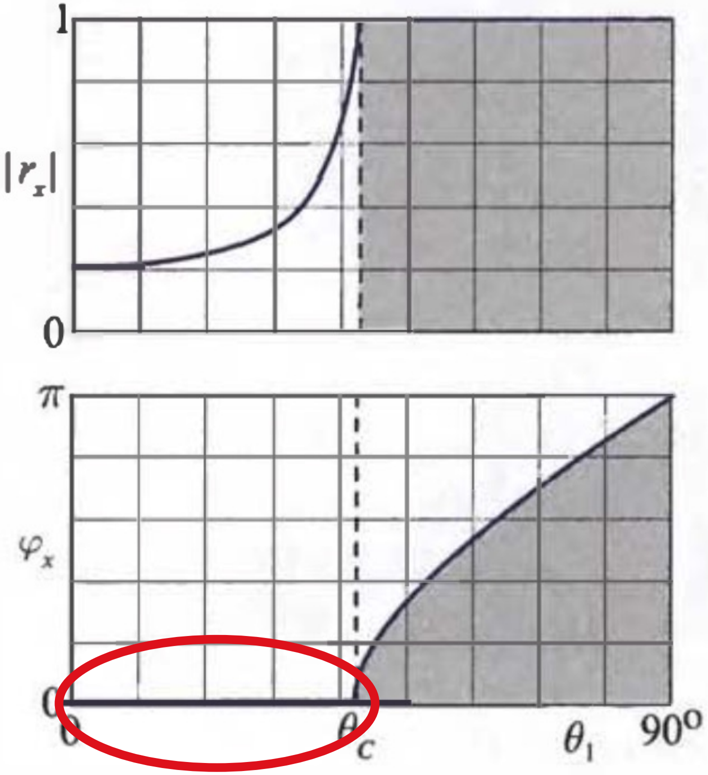

Note: reflection on optically less dense medium introduces no phase shift up to the critical angle

Saleh and Teich

TM Polarization / p-Polarization: External Reflection; $n_1 < n_2$

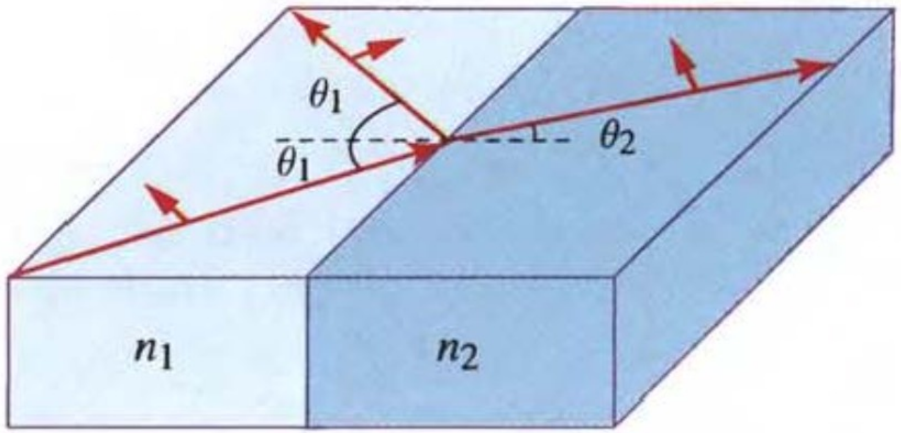

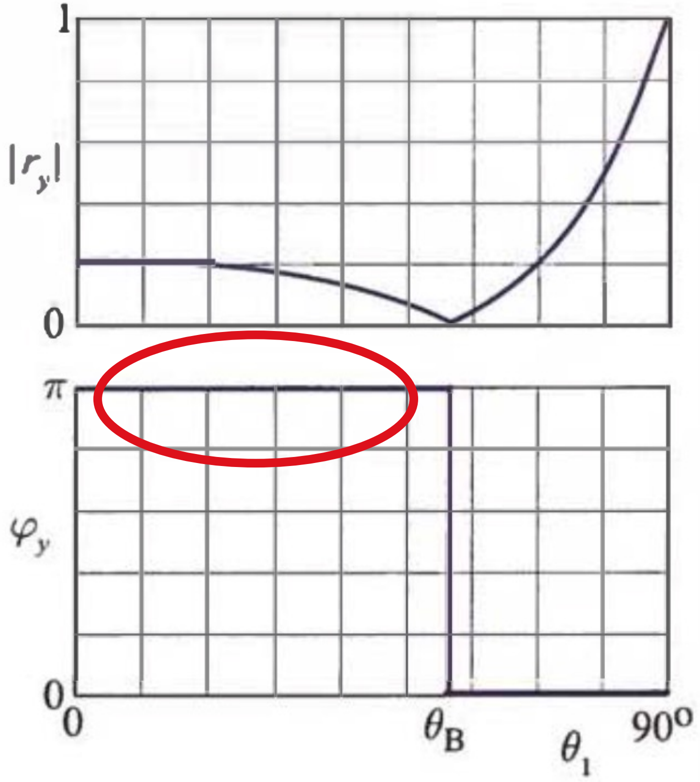

Figure 6.2-4 Magnitude and phase of the reflection coefficient as a function of the angle of incidence for *external reflection* of the *TM-polarized* wave ($n_2/n_1 = 1.5$).

Note: reflection on optically denser medium introduces a π phase shift

Saleh and Teich

TM Polarization / p-Polarization: Internal Reflection; $n_1 > n_2$

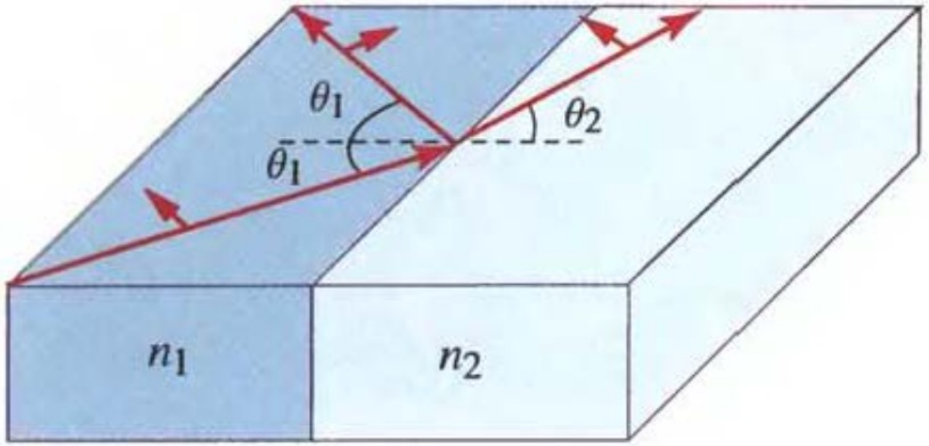

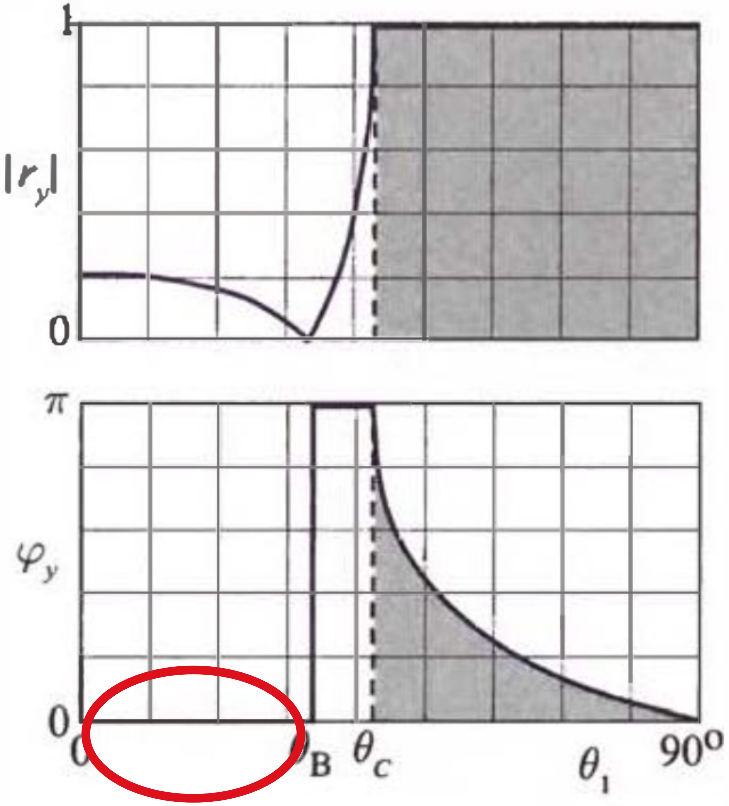

Figure 6.2-5 Magnitude and phase of the reflection coefficient as a function of the angle of incidence for *internal reflection* of the *TM-polarized wave* $(n_1/n_2 = 1.5)$.

Note: reflection on optically less dense medium introduces no phase shift up to Brewster-angle

Saleh and Teich

Basic idea of a distributed bragg reflector (DBR)

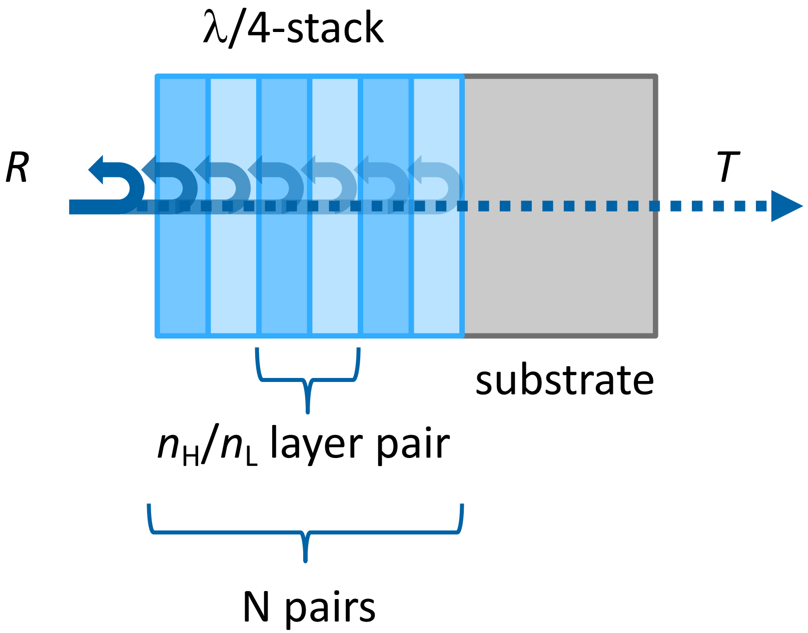

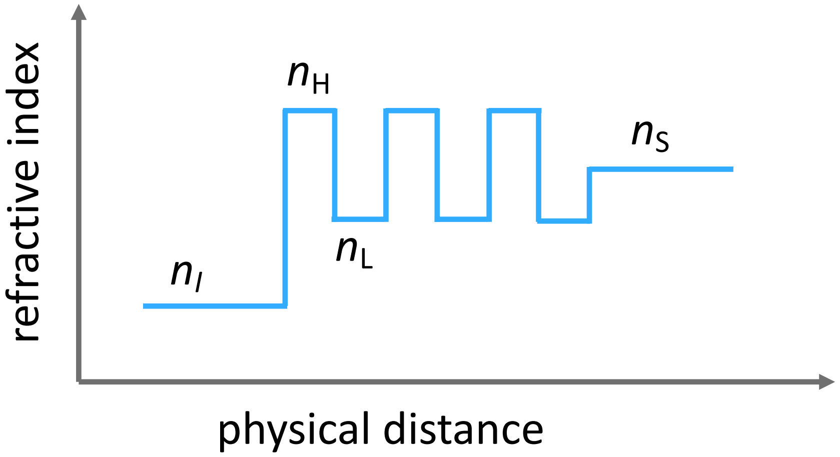

n_I: incident
n_H: high
n_L: low
n_S: substrate
T: transmission (intensity)
R: reflectivity (intensity)

λ_B: Bragg wavelength

- Individual reflections from each material boundary are added in phase
  Remember: reflection on optically denser medium introduces a π phase shift
- λ_B: twice the optical thickness of a layer pair

Calculation of DBR-stacks

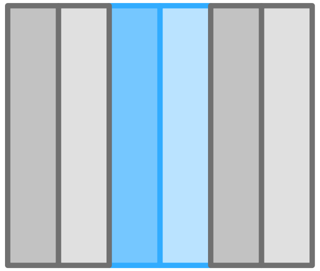

Calculation of DBR-stacks

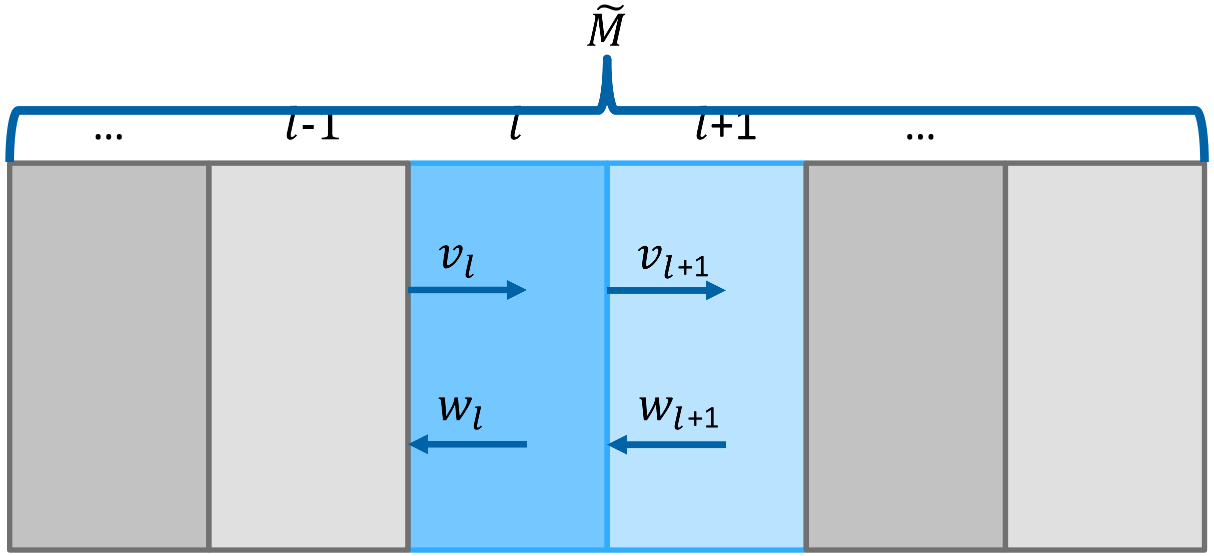

$r_{l,l+t}$: reflectivity (field) at interface l,l+1

$t_{l,l+1}$: transmissoin (field) at interface l,l+1

δ_l: accumulated phase by passing layer l

Transmission from layer l to l+1

$$v_{l+1} = e^{i\delta_l}\, t_{l,l+1} v_l + r_{l,l+1} w_{l+1}$$

$$w_l = e^{2i\delta_l}\, r_{l,l+1} v_l + e^{i\delta_l}\, t_{l,l+1} w_{l+1}$$

Clever matrix formulation

$$\begin{pmatrix} v_l \\ w_l \end{pmatrix} = \frac{1}{t_{l,l+1}} \begin{pmatrix} e^{-i\delta_l} & 0 \\ 0 & e^{i\delta_l} \end{pmatrix} \begin{pmatrix} 1 & r_{l,l+1} \\ r_{l,l+1} & 1 \end{pmatrix} \begin{pmatrix} v_{l+1} \\ w_{l+1} \end{pmatrix} = M_l \begin{pmatrix} v_{l+1} \\ w_{l+1} \end{pmatrix}$$

$$\widetilde{M} = \prod_{i=0}^{2N} M_l$$

A. Luce. A. Mahdavi, F. Marquardt, and H. Wankerl, JOSA A, Vor. 39, No. 6, June 2022

Calculation of DBR-stacks

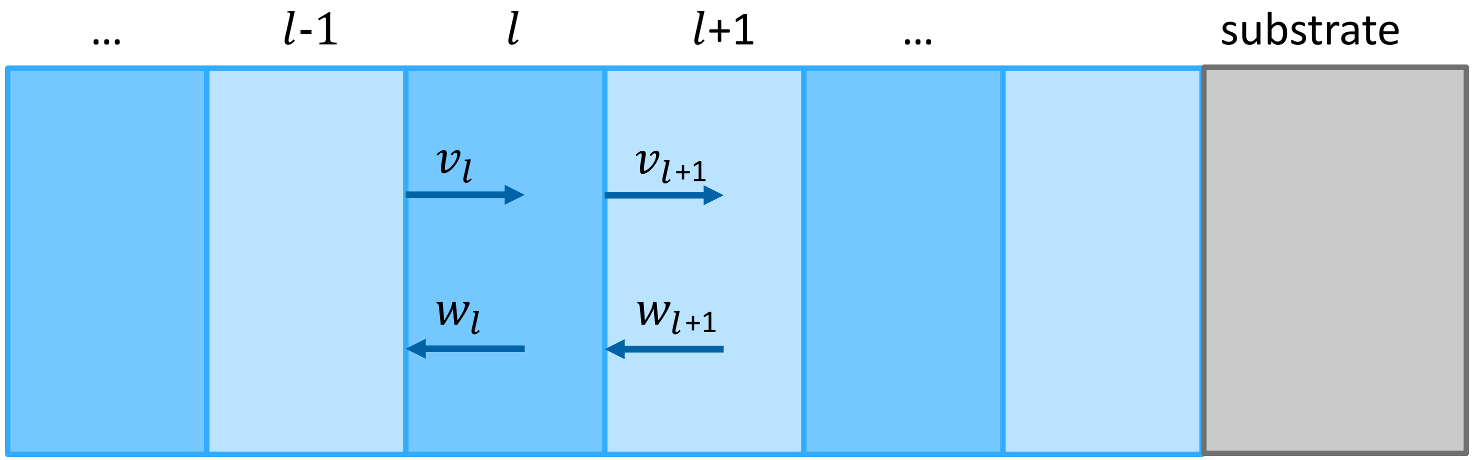

$r_{l,l+t}$: reflectivity (field) at interface l,l+1

$t_{l,l+1}$: transmissoin (field) at interface l,l+1

δ_l: accumulated phase by passing layer l

Transmission from layer l to l+1

$$v_{l+1} = e^{i\delta_l}\, t_{l,l+1} v_l + r_{l,l+1} w_{l+1}$$

$$w_l = e^{2i\delta_l}\, r_{l,l+1} v_l + e^{i\delta_l}\, t_{l,l+1} w_{l+1}$$

Clever matrix formulation

$$\begin{pmatrix} v_l \\ w_l \end{pmatrix} = \frac{1}{t_{l,l+1}} \begin{pmatrix} e^{-i\delta_l} & 0 \\ 0 & e^{i\delta_l} \end{pmatrix} \begin{pmatrix} 1 & r_{l,l+1} \\ r_{l,l+1} & 1 \end{pmatrix} \begin{pmatrix} v_{l+1} \\ w_{l+1} \end{pmatrix} = M_l \begin{pmatrix} v_{l+1} \\ w_{l+1} \end{pmatrix}$$

$$\widetilde{M} = \prod_{i=0}^{2N} M_l \qquad \begin{pmatrix} 1 \\ r \end{pmatrix} = \widetilde{M} \begin{pmatrix} t \\ 0 \end{pmatrix}$$

Transmitted light through DBR

Incident light on DBR

Incident light on exit-facet of the DBR

Reflected light from DBR

A. Luce. A. Mahdavi, F. Marquardt, and H. Wankerl, JOSA A, Vor. 39, No. 6, June 2022

Basic idea of a distributed bragg reflector (DBR)

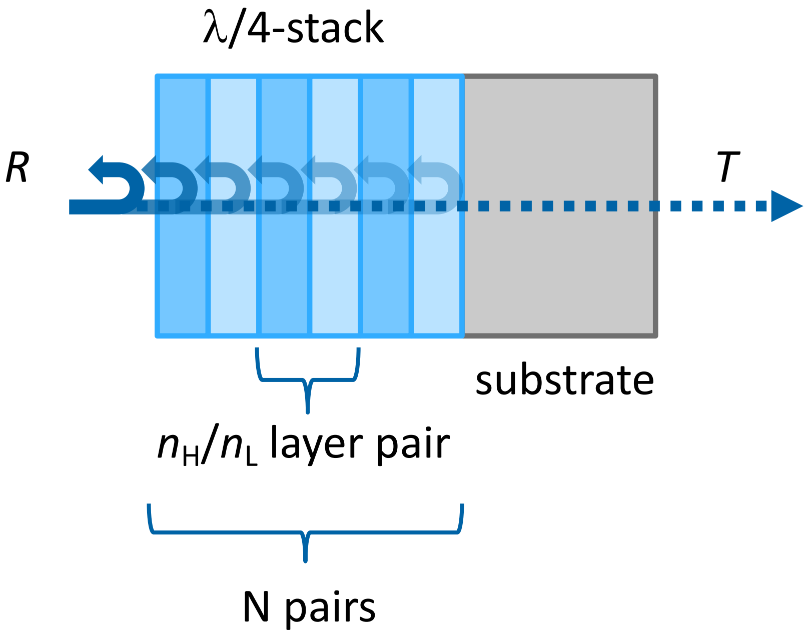

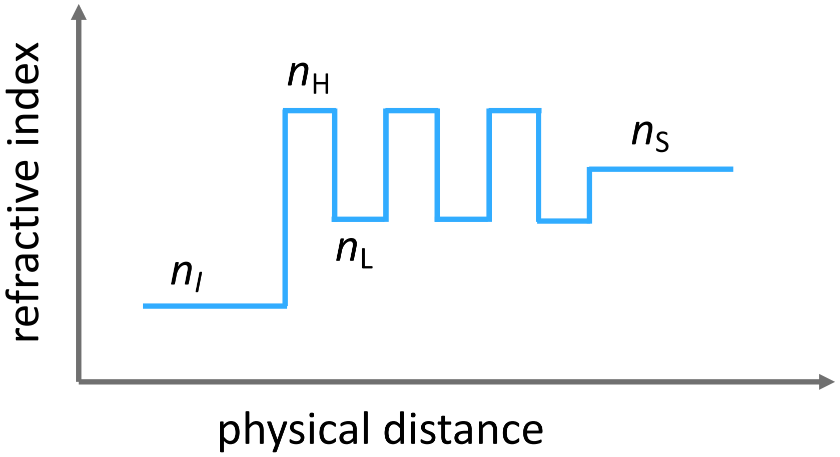

Matrix formulation:

$$\binom{1}{r} = \widetilde{M}\binom{t}{0} = \begin{pmatrix} \widetilde{M}_{0,0} & \widetilde{M}_{0,1} \\ \widetilde{M}_{1,0} & \widetilde{M}_{1,1} \end{pmatrix} \binom{t}{0}$$

A. Luce. A. Mahdavi, F. Marquardt, and H. Wankerl, JOSA A, Vor. 39, No. 6, June 2022

Transmission and reflection coefficients

$$r = r_{(\lambda,\theta)} = \frac{\widetilde{M}_{0,1}}{\widetilde{M}_{0,0}}; \quad R = r^2 \mathrm{t}$$

$$t = t_{(\lambda,\theta)} = \frac{1}{\widetilde{M}_{0,0}}; \quad T = \frac{n_2 \cos\theta_2}{n_1 \cos\theta_1} t^2$$

TMM-Fast Python package

Buildup of mirror and stopband: substrate only

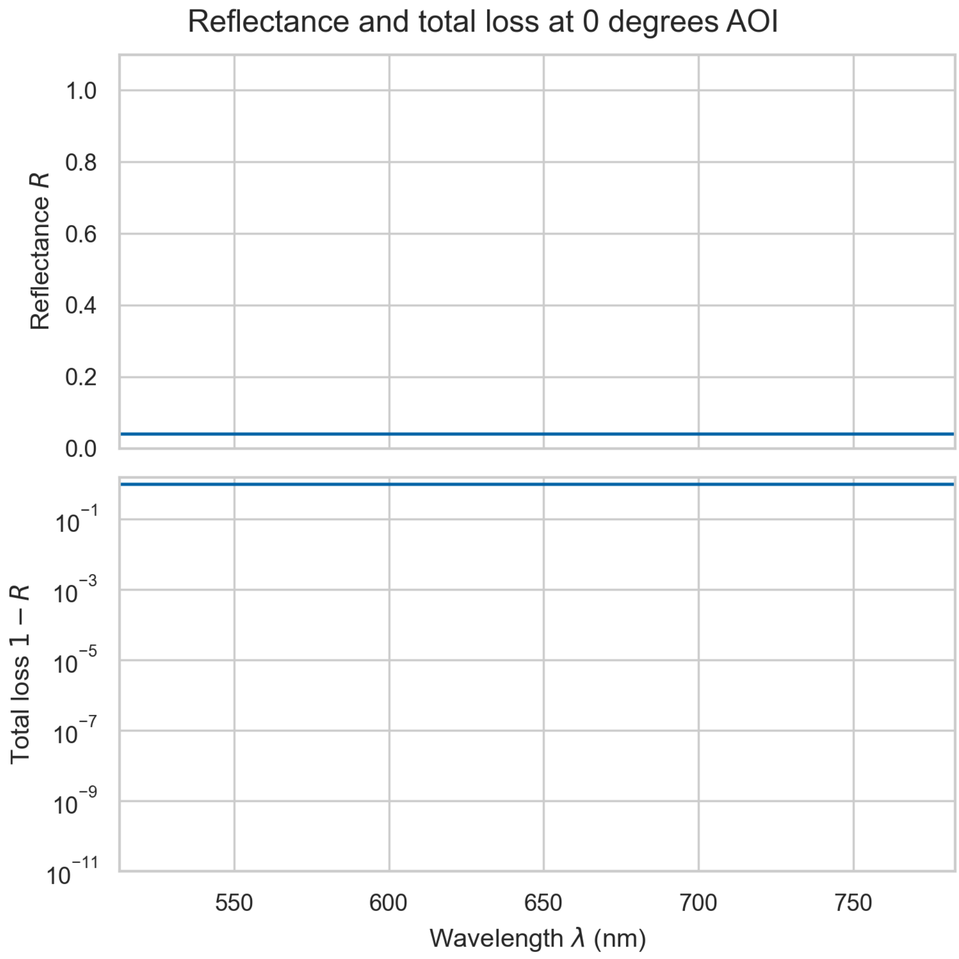

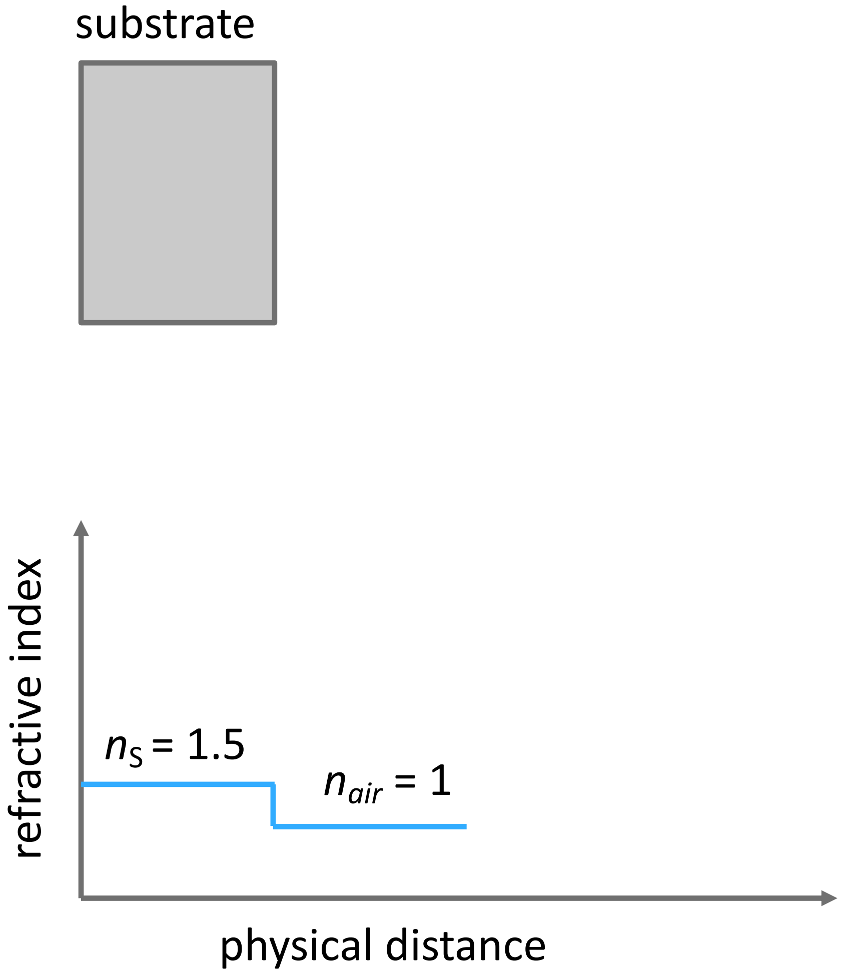

Buildup of mirror and stopband: N = 0

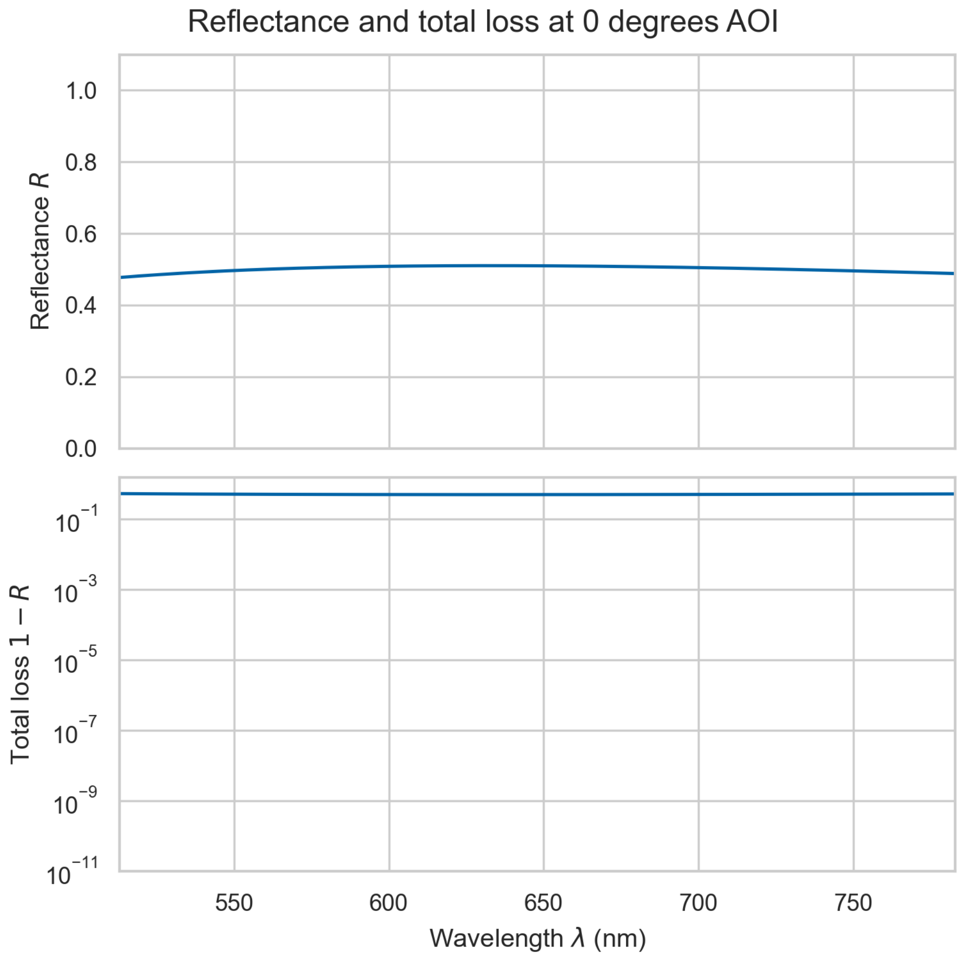

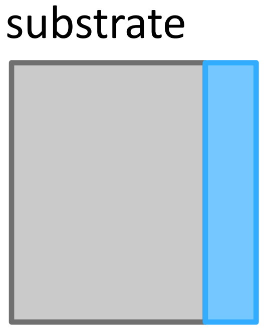

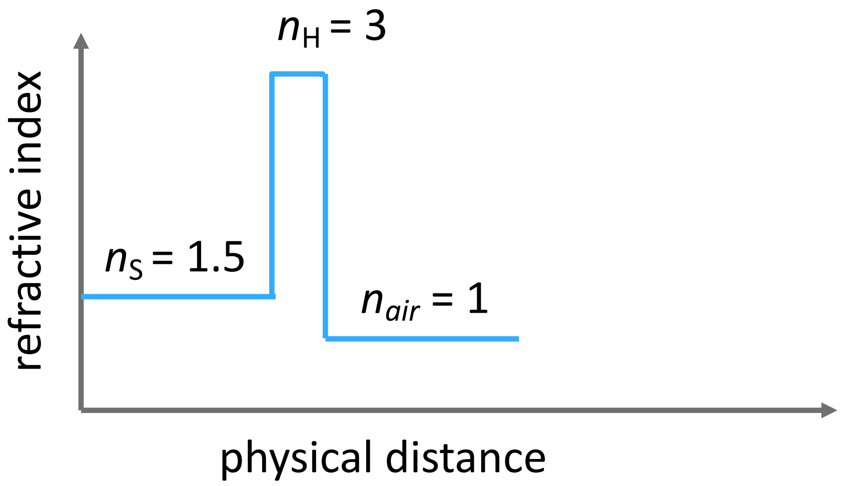

Buildup of mirror and stopband: N = 1

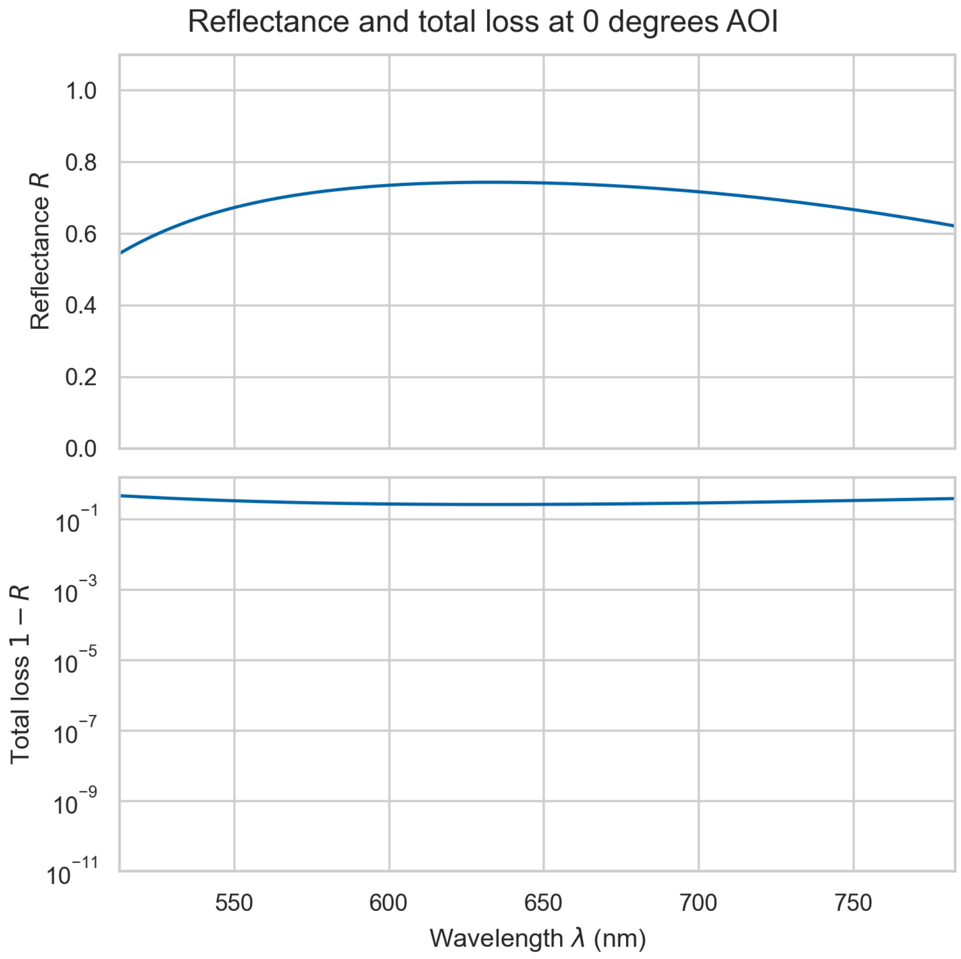

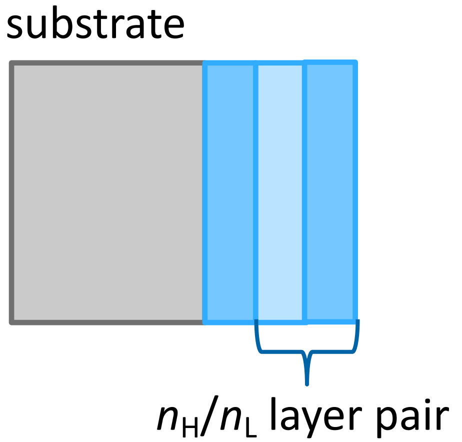

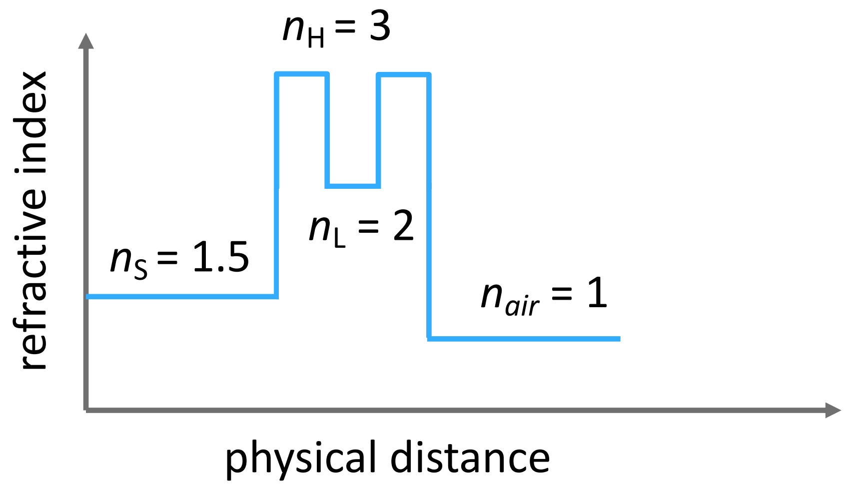

Buildup of mirror and stopband: N = 2

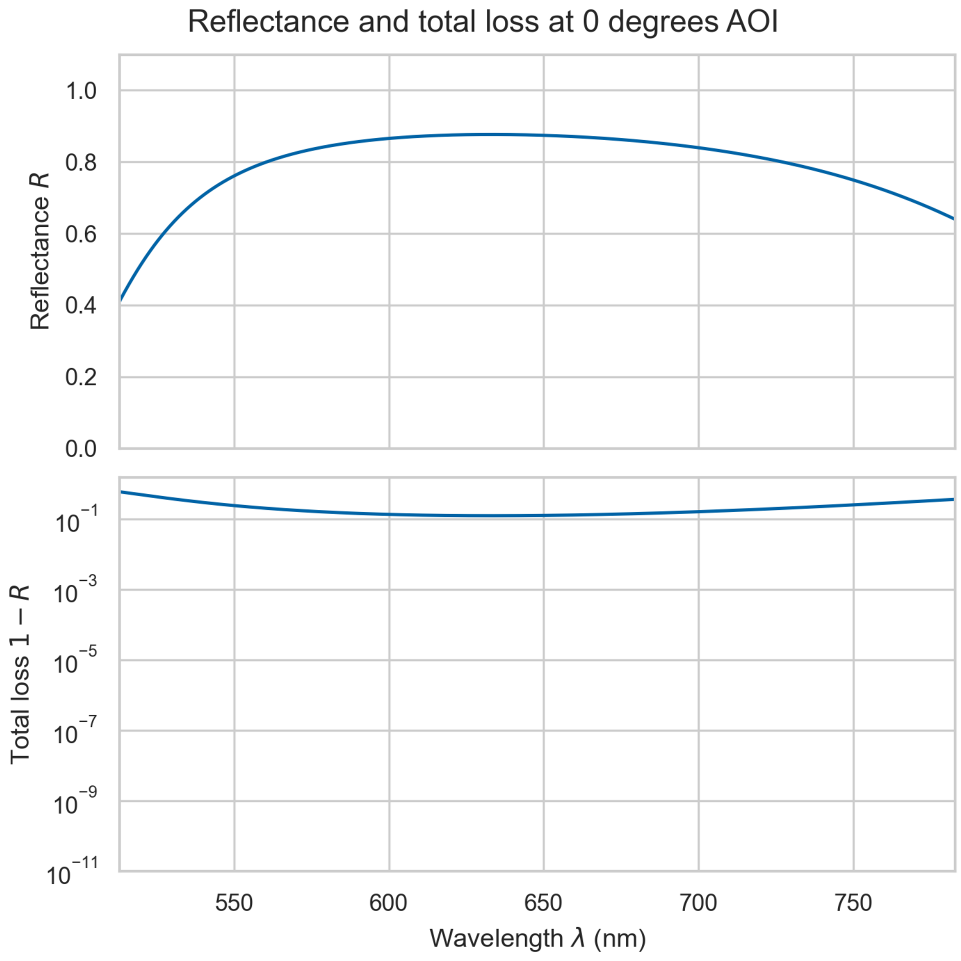

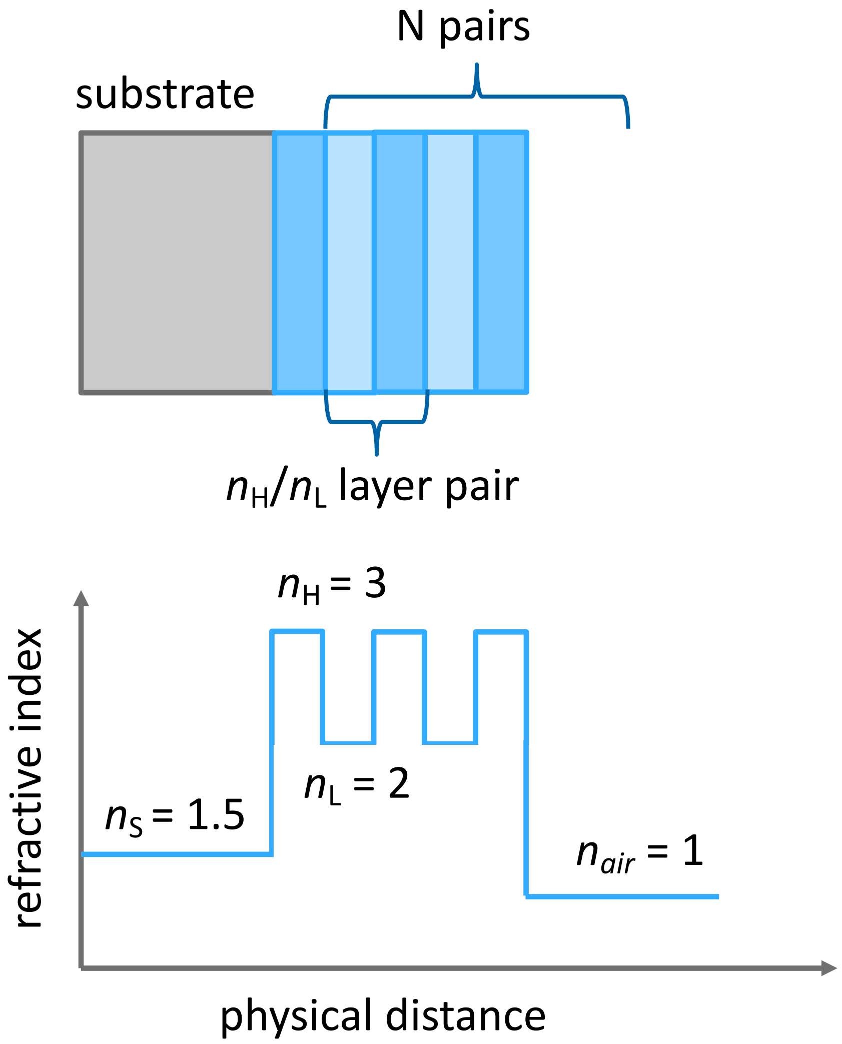

Buildup of mirror and stopband: N = 3

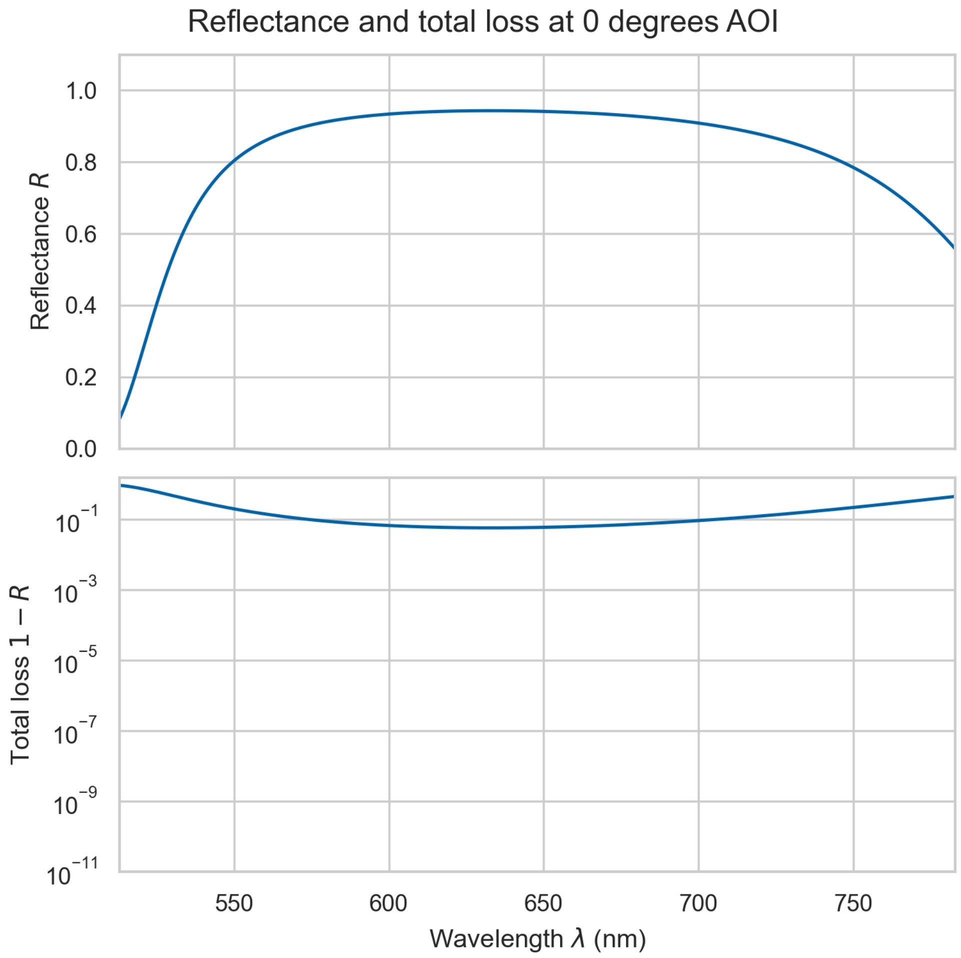

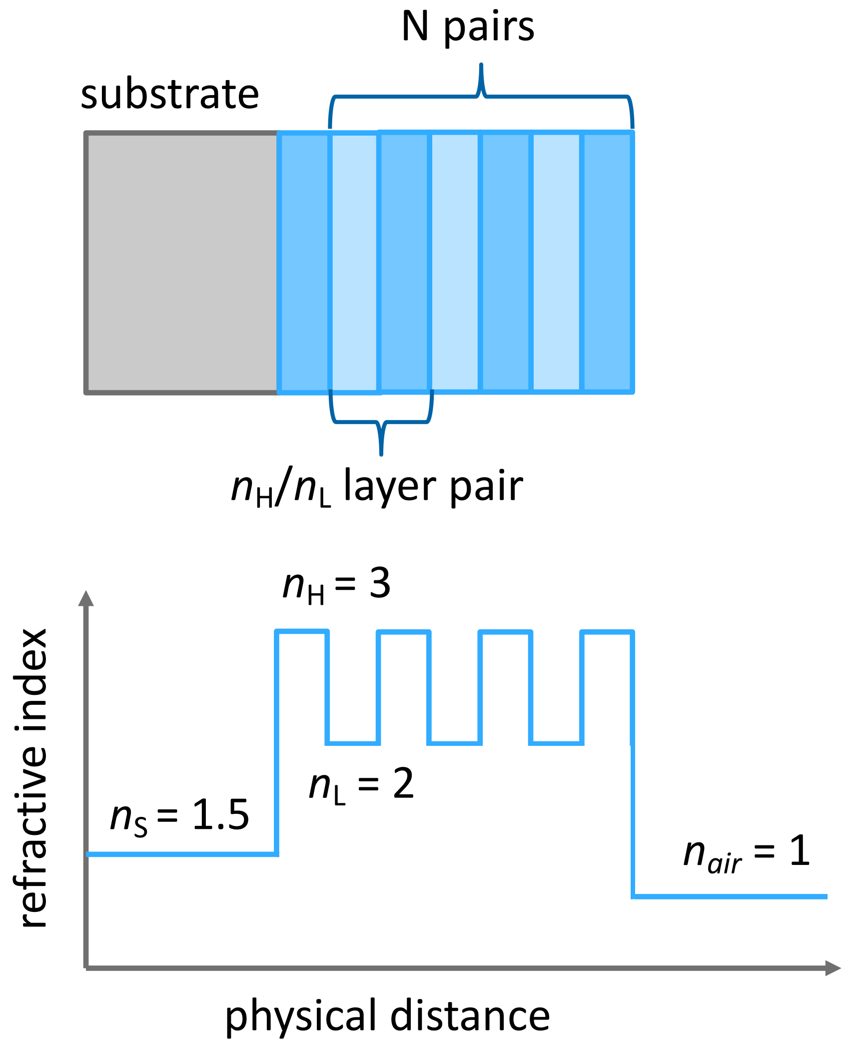

Buildup of mirror and stopband: N = 4

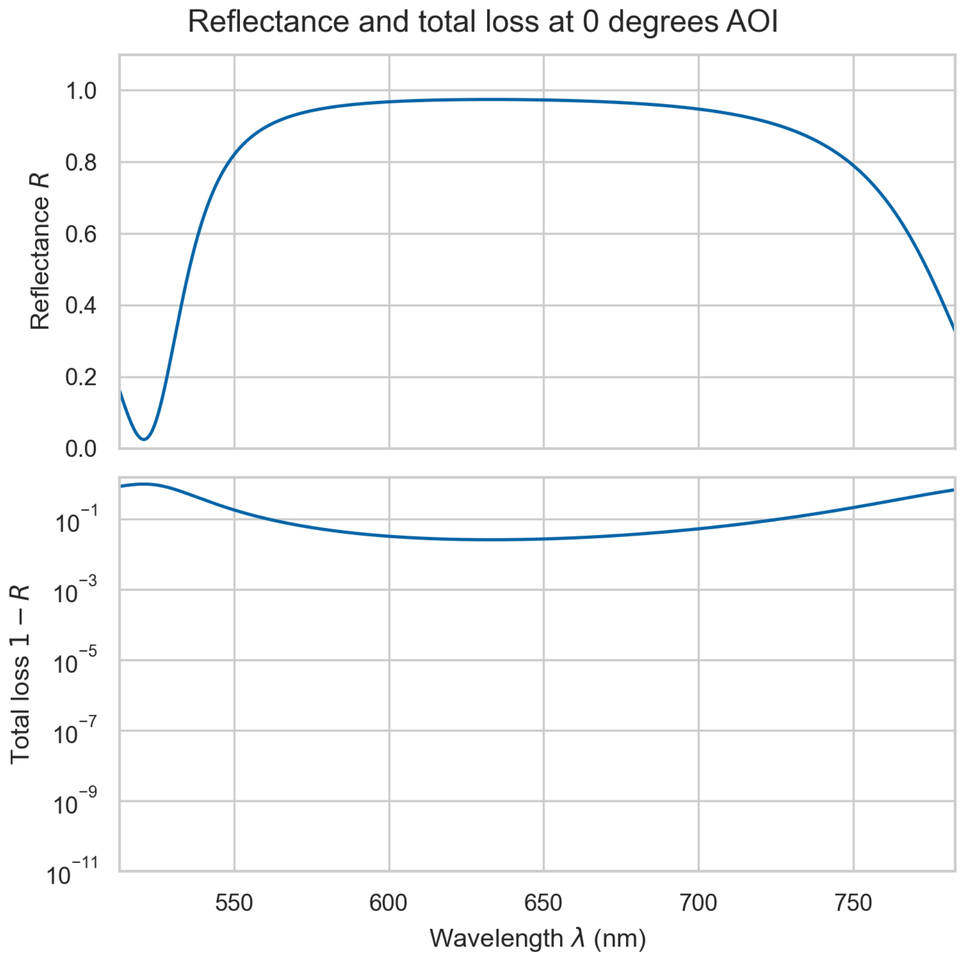

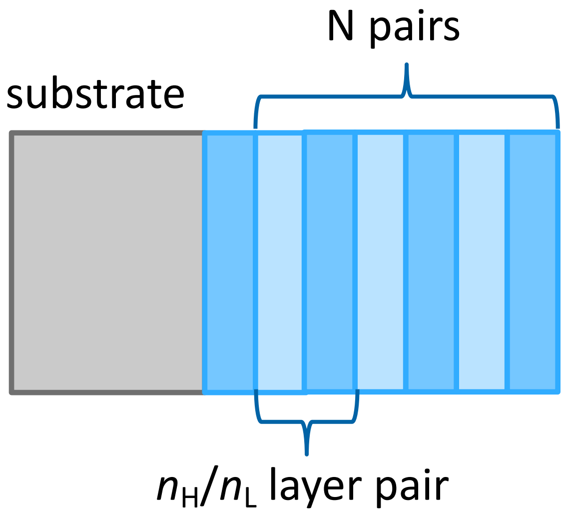

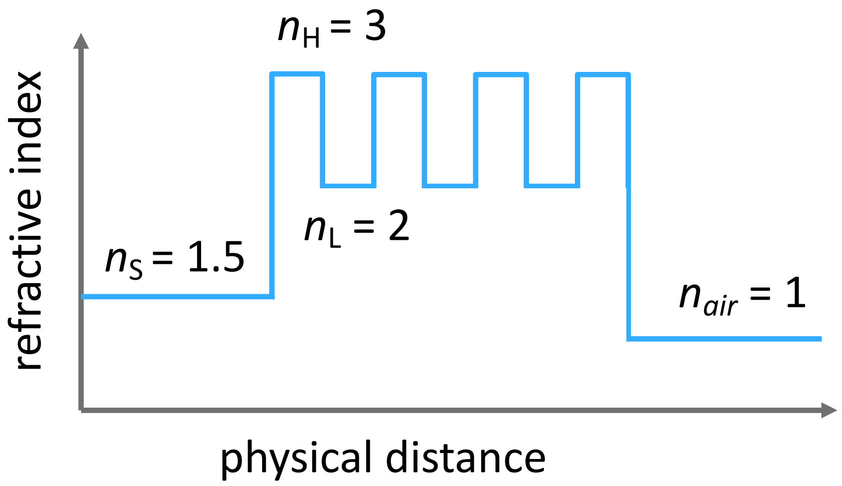

Buildup of mirror and stopband: N = 5

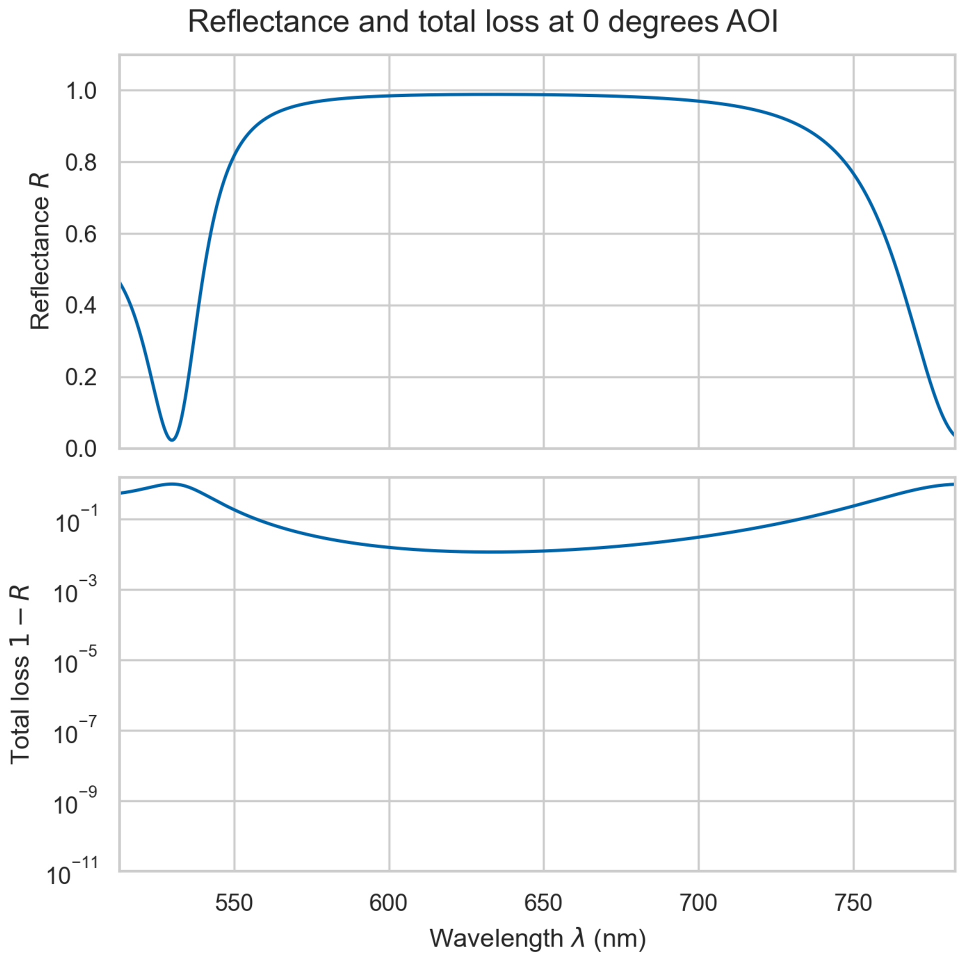

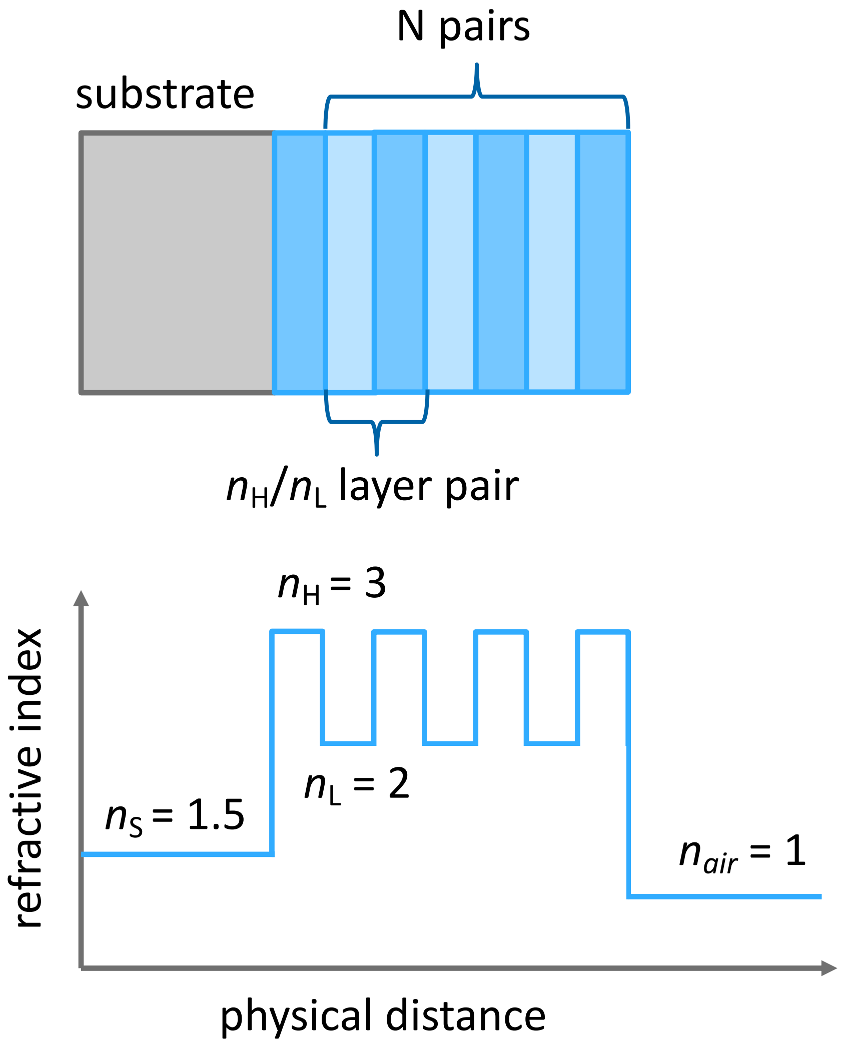

Buildup of mirror and stopband: N = 6

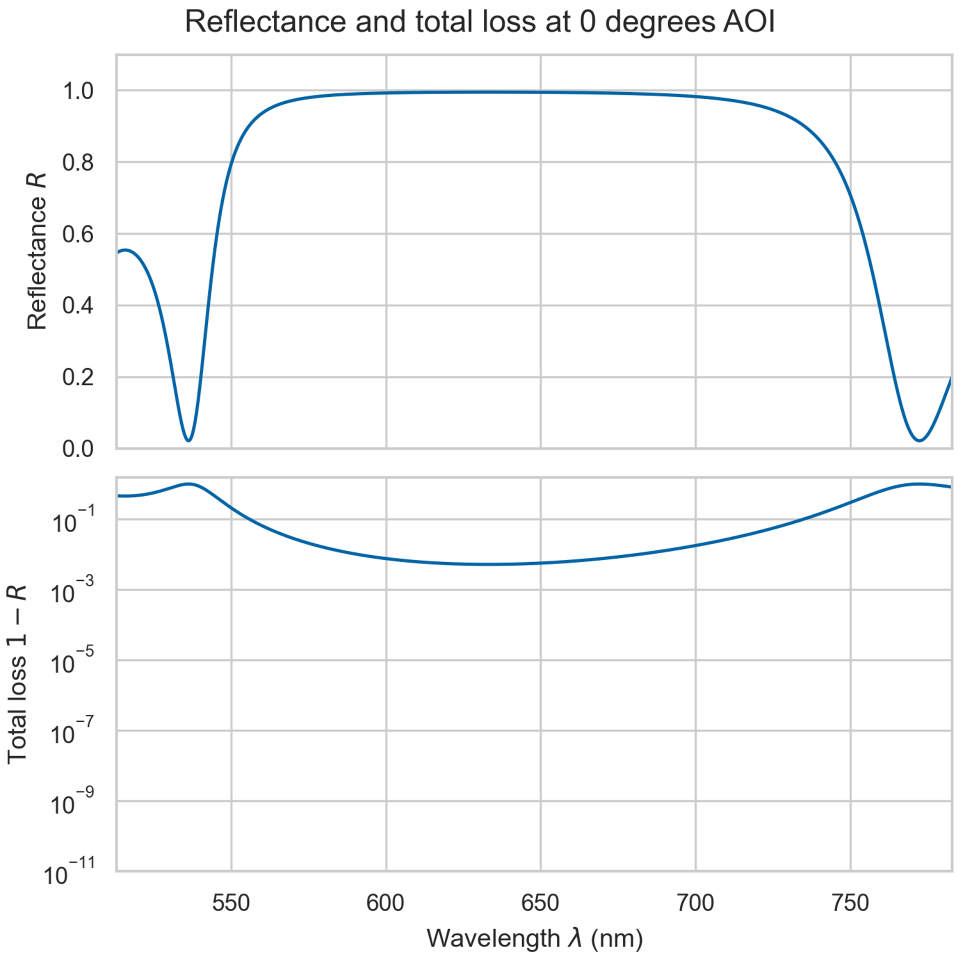

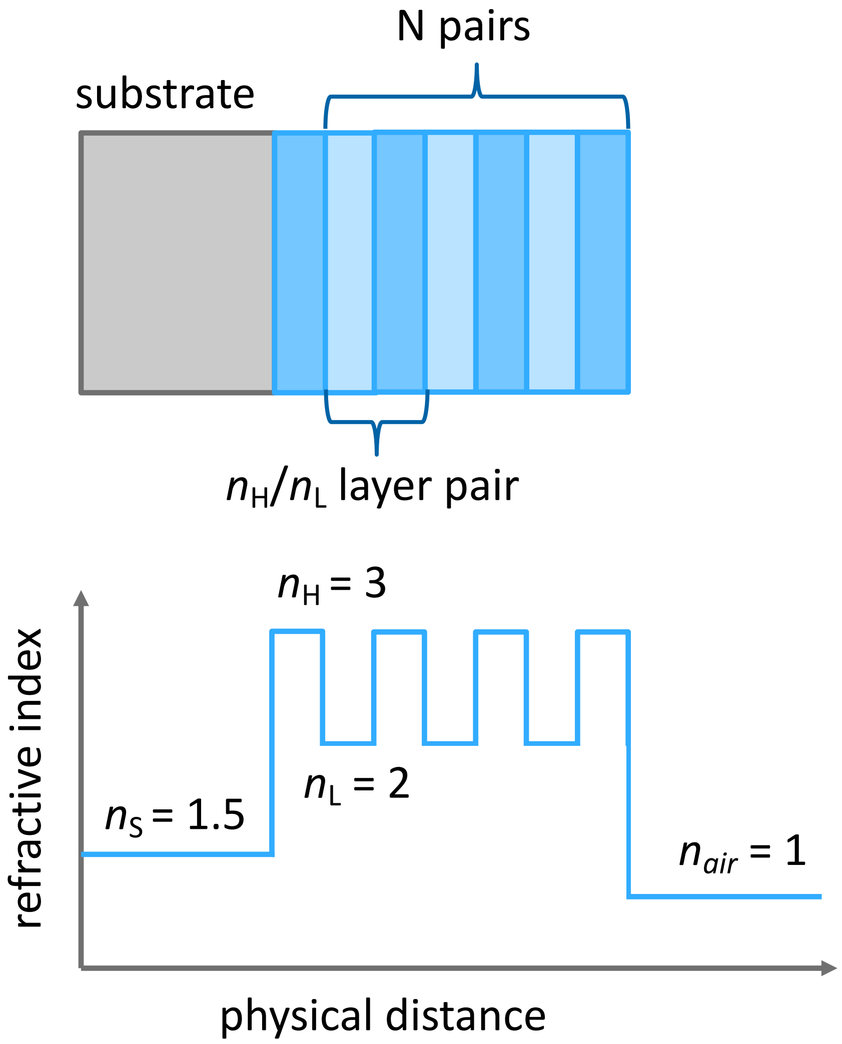

Buildup of mirror and stopband: N = 8

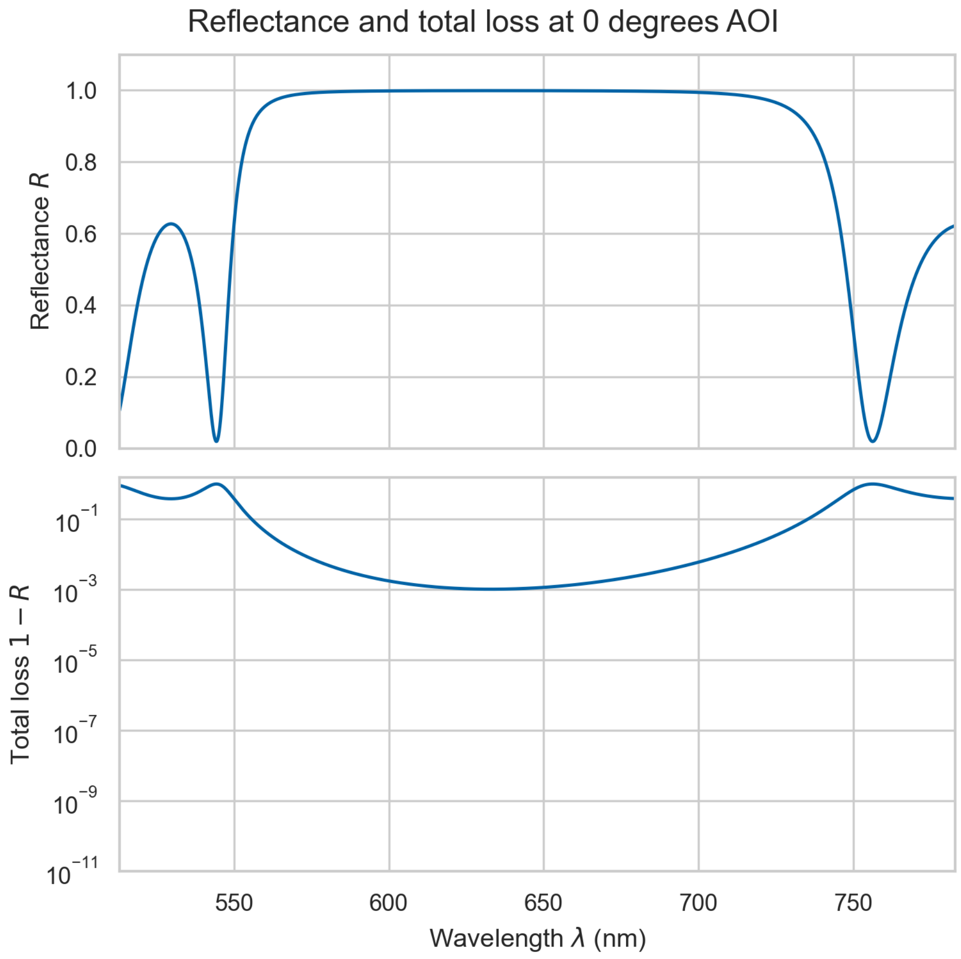

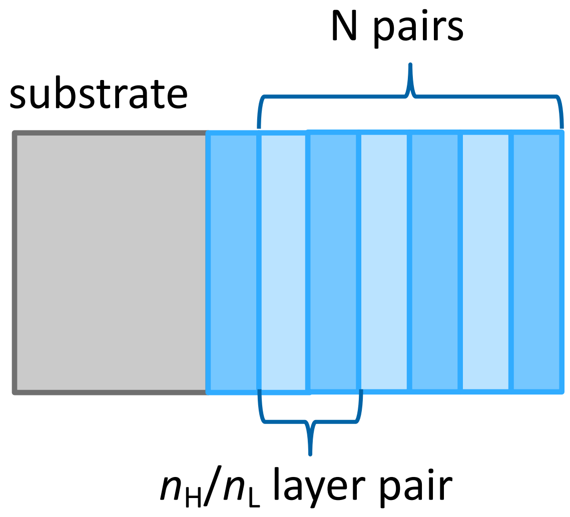

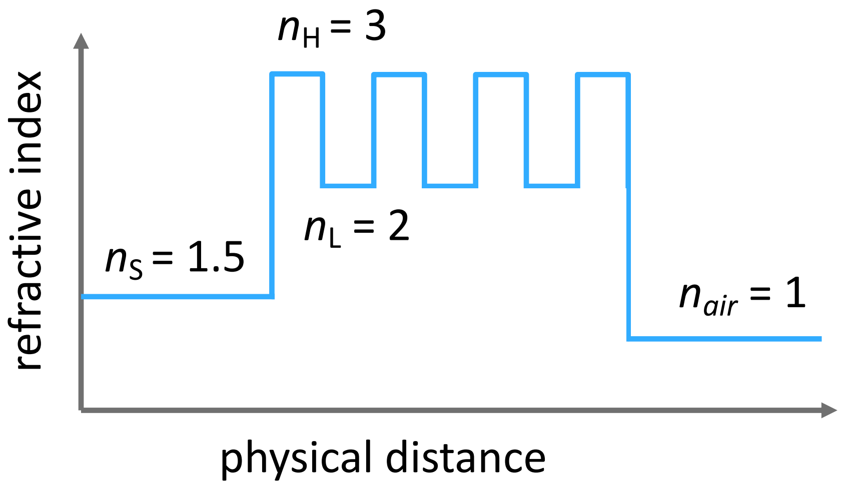

Buildup of mirror and stopband: N = 10

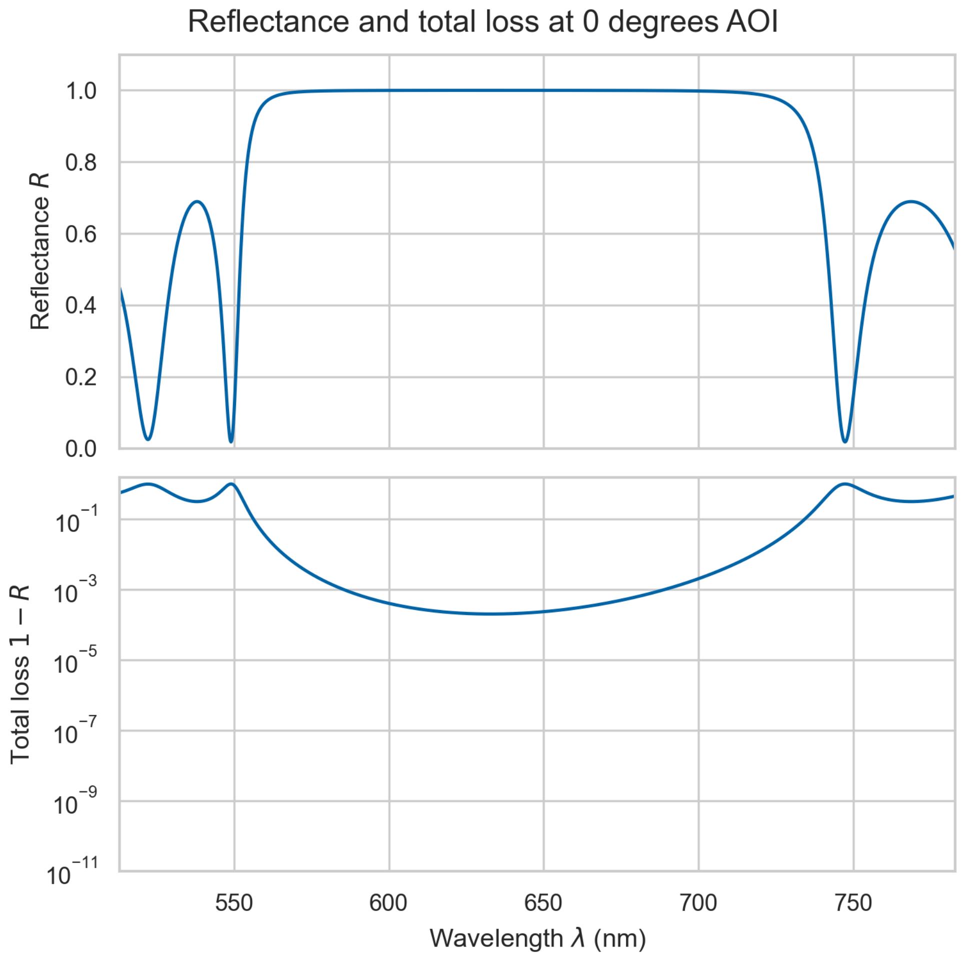

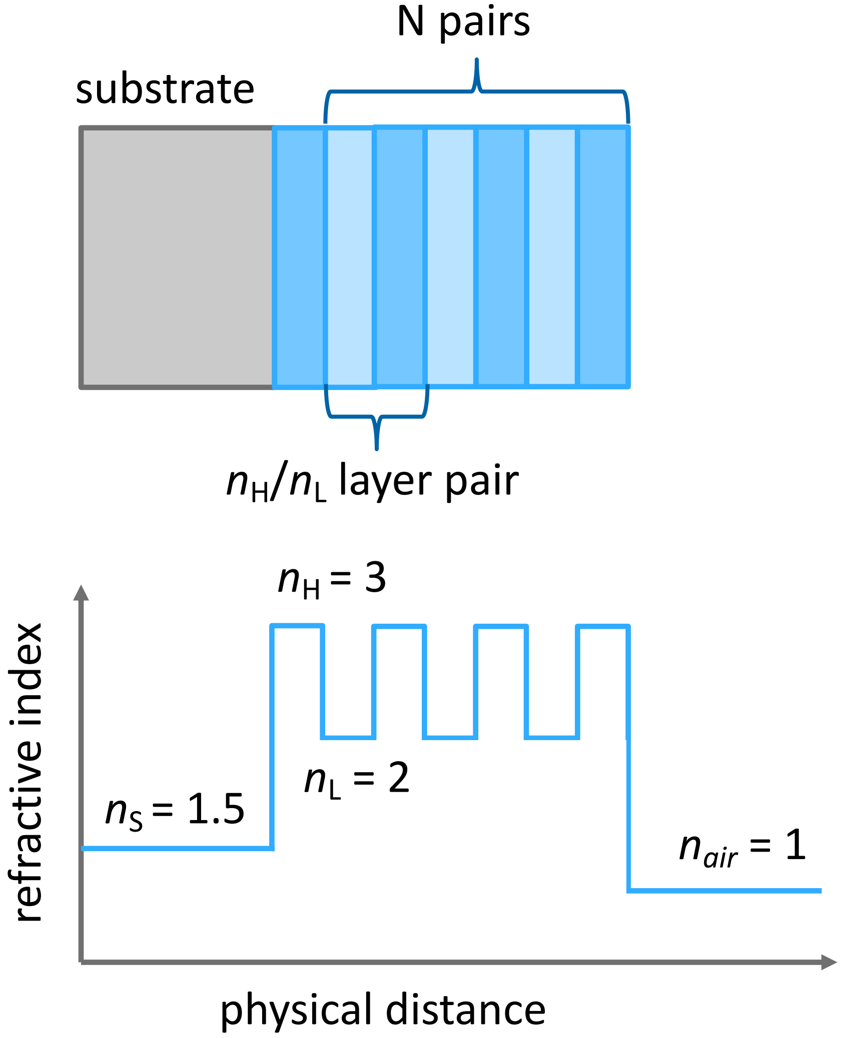

Buildup of mirror and stopband: N = 15

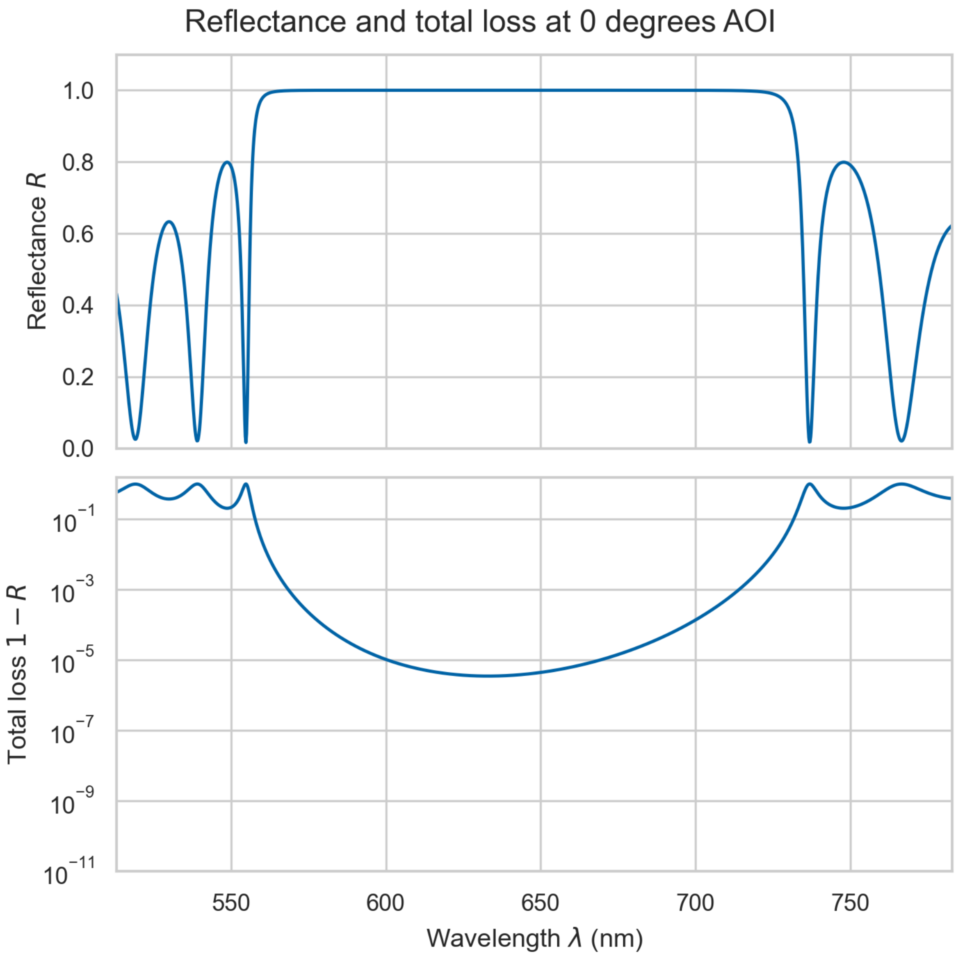

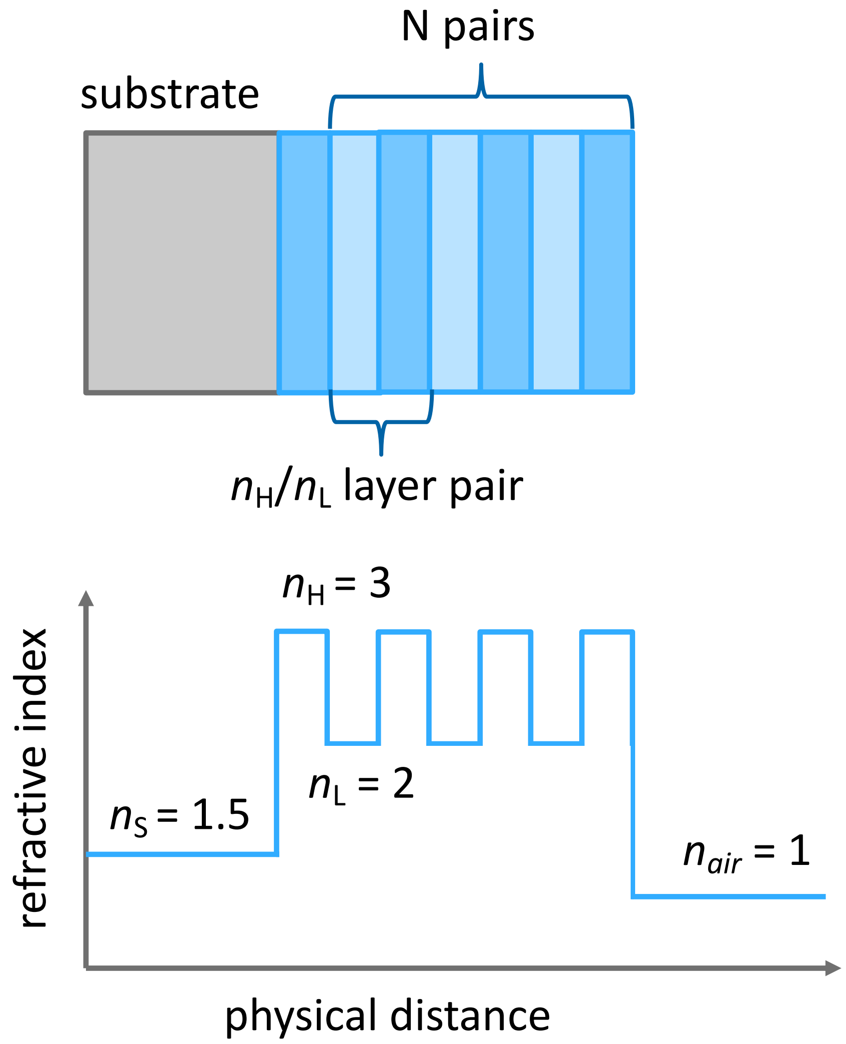

Buildup of mirror and stopband: N = 20

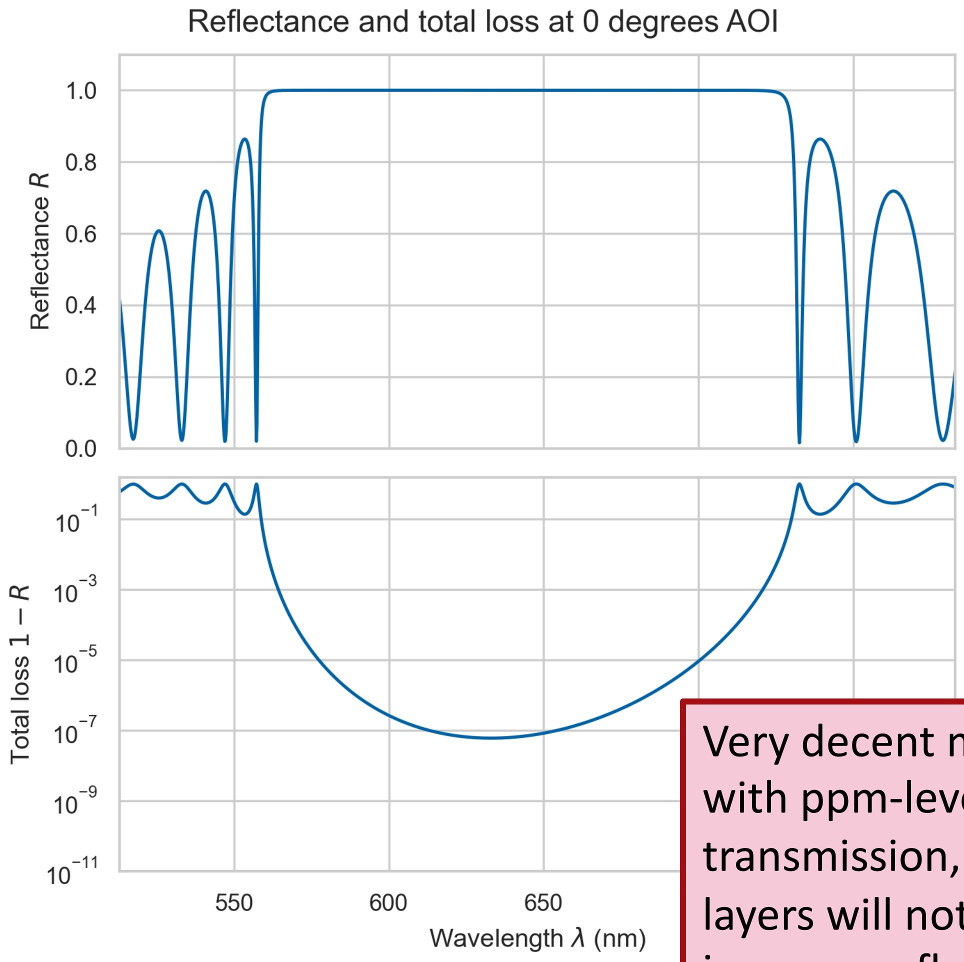

Very decent mirror with ppm-level transmission, further layers will not increase reflectivity

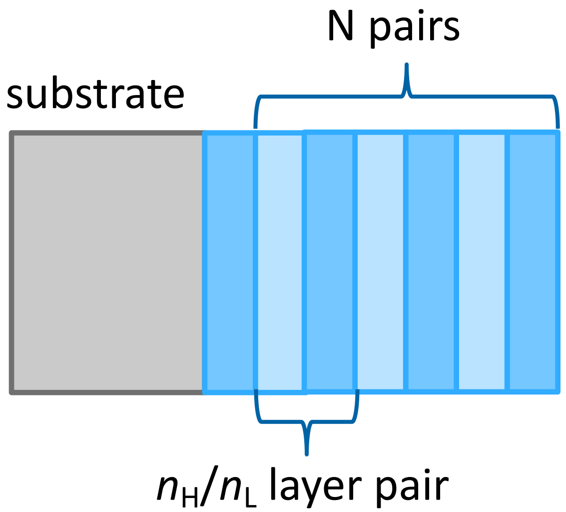

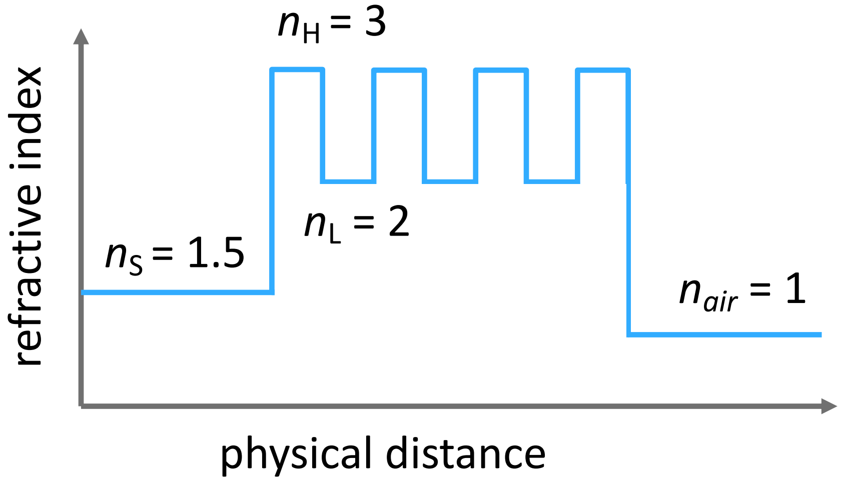

Buildup of mirror and stopband: N = 25

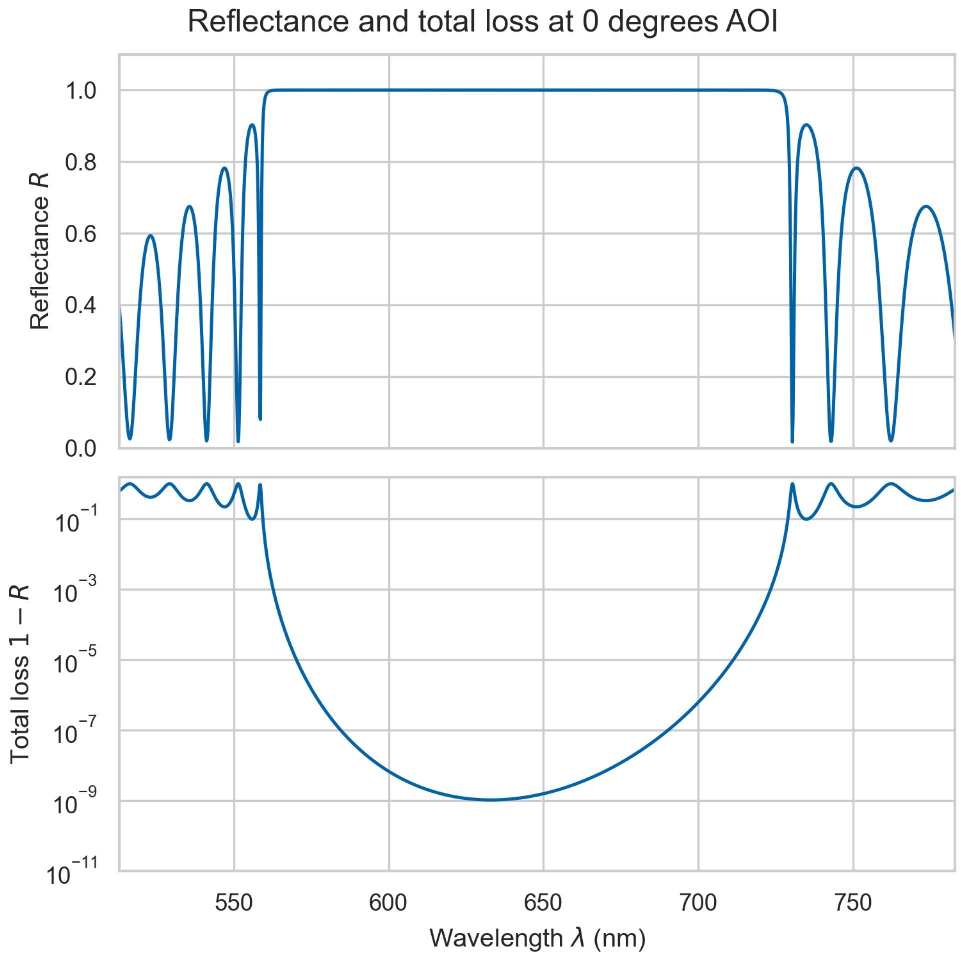

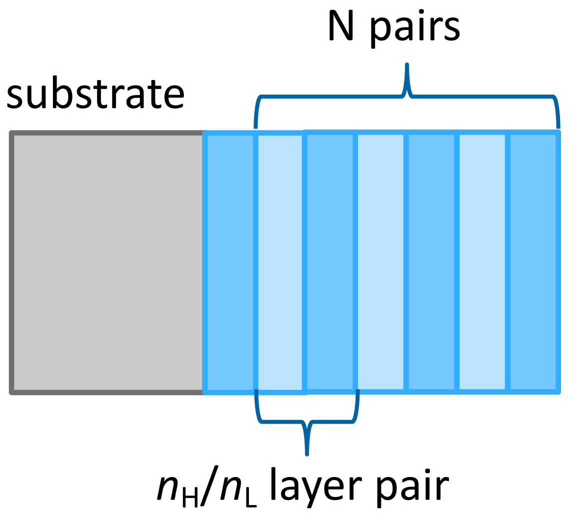

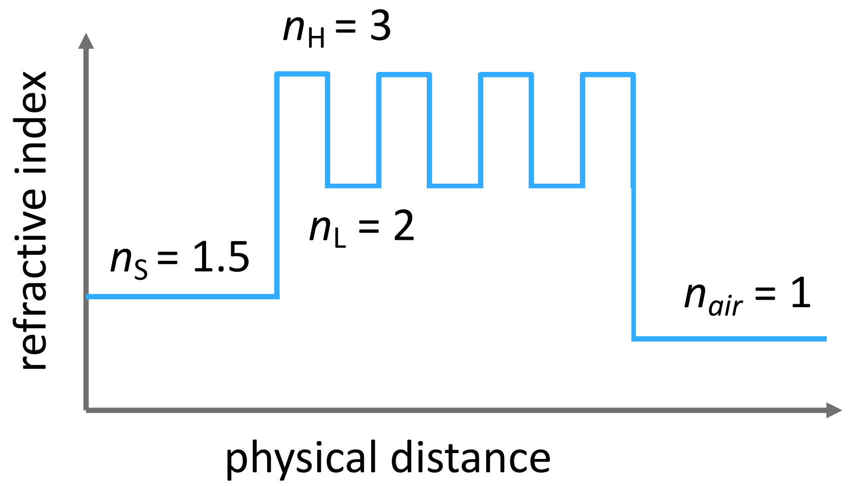

Buildup of mirror and stopband: N = 30

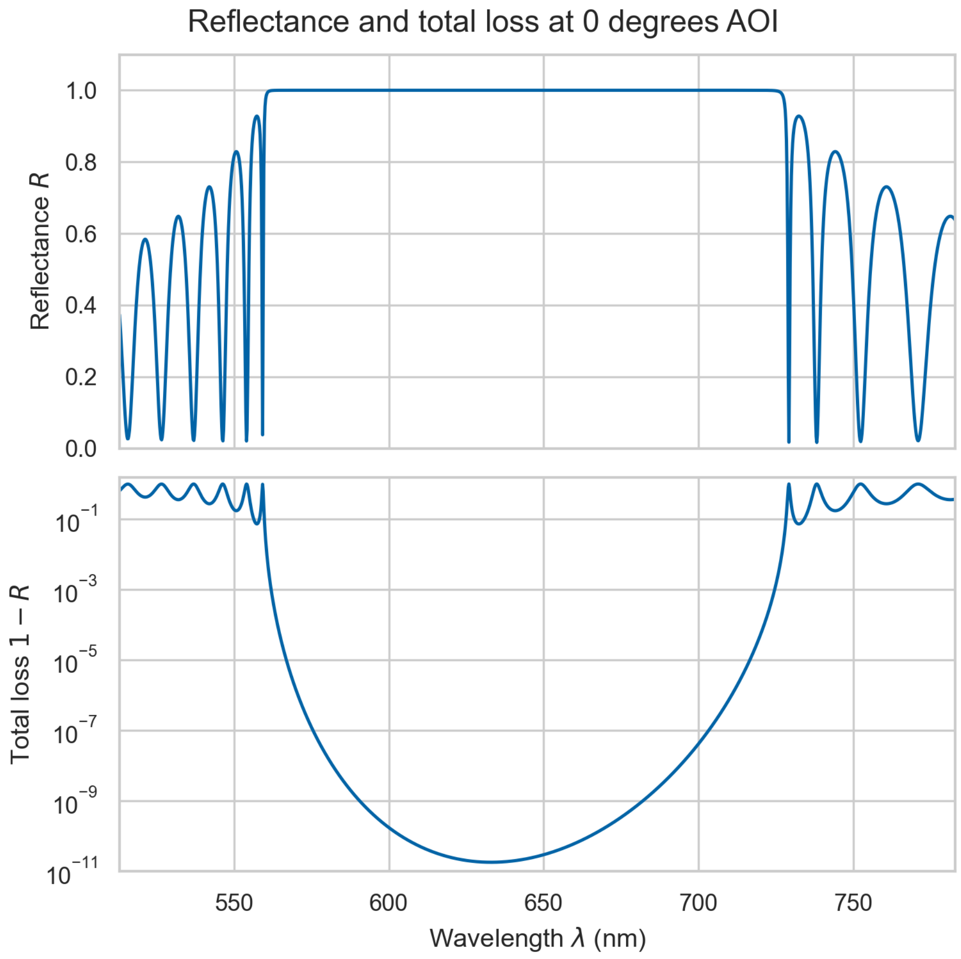

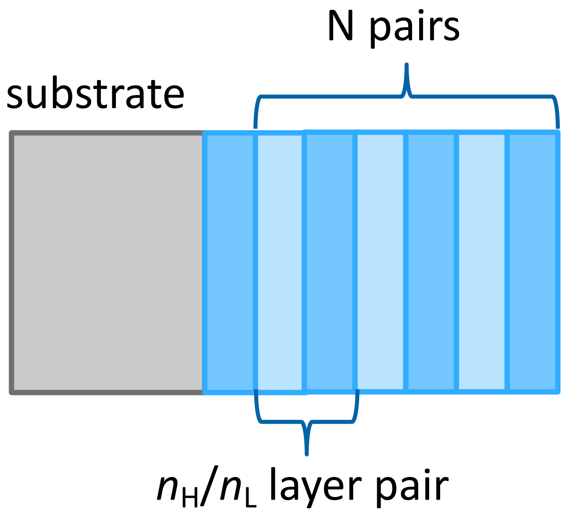

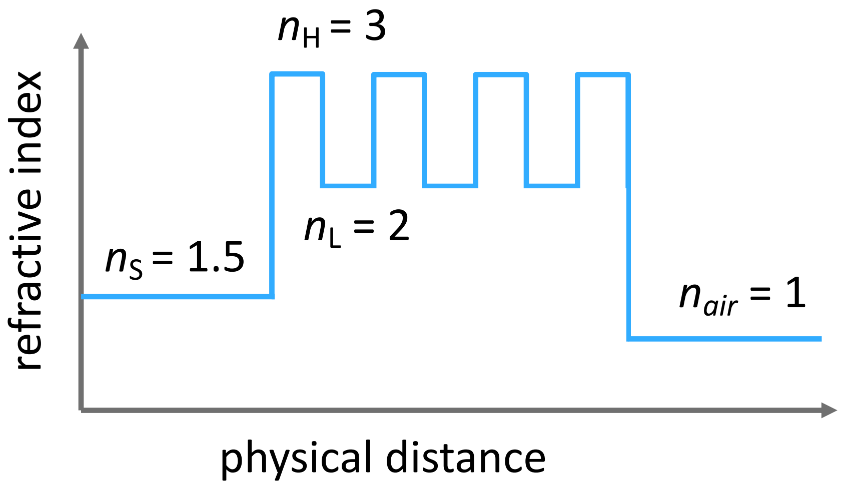

Analytical insights: width of stopband and angle-tuning

Fresnes reflection (0° AOI):

$$r = \frac{n_H - n_L}{n_H + n_L}$$

Relative width of stopband:

$$\frac{\Delta\omega}{\Delta\omega_{\mathrm{B}}} = \frac{4}{\pi}\sin^{-1} r$$

Technology	n_H	n_L	Relative width
Epitaxially grown semiconductors	~3.6	~3.0	~10%
Amorphous coatings (IBS)	2.1 (Ta_2O_5) 2.35 (TiO_2)	1.37 (MgF_2) 1.45 (SiO_2)	~30%

Higher contrast (large Δn) allows for wider stopband and fewer layers for a given reflectivity

U. Keller, Ultrafast Lasers, Springer, ISBN: 978-3-030-82531-7

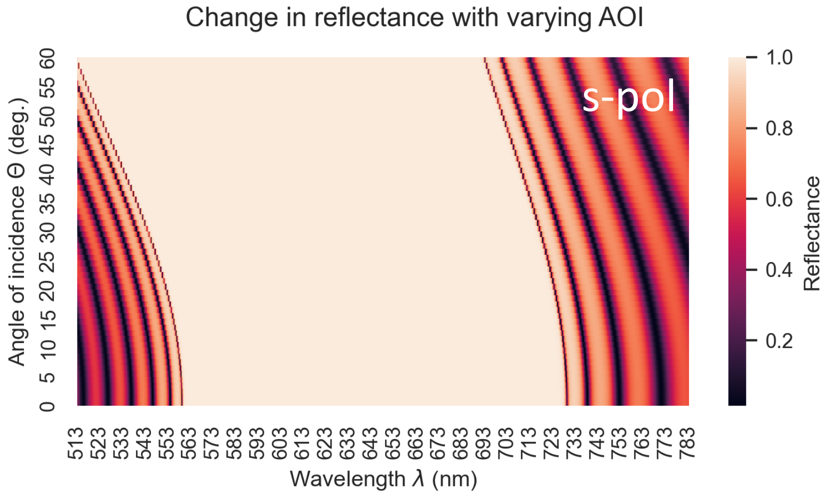
Change in reflectance with varying AOI

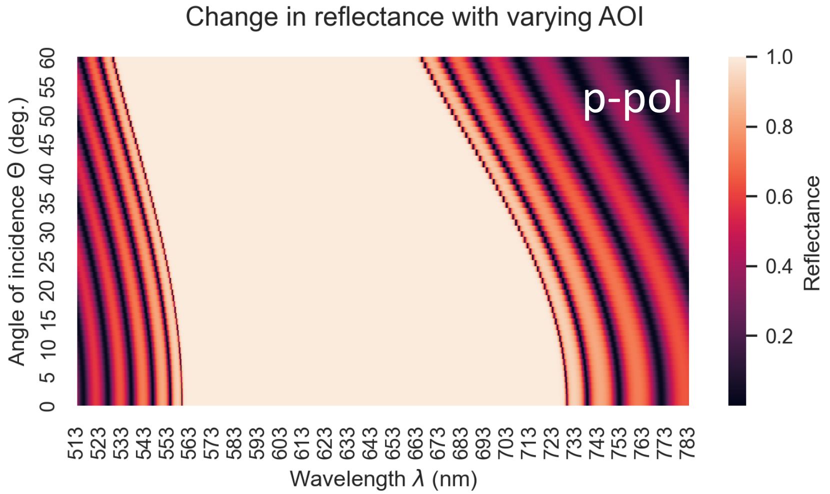
Change in reflectance with varying AOI

Excursion: chirped DBRs and dispersion measurements

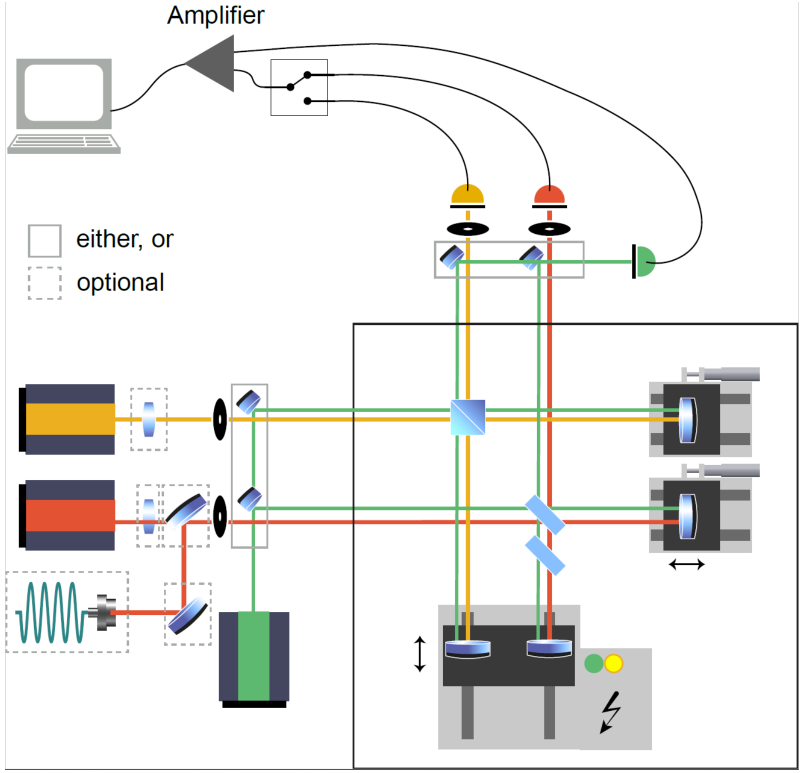

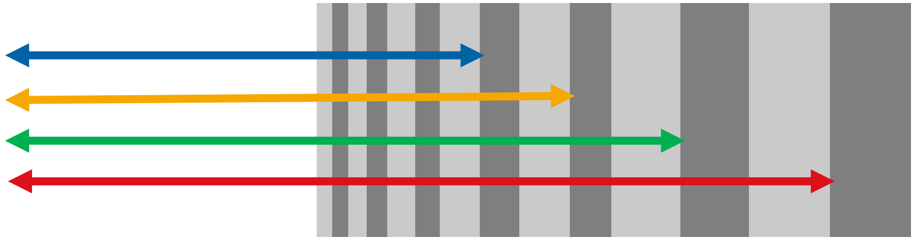

Chirped Distributed Bragg reflectors

- Spectrally dependent phase shifts due to different penetration depths
- GDD optimized designs possible

Group delay dispersion can be measured in an FTS if the sample is placed in one arm and not before the spectrometer

universität wien

CHRISTIAN DOPPLER LABORATORY FOR
MID-IR SPECTROSCOPY &
SEMICONDUCTOR OPTICS

High Finesse Mirror Design, **Fabrication** and Characterization

Optical Coating Technologies

Physical Vapor Deposition (PVD) of current amorphous coatings

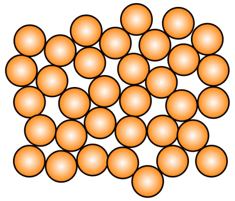

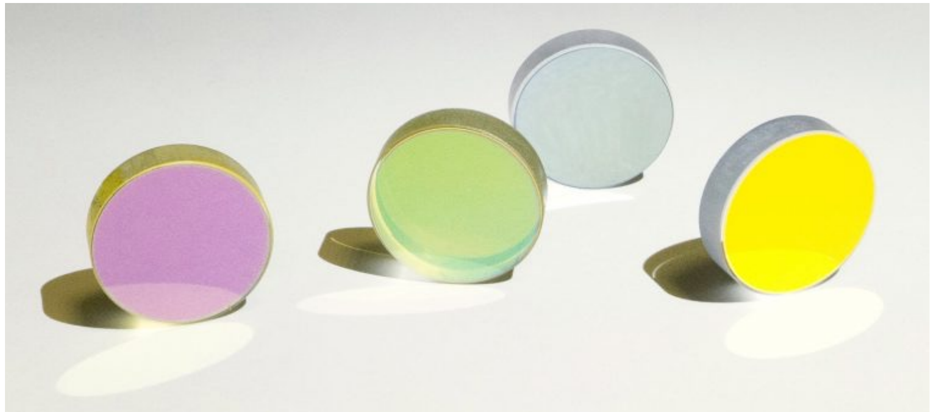

Substrate-Transferred crystalline semiconductor supermirrors

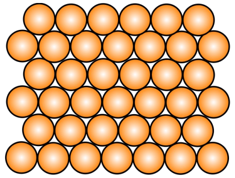

1857
Arc Evaporation

1907
E-beam Evaporation

1939
Magnetron Sputtering

1979
Ion-beam Sputtering

2012
Crystalline Coatings

New state-of-the-art low-loss mirrors:
GaAs/AlGaAs deposited via molecular beam epitaxy

State-of-the-art multilayer mirrors:
ion-beam sputtered Ta_2O_5/SiO_2

E-beam evaporation

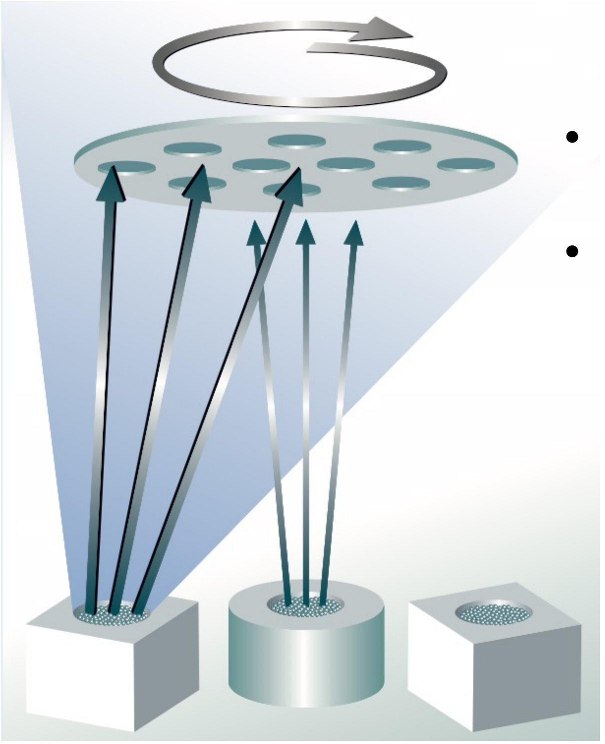

Evaporation sources heated by e-beam or resistive heating

- Rotating substrates to ensure coating homogeneity
- Substrate temperature between 150 and 400°C

Challenges:
- Low packing density allows atmospheric water to enter coating → absorption and shift of stopband
- Formation of micro crystallites leading to high scattering losses (up to percent level)

Advantages
- High laser damage thresholds and low absorption
- Often used for laser mirrors
- Best technology for UV-mirrors

Layertec, Optics and Coatings

Sputtering

Extraction of ionized particles by ion bombardment
→ acceleration with electric fields and deposition on substrate

Magnetron Sputtering

- Gas discharge in front of target
- Potentially combined with reactive gas to create compunds

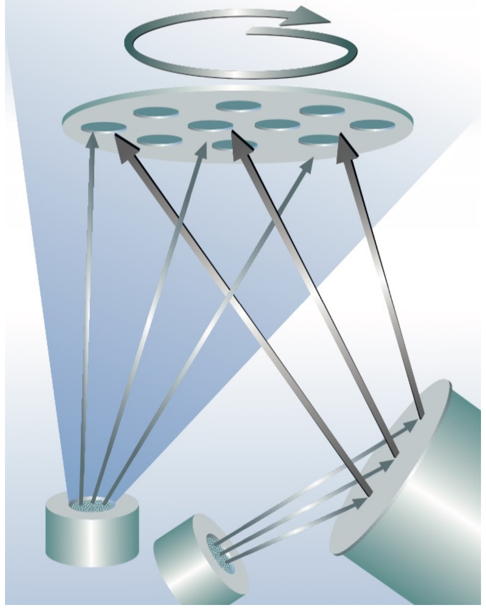

Ion Beam Sputtering (IBS)

- Separate ion source generates target ions and reactive gas (oxygen)

Layertec, Optics and Coatings

Advantages

- **Gold standard** for mirror production from VIS-NIR
- High laser damage thresholds and low absorption
- Fully amorphous microstructure (no micro crystallites)
- High package density (no water-vapor issues)
- High mechanical stability

Challenges:

- Mid-IR wavelength coverage (relatively high absorption)
- Amorphous structure leads to scattering losses

Molecular Beam Epitaxy (MBE)

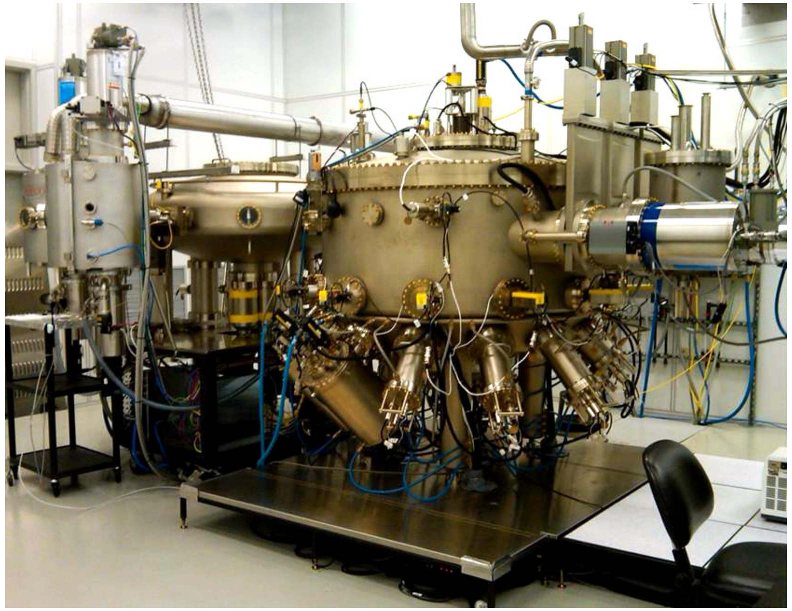

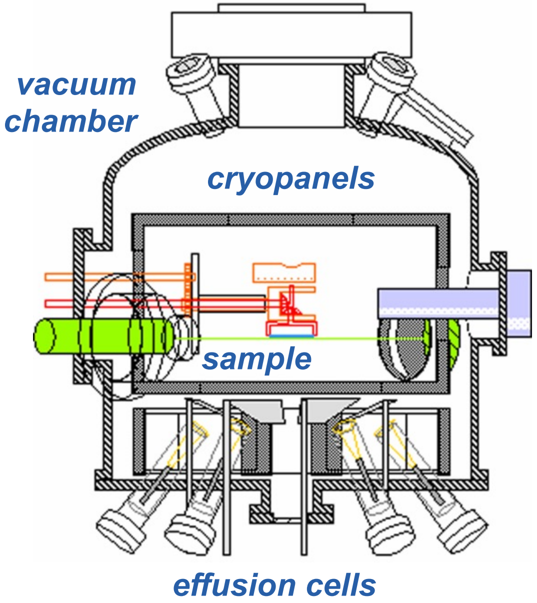

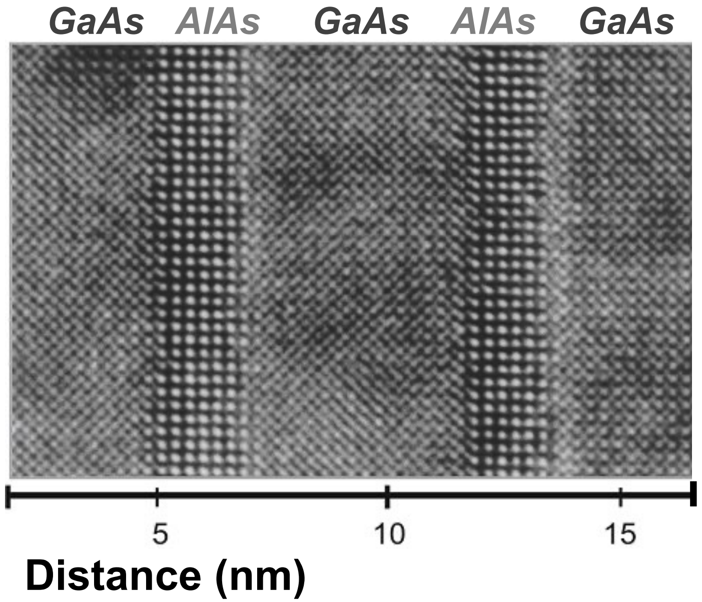

- Molecular beam epitaxy is employed to grow single-crystal GaAs/AlGaAs heterostructures
- The single-crystalline multilayer is removed and directly bonded to a super-polished (curved) substrate
- Alternating layers GaAs/$Al_{0.92}Ga_{0.08}As$ form distributed Bragg reflector

TEM micrograph courtesy of the University of Cambridge

Molecular Beam Epitaxy (MBE) – Crystalline Mirrors

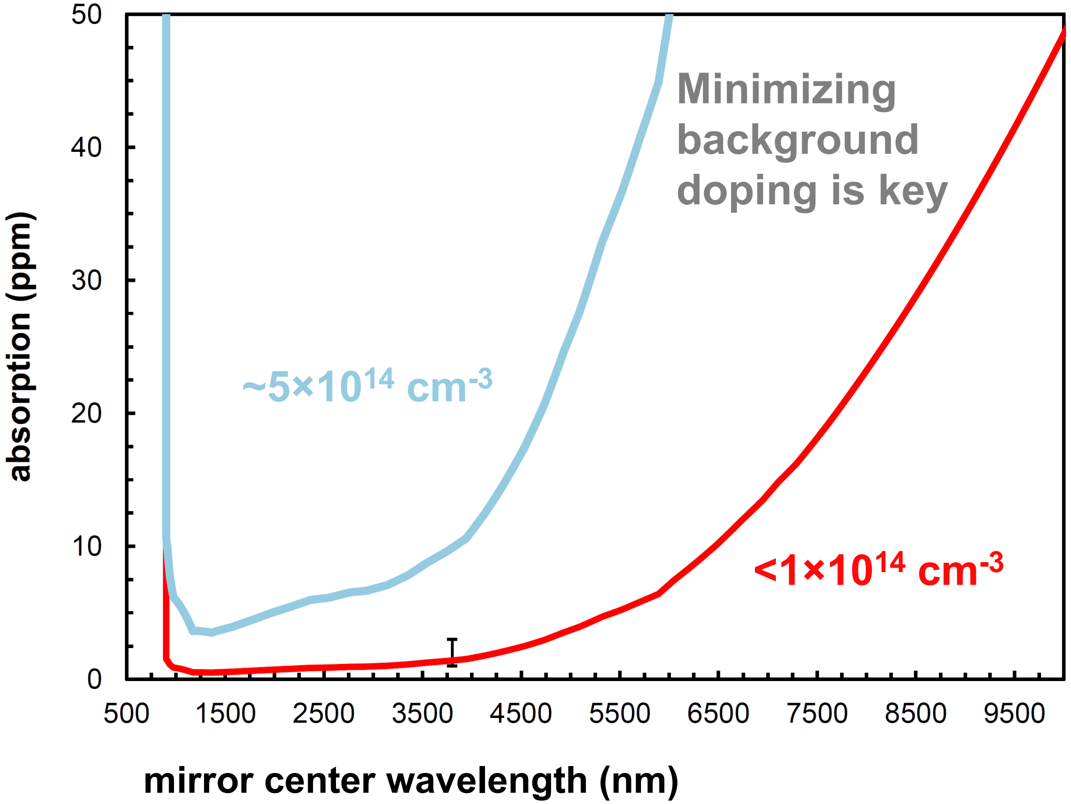

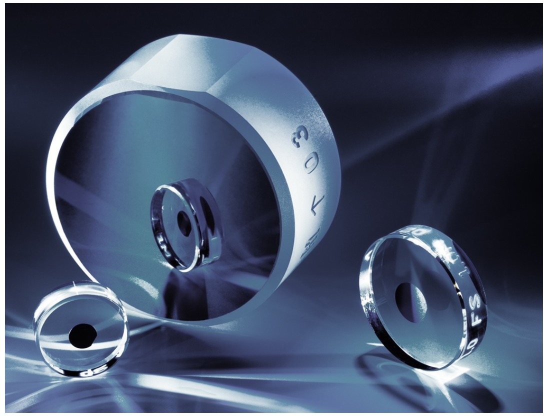

Challenges:

- Involved (and expensive) production process
- Low Δn → reduced relative stopband compared to near-IR mirror technology (~10%)

Advantages

- High thermal conductivity
- Minimal absorption in mid-IR spectral range (sensitive mid-IR spectroscopy, high cavity transmission)
- Negligible scatter due to crystalline surface quality
- Excellent Brownian noise performance (reference cavities, gravitational wave detection, ring-laser gyroscopes, …)
- Potential for **ppm-level optical losses** in the mid-IR

For absorption coefficients see: W. G. Spitzer and J. M. Whelan, *Physical Review* **114** 59 (1959)

universität wien

CHRISTIAN DOPPLER LABORATORY FOR
MID-IR SPECTROSCOPY &
SEMICONDUCTOR OPTICS

High Finesse Mirror Design, Fabrication and **Characterization**

Low Loss Crystalline Coatings

28.5 period GaAs/AlGaAs crystalline coating

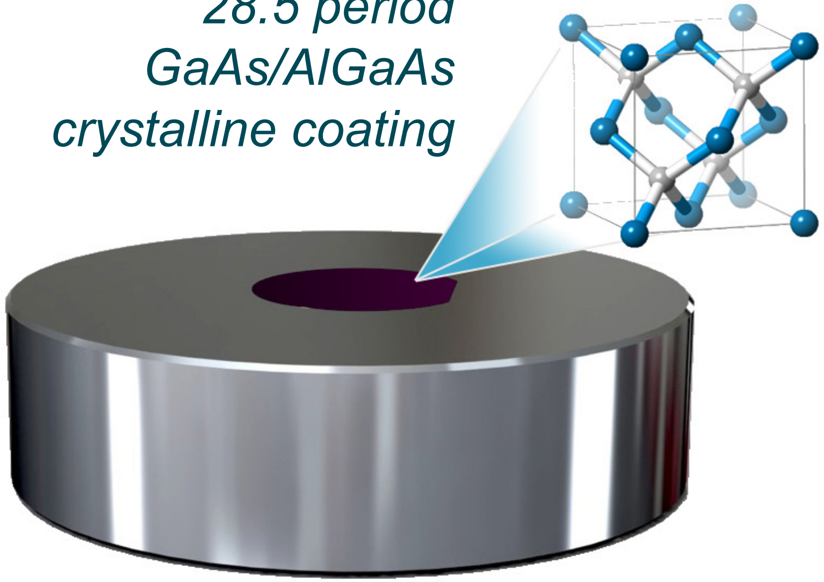

single-crystal Si (SCS) substrate

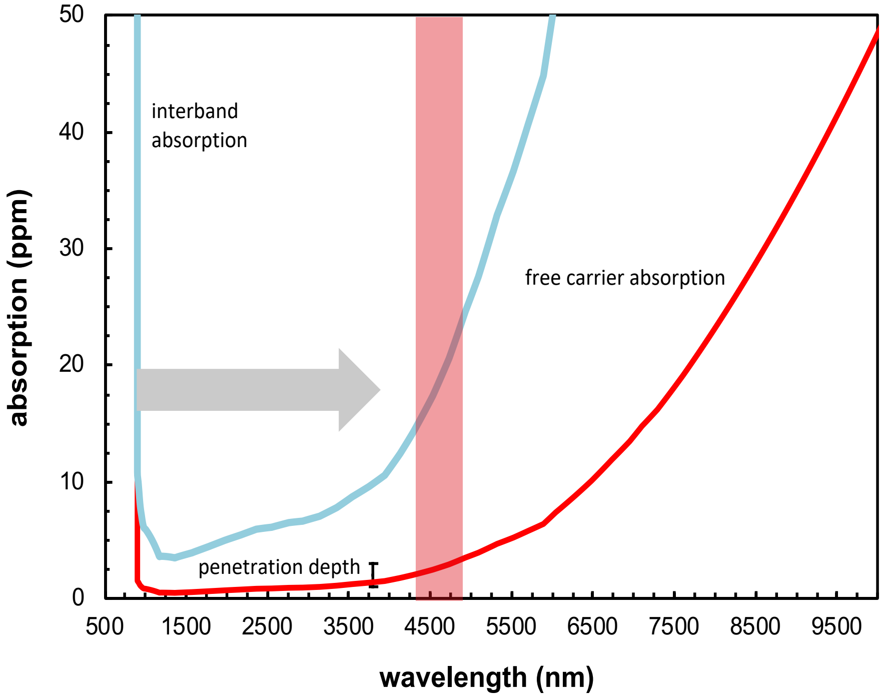

- Monocrystalline mirror discs transferred to curved substrates
- Alternating layers GaAs/$Al_{0.92}Ga_{0.08}As$ form distributed Bragg reflector
- Potential for **ppm-level optical losses** in the mid-IR

Crystalline Coatings

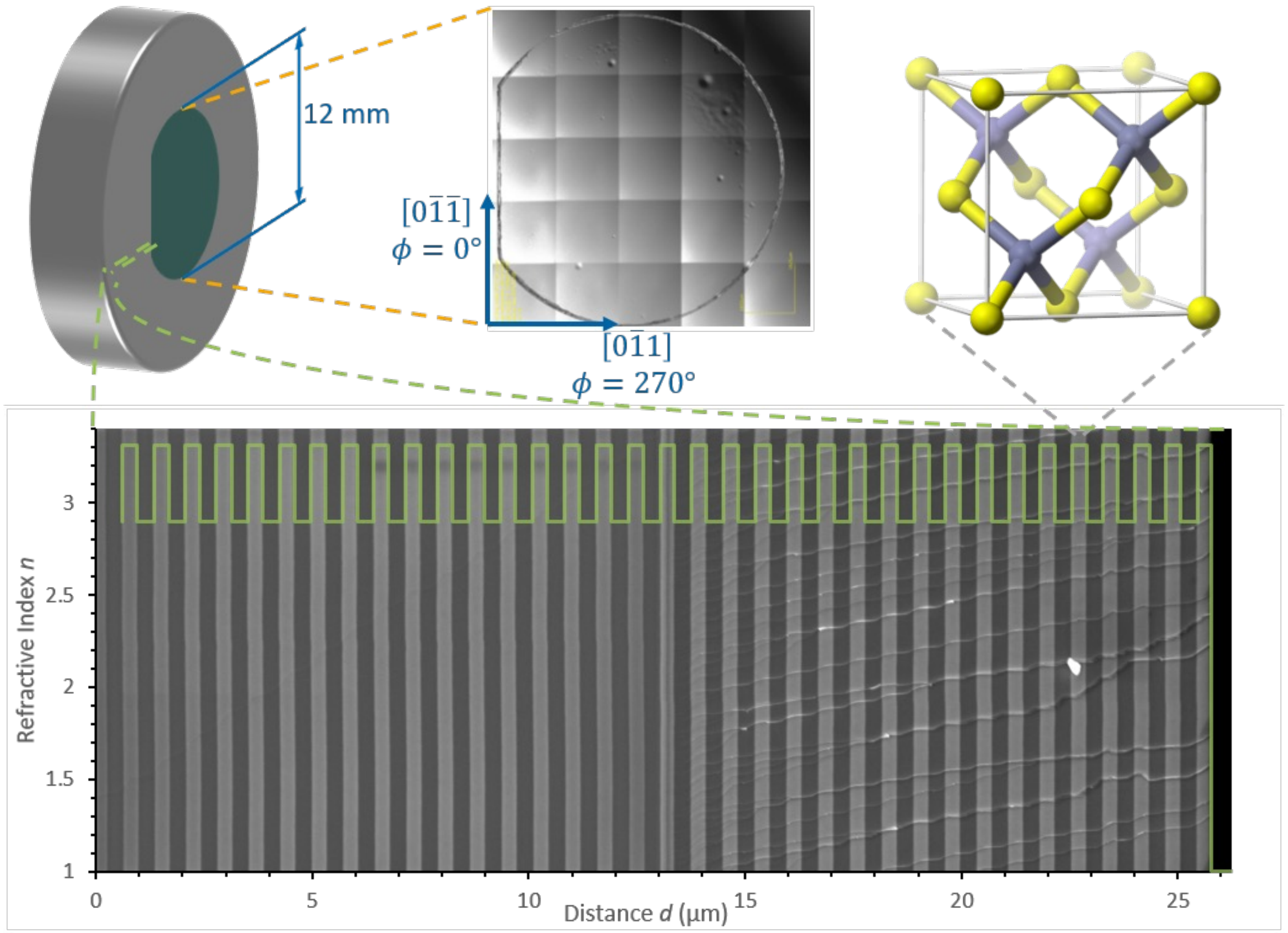

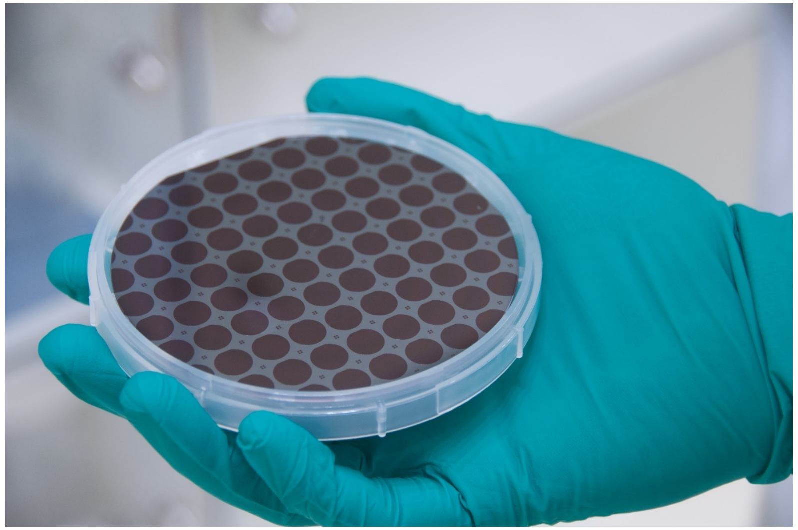

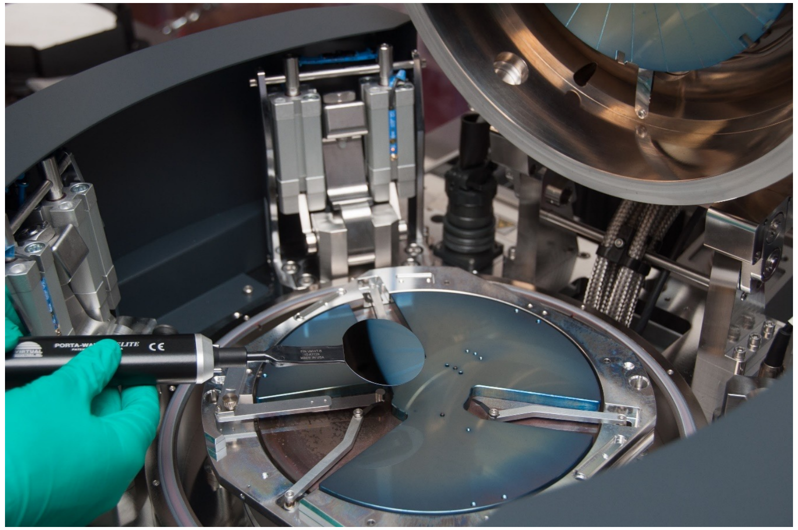

Predicting Transmission via a Model Based on FTIR and SEM Data

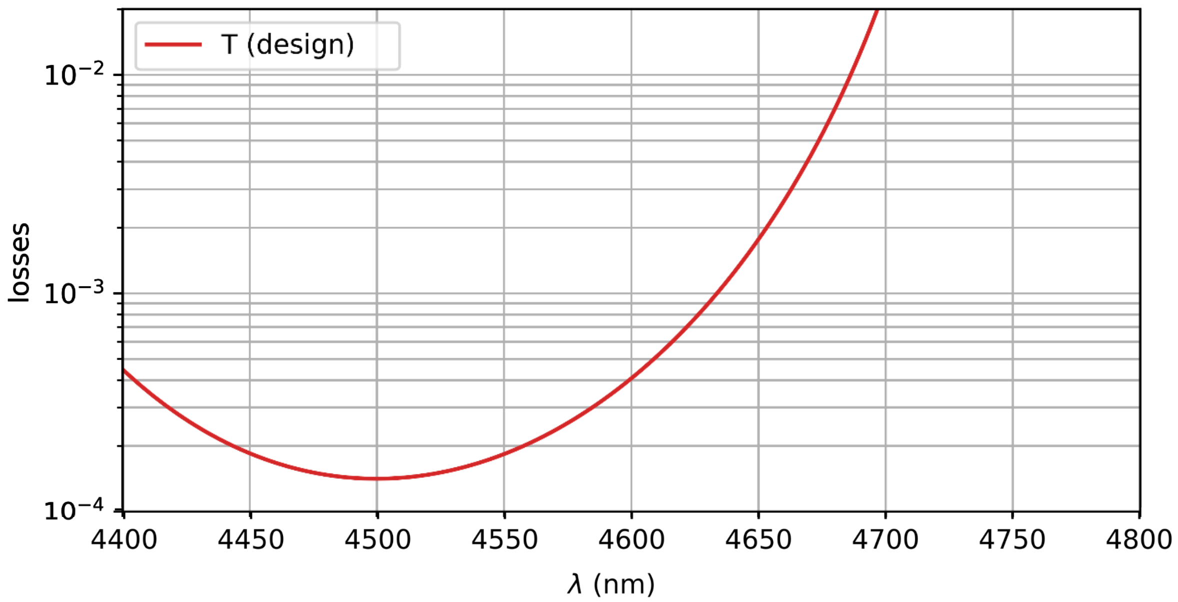

	Loss (ppm)	λ_{min} (nm)
T (design)	142	4500

Fourier-Transform Spectroscopy

Resolution

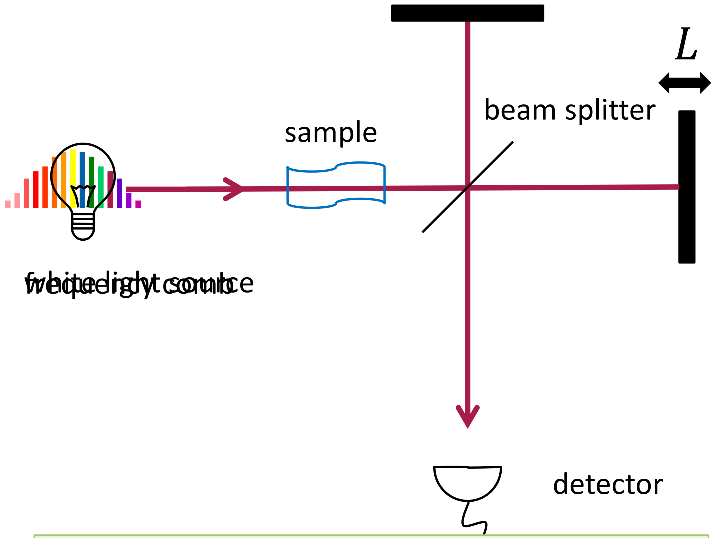

Resolution: $\Delta\nu = \frac{1}{2L} > f_{\text{rep}}$

Typical value: ≈ 6 GHz – 1.8 MHz

Comb:
$\Delta\nu \approx 10\ \text{kHz};\ \mathbf{L} = \mathbf{1\ m}$

Corresponds to L= **15 km** !!!

See summer school lecture of Lucile Rutkowski on
“Cavity-enhanced optical frequency comb spectroscopy“

Fourier-Transformation Spectroscopy

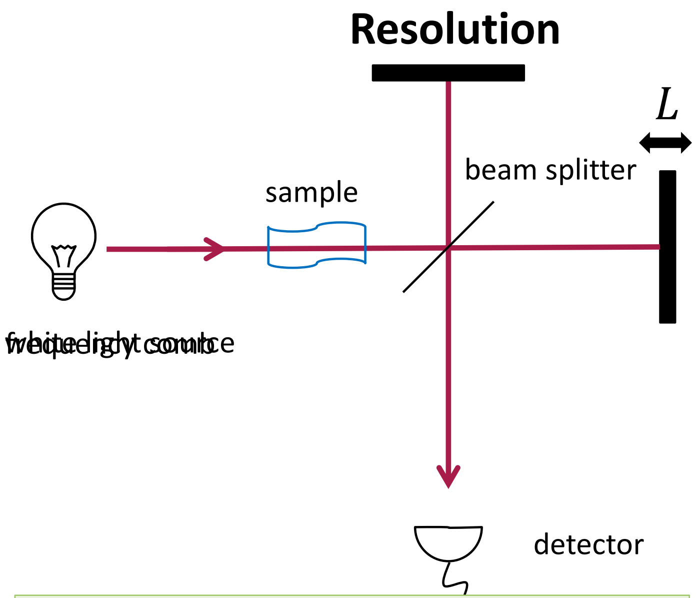

Resolution: $\Delta\nu = \frac{1}{2L} > f_{\mathrm{rep}}$

Typical value: ≈ 6 GHz – 1.8 MHz

Comb:
$\Delta\nu \approx 10\ \mathrm{kHz};\ \mathbf{L = 1\ m}$

Corresponds to L= **15 km** !!!

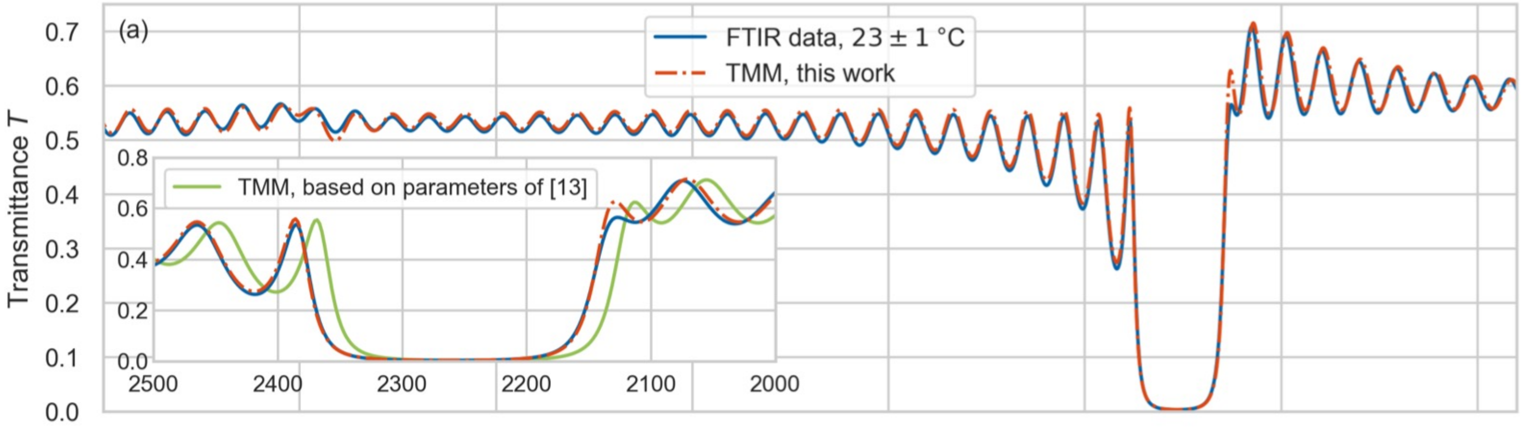

Poster: L. Perner, *et al.*
“High-Accuracy Measurement of Mid-IR Refractive Indices of GaAs/AlGaAs in Thin-Film Multilayers”

L. Perner, M. Prinz, O. H. Heckl, Mid-infrared refractive index of crystalline thin-film GaAs/AlGaAs multilayers , writeup in progress

Predicting Transmission via a Model Based on FTIR and SEM Data

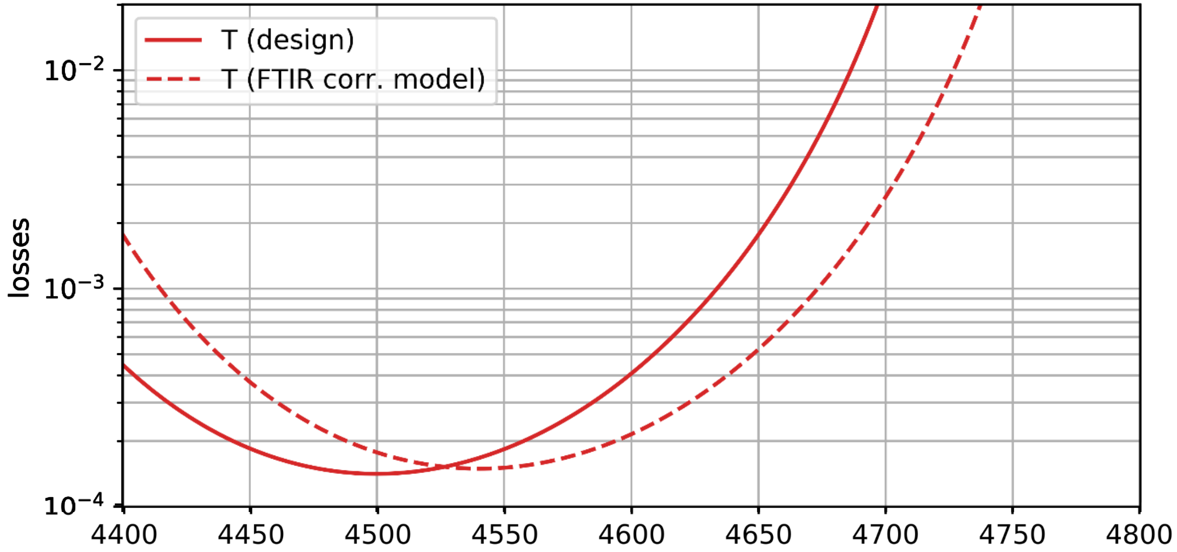

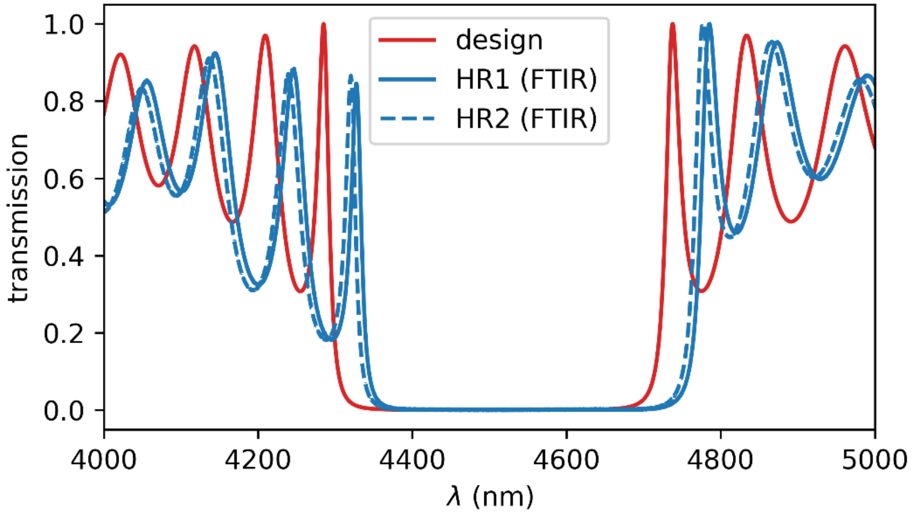

	Loss (ppm)	λ_{min} (nm)
T (design)	142	4500
T (FTIR corr.)	144 ± 2	4538 ± 1

- FTIR can be used to determine growth (thickness) errors and thus the center wavelength
- **However**, this system cannot independently resolve the minimum transmission value

Loss Components in Optical Interference Coatings

$$\underbrace{T + \underbrace{A + S}_{l}}_{L} = 1 - R$$

l … Excess loss

L … Total loss

Precise measurements at ppm level challenging, most often not provided by manufacturers.

→ A major inhibition for progress in the field!

Transmission (T)

Design parameter, controlled by # of mirror periods and index contrast

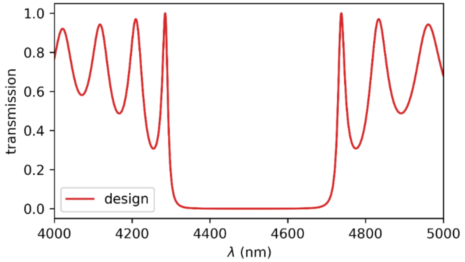

Absorption (A)

Determined by free-carrier absorption

Excess losses:
Scatter and absorption reduce cavity transmission
$$\frac{P_{\text{trans}}}{P_{\text{in}}} \propto \frac{T^2}{L^2}$$

Scatter (S)

Measure of surface and bond quality

- typical micro-roughness of < 0.2 nm leads to $S <$ 5 ppm in NIR

Assumption:
< 1 ppm in mid-IR

Reflectance (R)

Final reflectivity defined by total losses

- aim is to achieve $l < T$
- determines cavity enhancement and linewidth (finesse)

Excess Loss Measurements

Transmission (*T*)

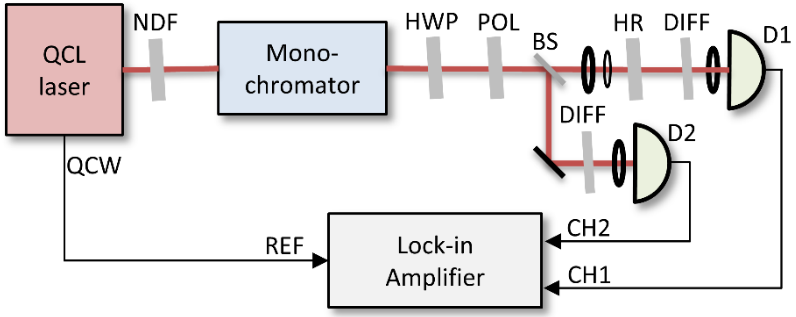

Direct transmission

Simple, but high-precision direct transmission measurement

Absorption (*A*)

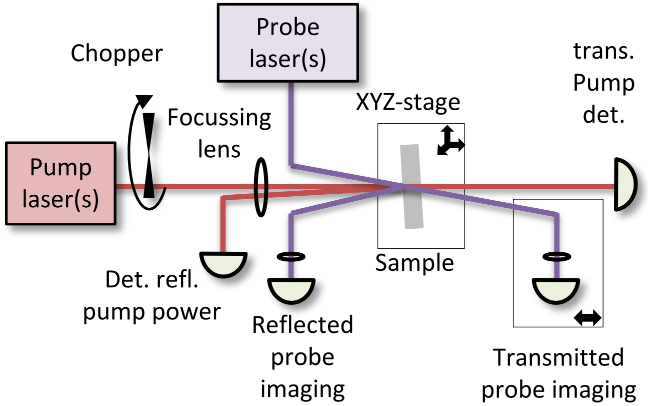

Photothermal common-path interferometry (PCI)

Allows for direct absorption measurements < 10 ppm
(<1 ppm with W-level pump)

Reflectance (*R*)

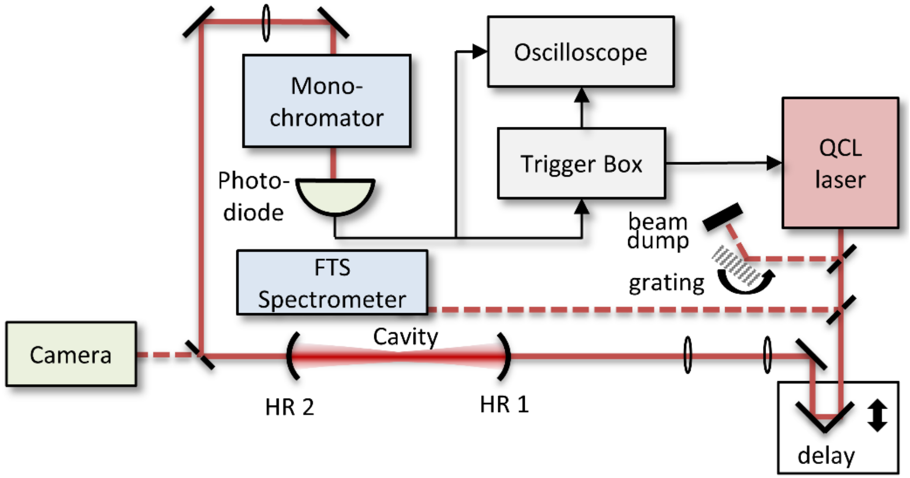

Cavity ring-down (CRD)

Broadband (~200 nm) QCL @ 4.55 µm with passive feedback

Excess Loss Measurements

Transmission (*T*)

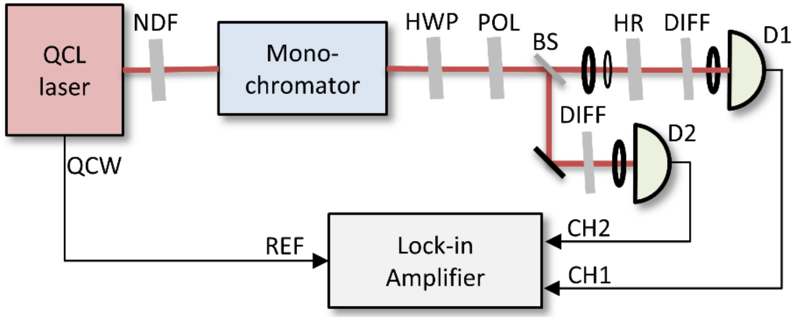

Direct transmission

Simple, but high-precision direct transmission measurement

Absorption (*A*)

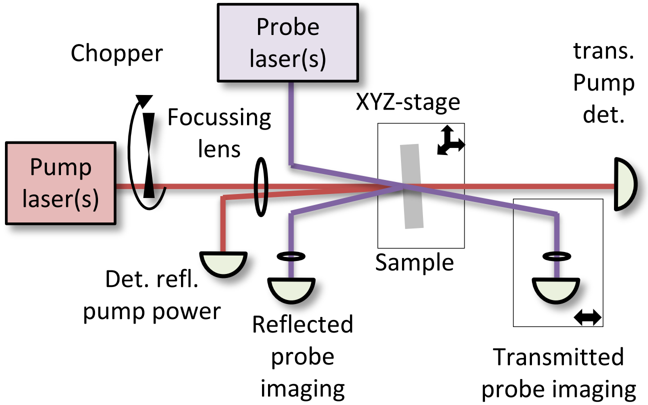

Photothermal common-path interferometry (PCI)

Allows for direct absorption measurements < 10 ppm
(<1 ppm with W-level pump)

Reflectance (*R*)

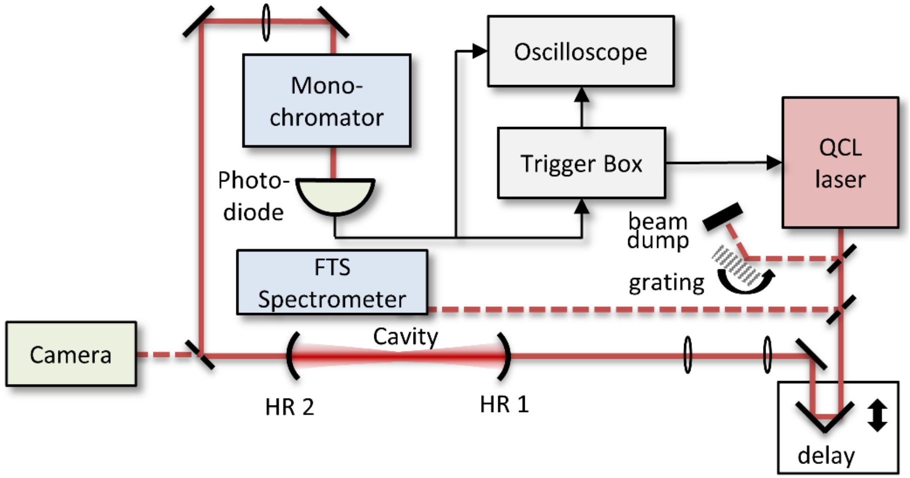

Cavity ring-down (CRD)

Broadband (~200 nm) QCL @ 4.55 µm with passive feedback

Direct Transmission Measurment (DIRT)

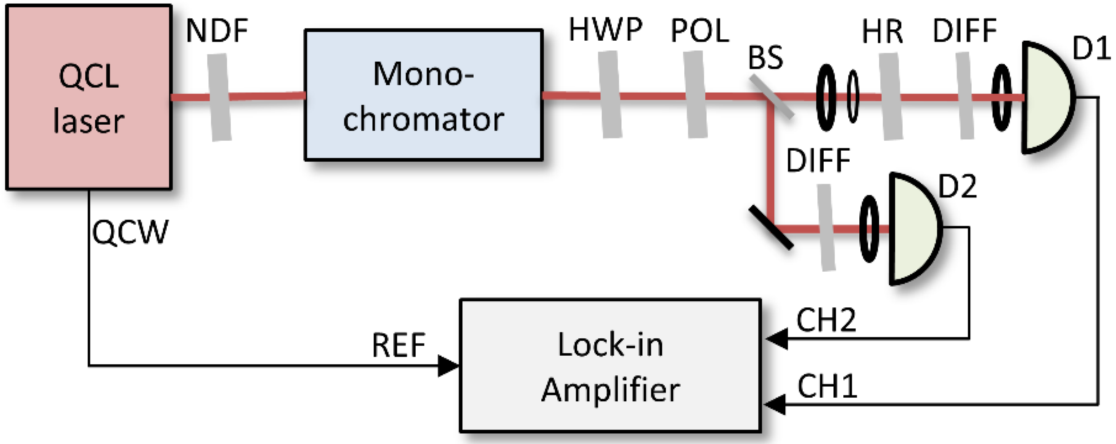

- Differential measurement
  - To deal with QCL probe power fluctuation
- Lock-in detection
  - enhances detector sensitivity given the low power per wavelength
  - increase of detector dynamic range (allowing measurement of P_{in} and P_{trans} with same detector)
- Blocking of stray light is crucial for a trustworthy measurement

DIRT Measurement Results

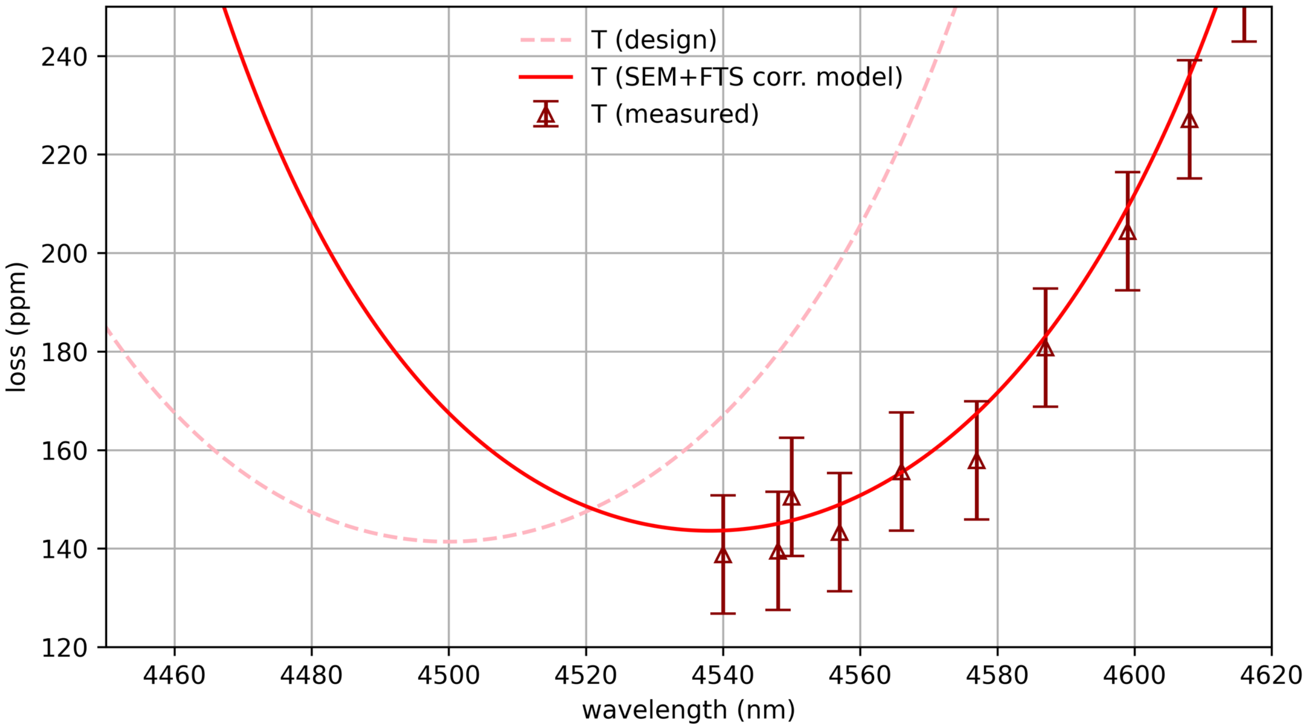

	Loss (ppm)	λ_{min} (nm)
T (design)	142	4500
T (FTIR corr.)	144 ± 2	4538 ± 1
T (measured)	143 ± 3	4536 ± 5

- We observe excellent agreement between direct measurements and FTIR-corrected transmission values – accurate dispersion curves.

Excess Loss Measurements

Transmission (*T*)

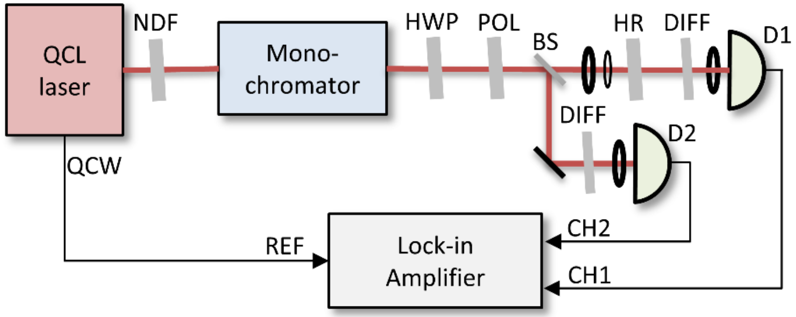

Direct transmission

Simple, but high-precision direct transmission measurement

Absorption (*A*)

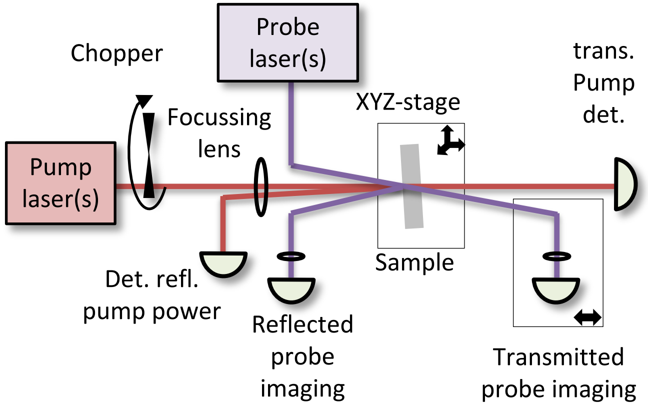

Photothermal common-path interferometry (PCI)

Allows for direct absorption measurements < 10 ppm
(<1 ppm with W-level pump)

Reflectance (*R*)

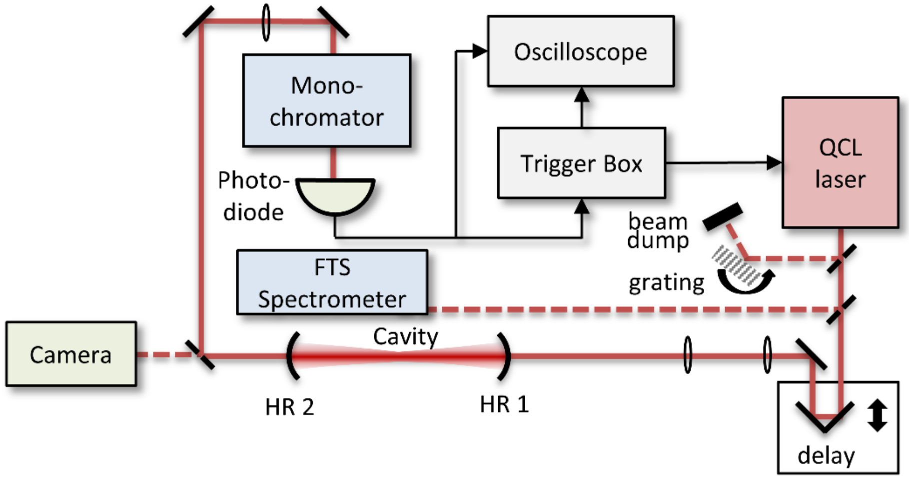

Cavity ring-down (CRD)

Broadband (~200 nm) QCL @ 4.55 µm with passive feedback

Measuring Optical Absorption via Photothermal Commonpath Interferometry (PCI)

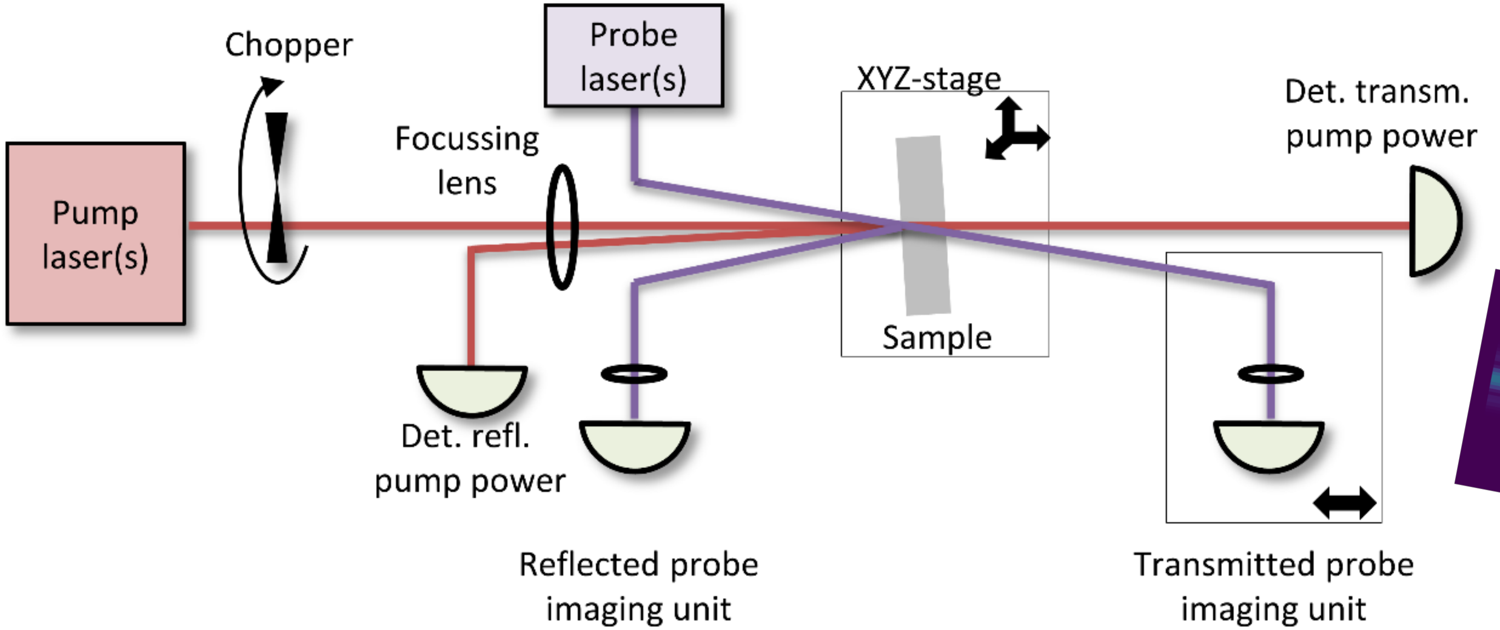

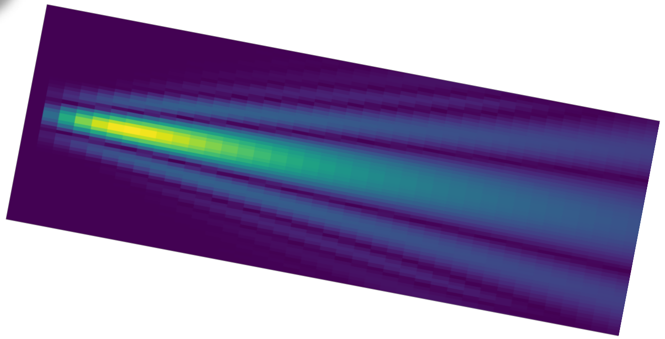

Sensitivity limit below 10 ppm with our current 4.5 µm QCL pump laser

Alexandrovski, Photothermal common-path interferometry: new developments. SPIE 7193 (2009)

Absorption Measurements via Photothermal Common Path Interferometry (PCI)

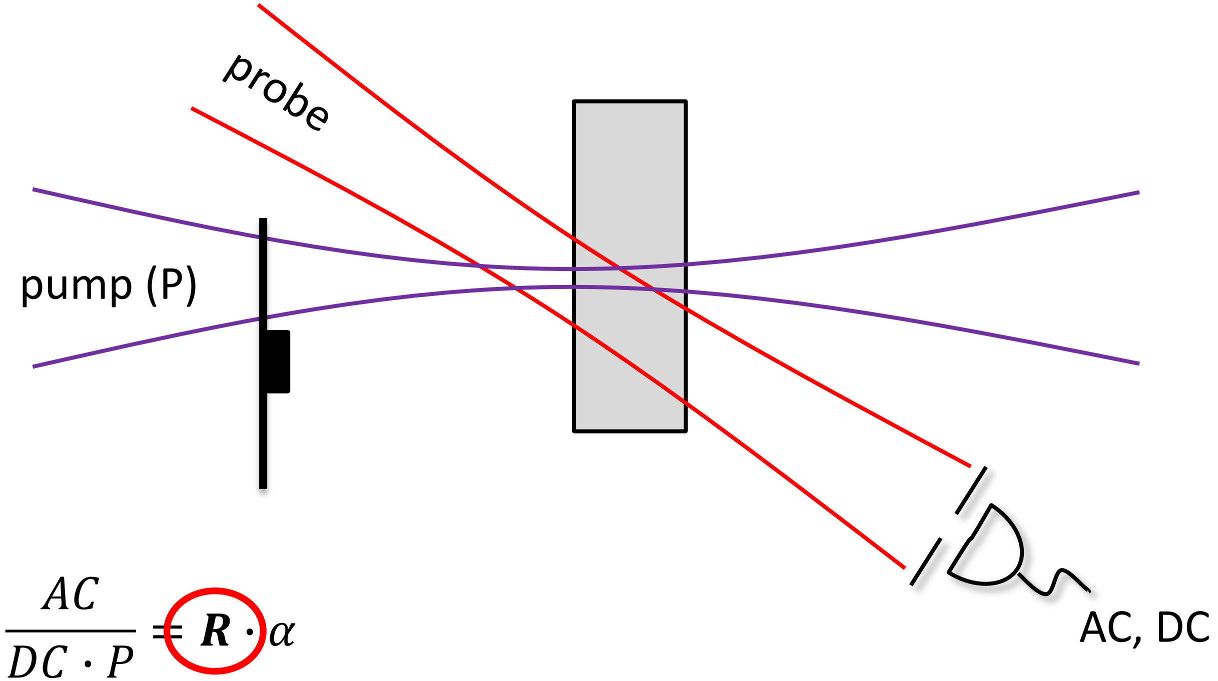

$$\frac{AC}{DC\cdot P} = \boxed{\boldsymbol{R}}\cdot\alpha$$

α	… Absorption
R	… Responsivity
AC	… Amplitude of probe signal modulation at pump chopping frequency
DC	… Average probe signal
P	… Average pump power at pump/probe crossing

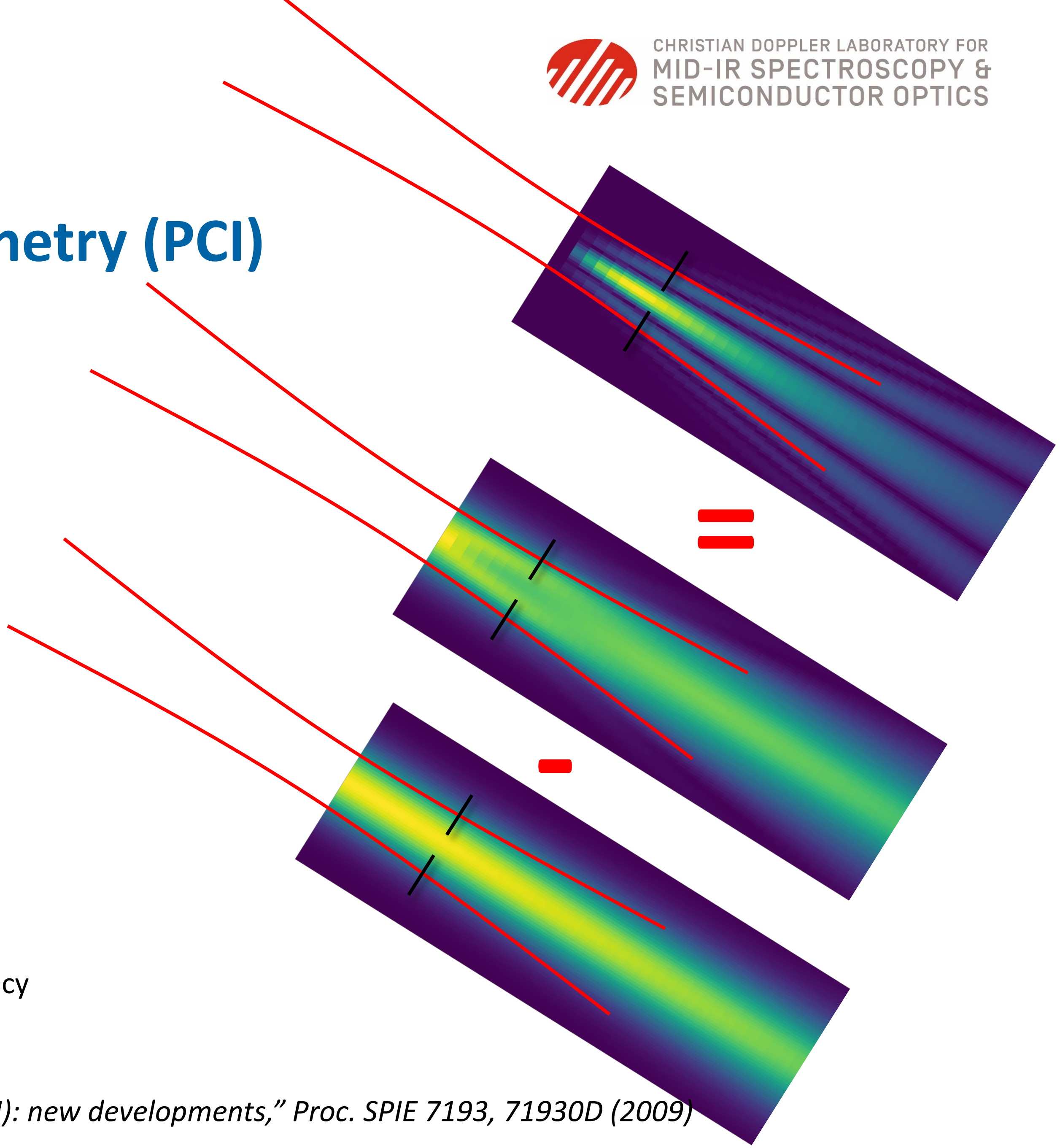

A. Alexandrovski, M. Fejer et al., "Photothermal common-path interferometry (PCI): new developments," Proc. SPIE 7193, 71930D (2009)

PCI setup

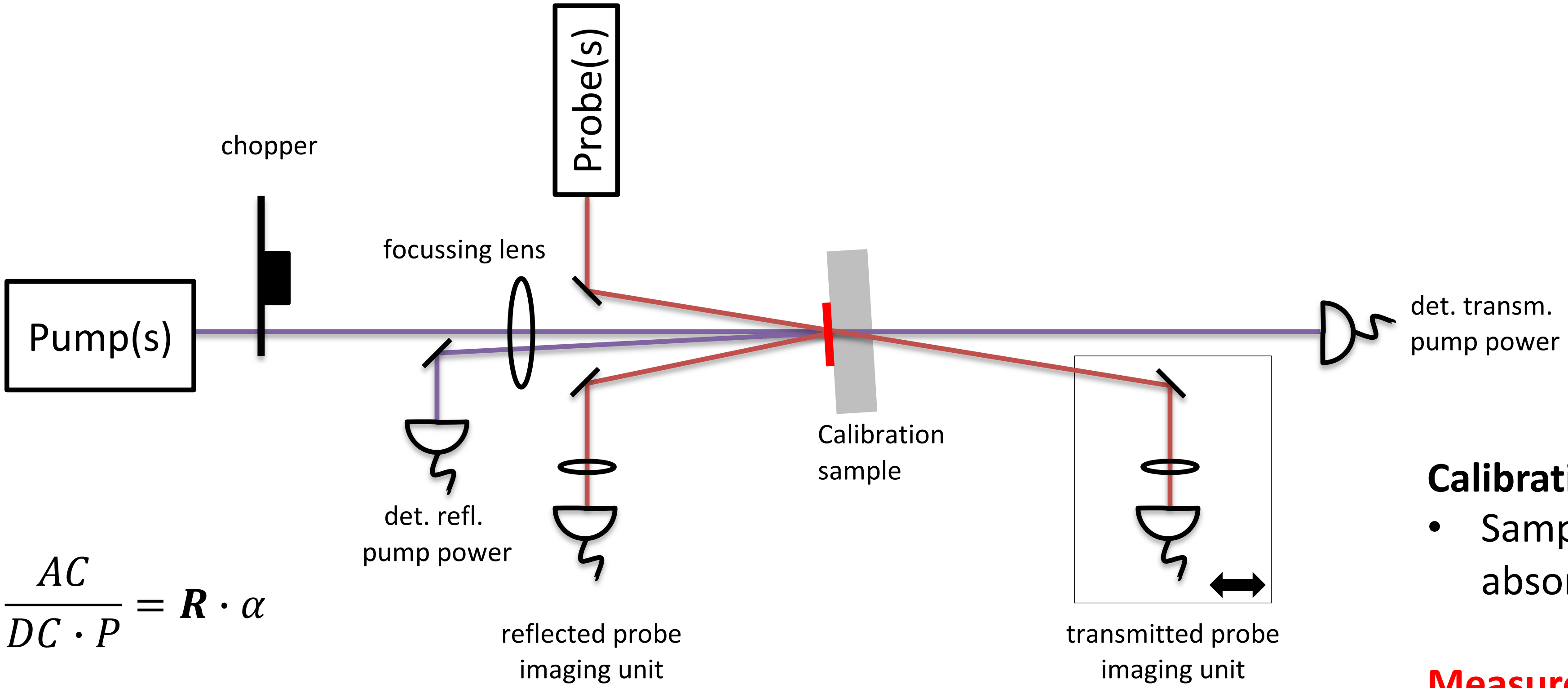

$$\frac{AC}{DC \cdot P} = \boldsymbol{R} \cdot \alpha$$

α	… Absorption
R	… Responsivity
AC	… Amplitude of probe signal modulation at pump chopping frequency
DC	… Average probe signal
P	… Average pump power at pump/probe crossing

Calibration

- Sample on same substrate with ~40% absorption

Measurement

- Relative comparision of signals allows measurement of <40 ppm absorption

PCI setup

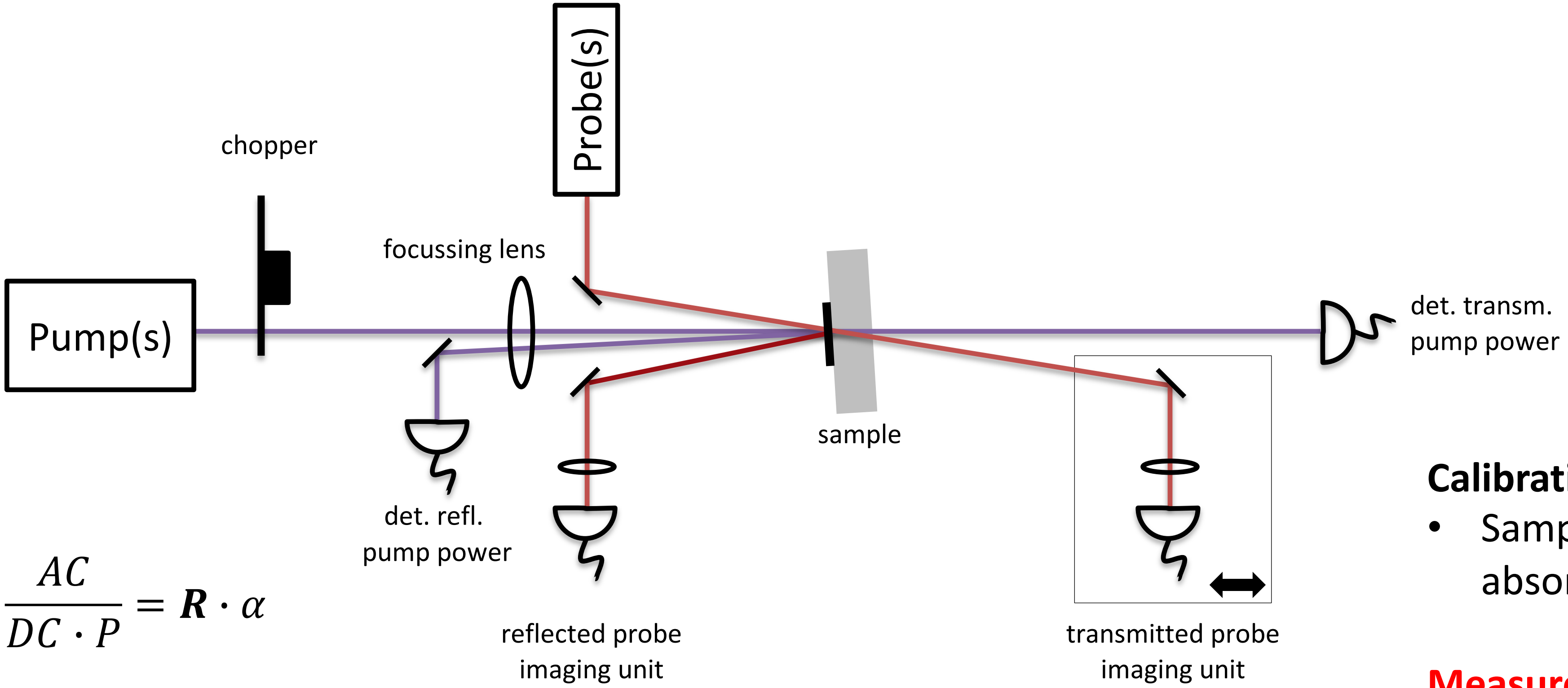

$$\frac{AC}{DC \cdot P} = \boldsymbol{R} \cdot \alpha$$

α	… Absorption
R	… Responsivity
AC	… Amplitude of probe signal modulation at pump chopping frequency
DC	… Average probe signal
P	… Average pump power at pump/probe crossing

Calibration

- Sample on same substrate with ~40% absorption

Measurement

- Relative comparision of signals allows measurement of <40 ppm absorption

PCI calibration

$$\frac{AC}{DC \cdot P} = \boldsymbol{R} \cdot \alpha$$

Standard calibration (using calibration piece)

- $P_{\text{absorbed}} = P_{\text{in}} - P_{\text{refl}} - P_{\text{trans}}$

  $\alpha_{\text{calib}} = \dfrac{P_{\text{absorbed}}}{P_{\text{in}}}$

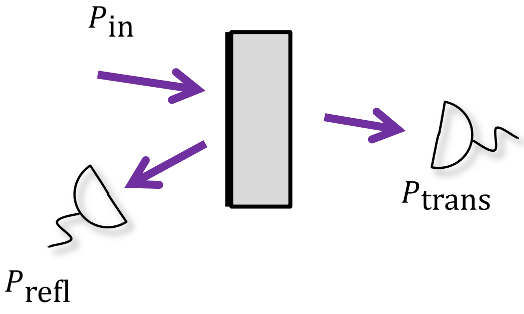

- $\alpha_{\text{calib}} \to \boldsymbol{R}$

  $\uparrow$
  (%-level)

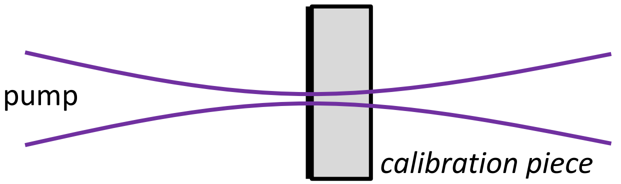

- $R \to \boldsymbol{\alpha_{\text{sample}}}$

  $\uparrow$
  (ppm-level)

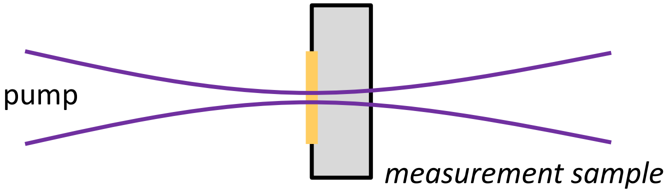

In-Situ calibration (using „proxy pump“)

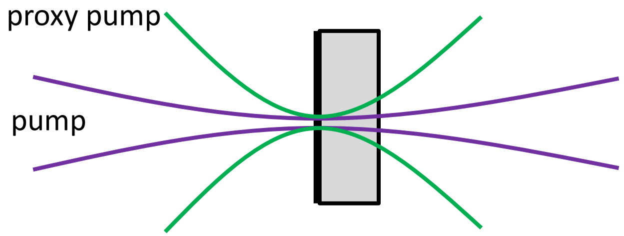

- Check equal spotsize for both pumps (e.g. via equal R)

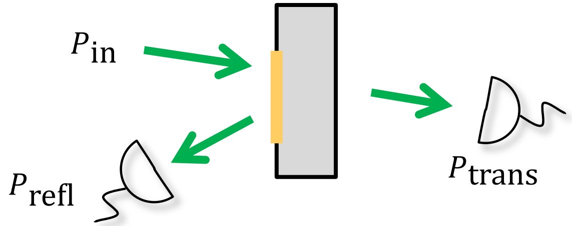

- $\alpha_{proxy} = \dfrac{P_{\text{absorbed}}}{P_{\text{in}}}$

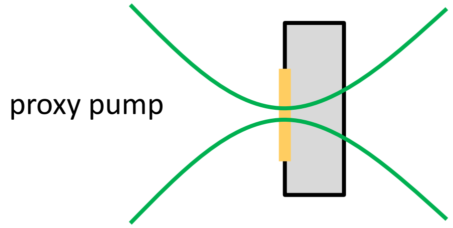

- $\alpha_{\text{proxy}} \to \boldsymbol{R}$

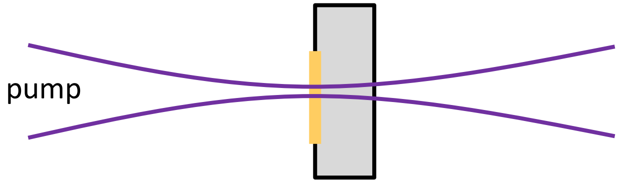

- $R \to \boldsymbol{\alpha_{\text{sample}}}$

PCI setup

Challenges of extension to Mid-IR:

- Low-power pump
- Substrate response / absorption
- Thermal lens contribution by thicker coatings
- Probe-induced absorption
- Atmospheric effects
- Polarization-dependence

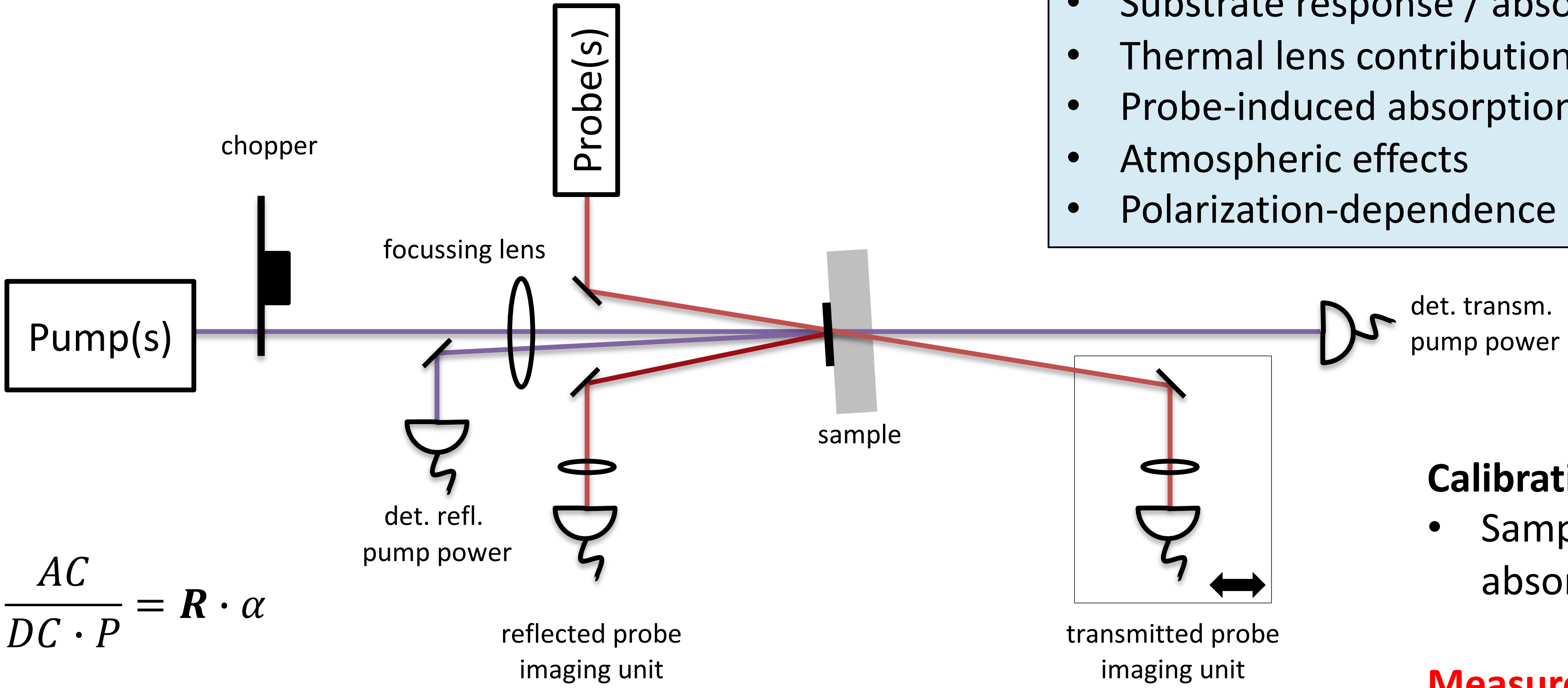

$$\frac{AC}{DC \cdot P} = \boldsymbol{R} \cdot \alpha$$

α	… Absorption
R	… Responsivity
AC	… Amplitude of probe signal modulation at pump chopping frequency
DC	… Average probe signal
P	… Average pump power at pump/probe crossing

Calibration

- Sample on same substrate with ~40% absorption

Measurement

- Relative comparision of signals allows measurement of <40 ppm absorption

PCI Measurement Results

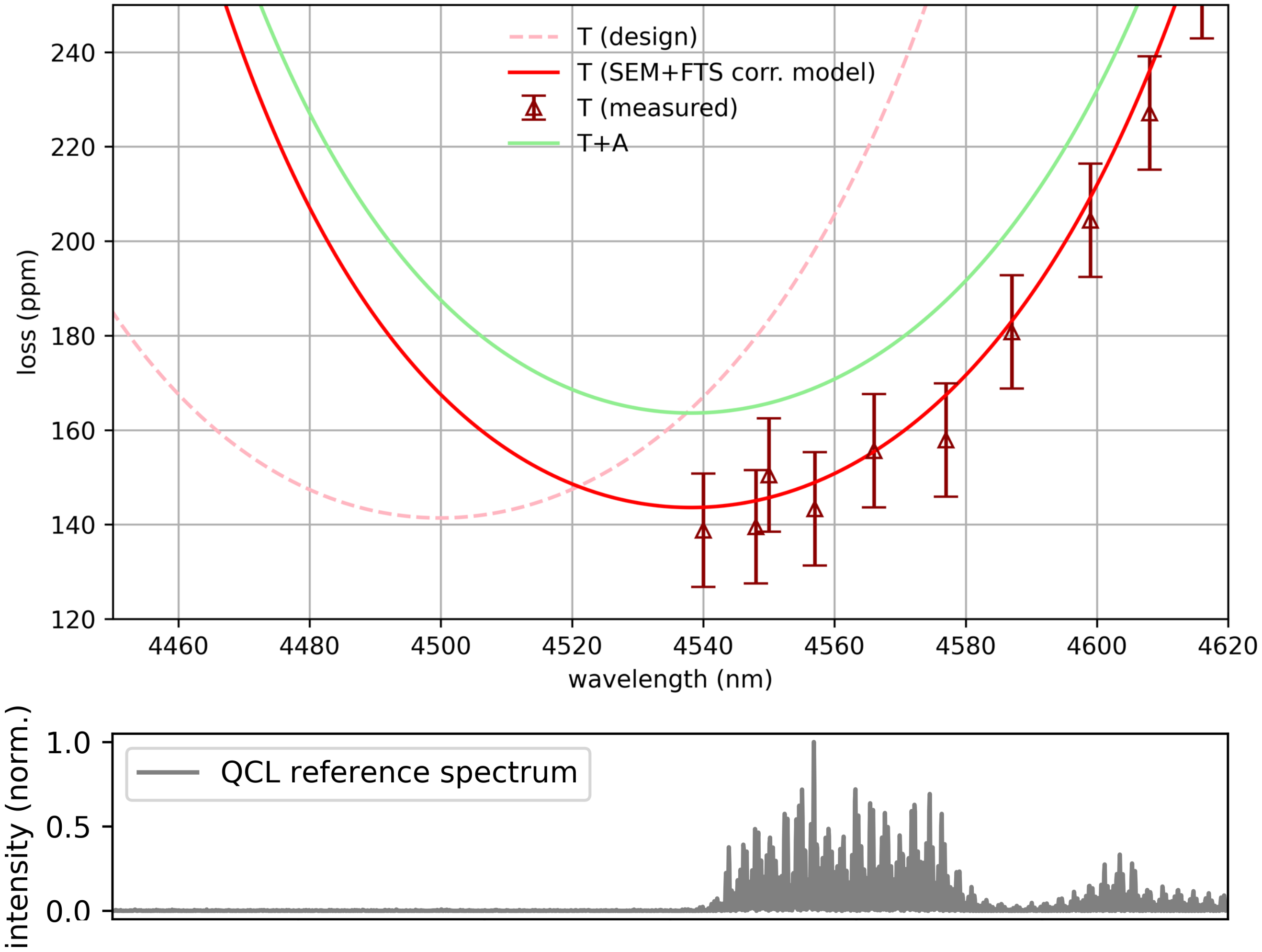

	Loss (ppm)	λ_{min} (nm)
T (measured)	143 ± 3	4536 ± 5
A (measured)	< 20	4550-4700

- PCI reveals an upper limit of for optical absorption (4.55-4.70 µm)
- The broad spectral range of the QCL pump overstates absorption losses in the stopband center.

Polarization-dependent Absorption

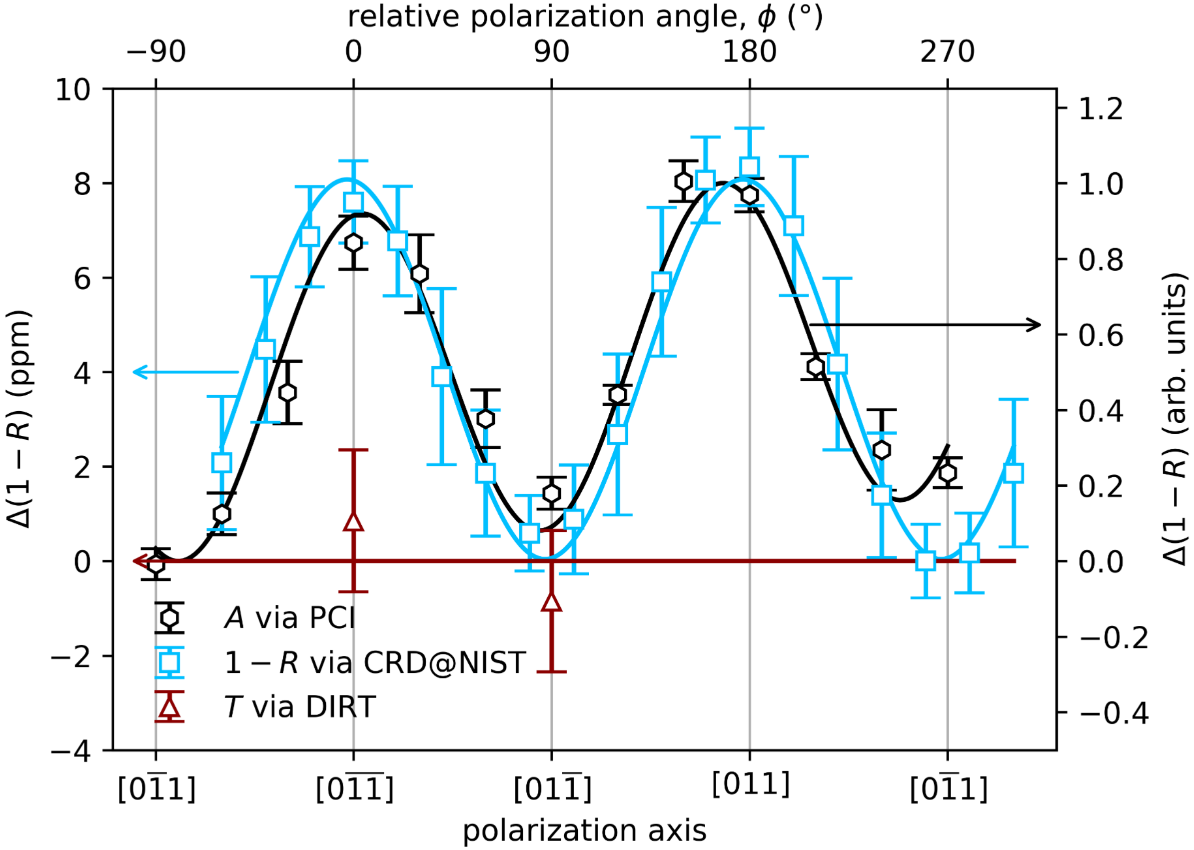

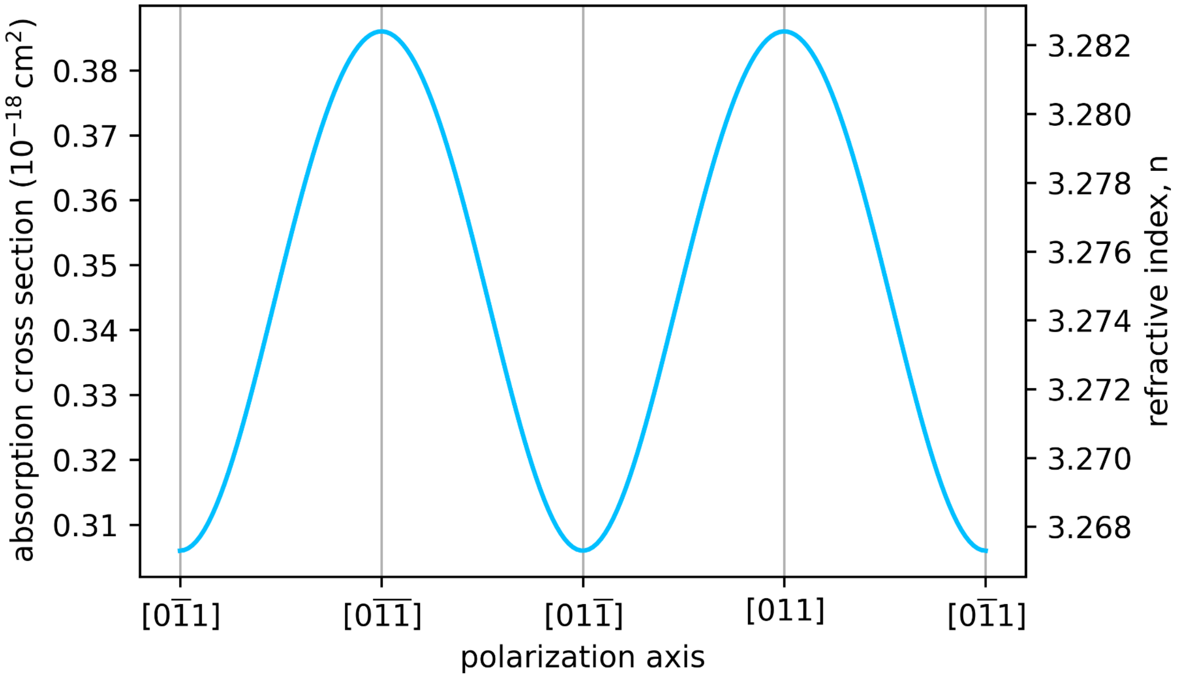

- First-time observation of this effect – allowed to optimize mirror orientation in cavity for lowest losses.
- Data in agreement with density functional theory model of uniaxially strained GaAs.

Excess Loss Measurements

Transmission (*T*)

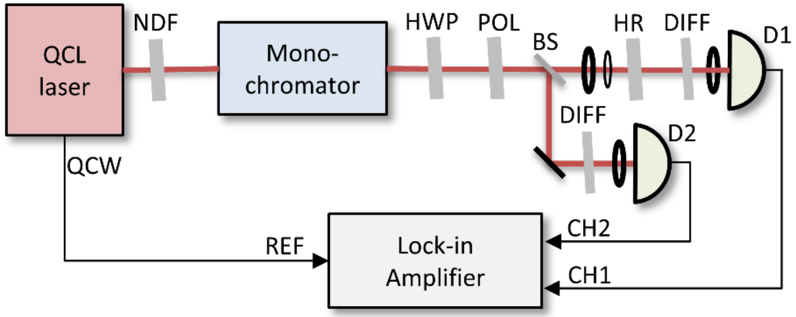

Direct transmission

Simple, but high-precision direct transmission measurement

Absorption (*A*)

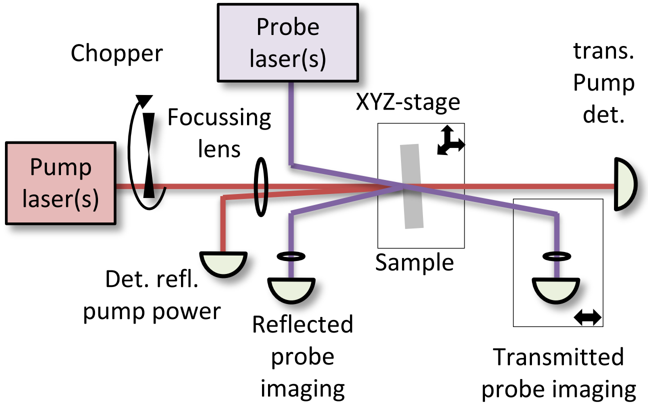

Photothermal common-path interferometry (PCI)

Allows for direct absorption measurements < 10 ppm
(<1 ppm with W-level pump)

Reflectance (*R*)

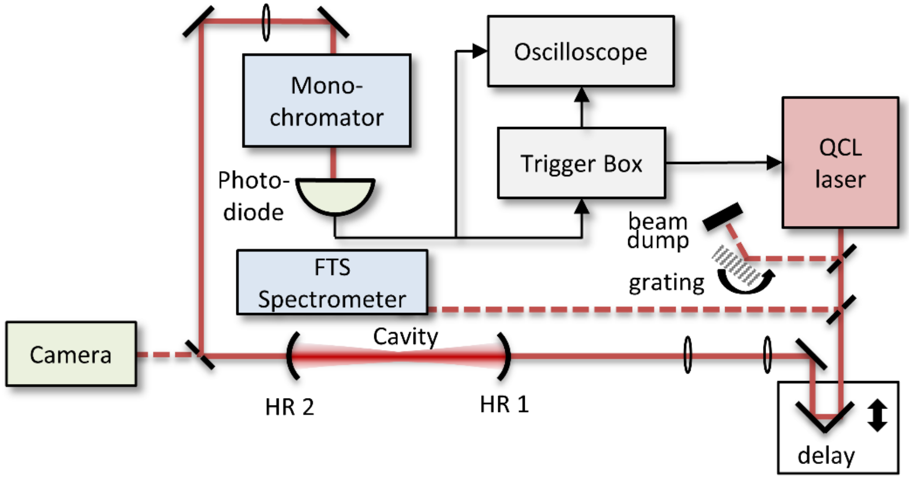

Cavity ring-down (CRD)

Broadband (~200 nm) QCL @ 4.55 µm with passive feedback

Measuring Total Loss L = (1-R) via Cavity Ringdown (CRD)

$$R + \underbrace{T + A + S}_{L} = 1$$

$$\tau = \frac{d}{cL}$$

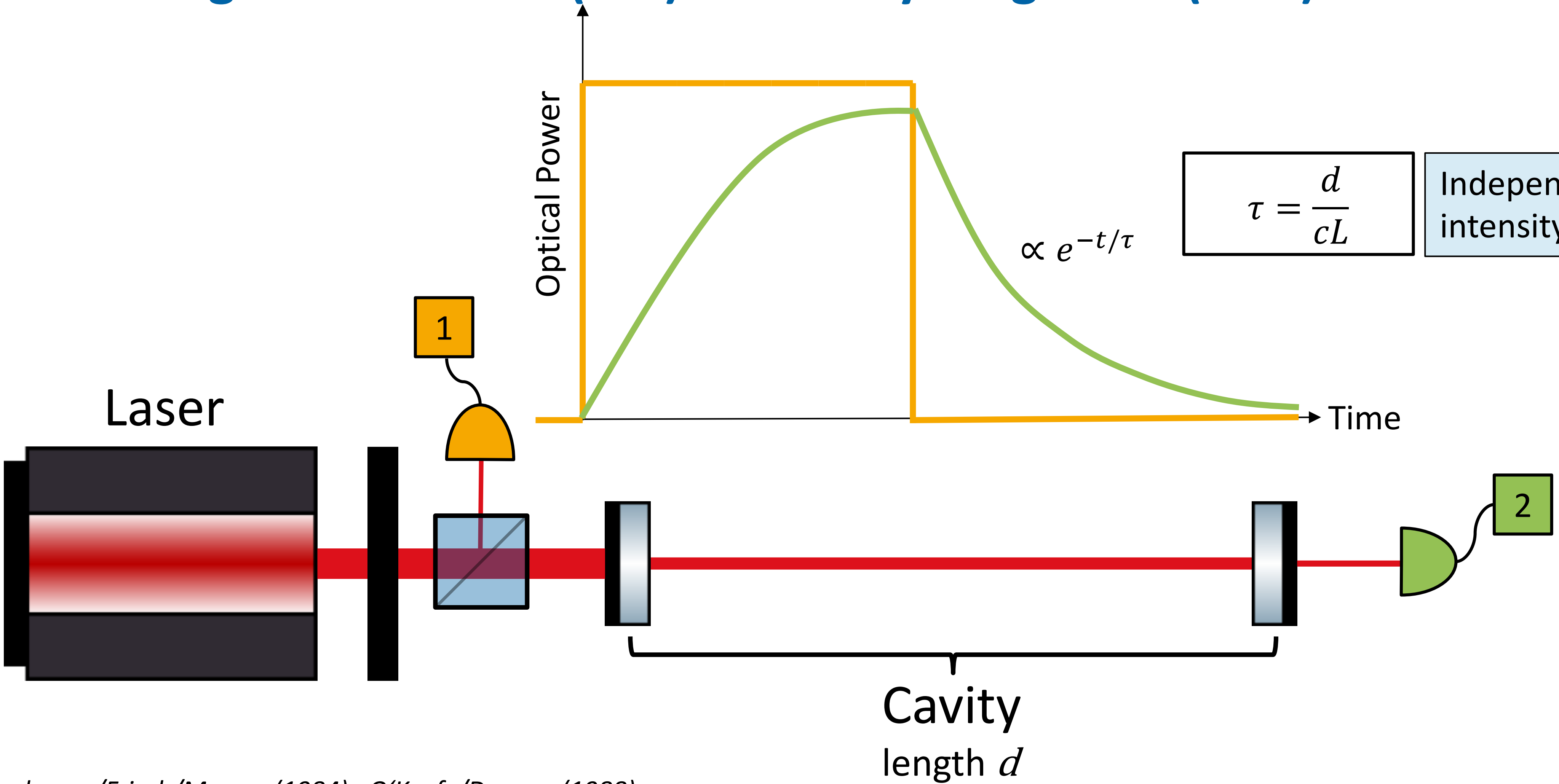

$$\boxed{\tau = \frac{d}{cL}}$$

Independent of laser intensity fluctuations!

Anderson/Frisch/Masser (1984); O‘Keefe/Deacon (1988)

CRD with Broadband Excitation

$$R + \underbrace{T + A + S}_{L} = 1$$

$$\tau = \frac{d}{cL}$$

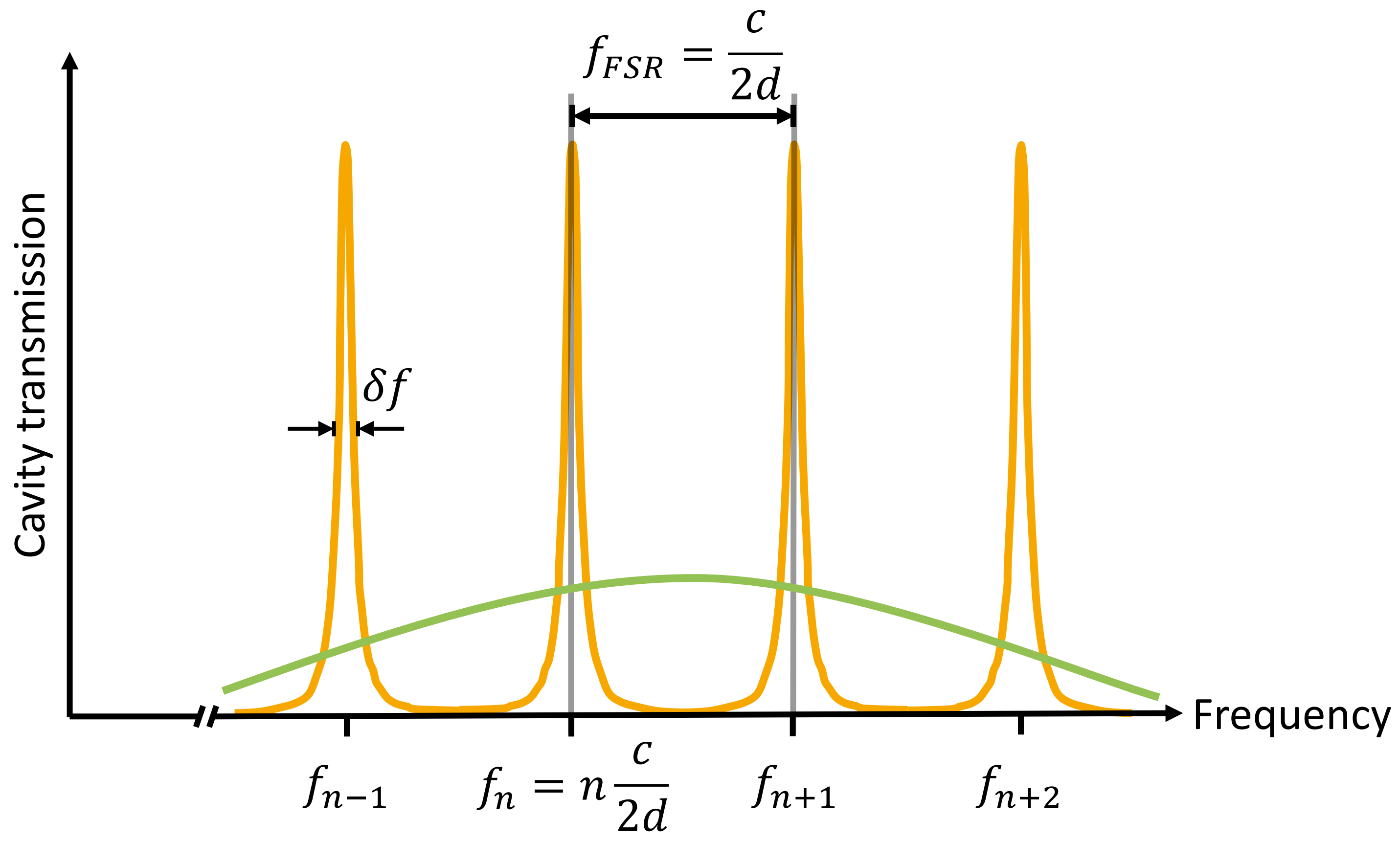

Finesse

$$\mathcal{F} := \frac{f_{FSR}}{\delta f} = \frac{\pi c}{d}\tau$$

- Tuneable source (e.g. DFB QCL)
  - Narrow tuning range
  - Expensive

- Broadband source (e.g. FP QCL)
  - High coupling loss (incoupled power ratio given by Finesse)
    - ➢ Feedback

QCL … Quantum cascade laser
DFB … direct feedback
FP … Fabry Perot

Characterization of Total Loss via Cavity Ringdown

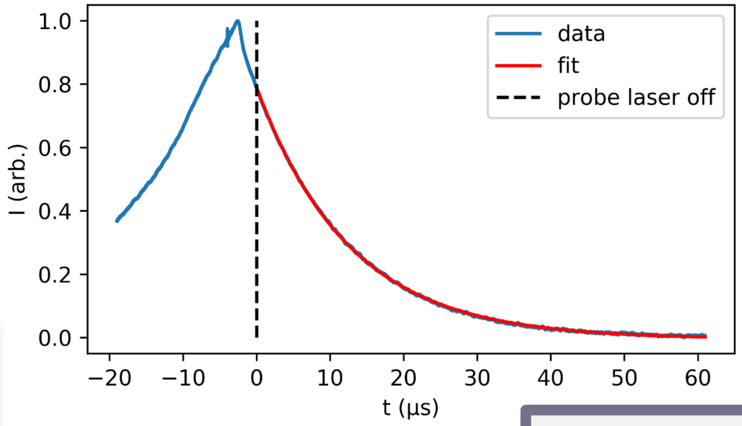

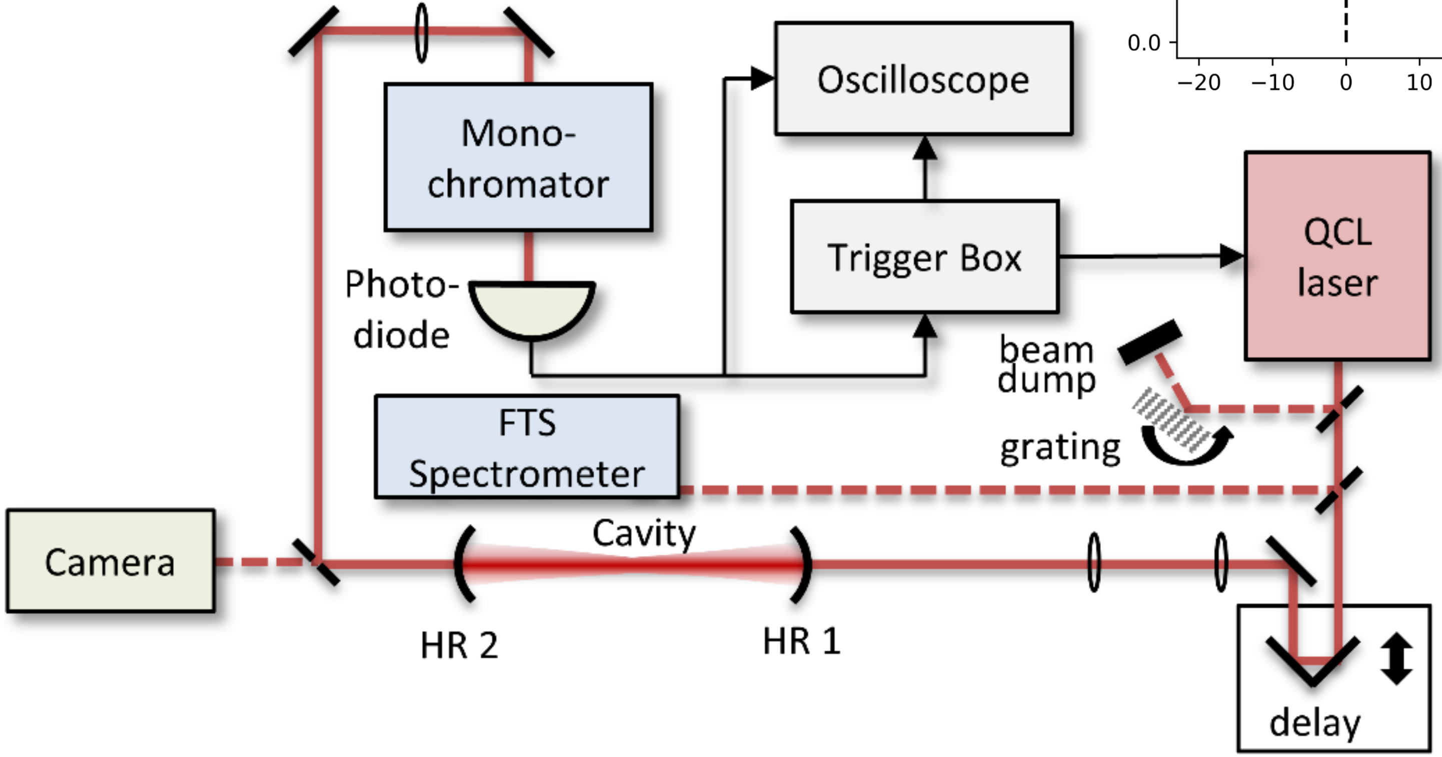

- 4.55 µm Fabry-Perot QCL without isolation and no servo system
- Delay stage to match external cavity and enhance feedback
- Monochromator for wavelength resolved measurements

Ultralow-Loss 4.5 µm Optical Interference Coatings

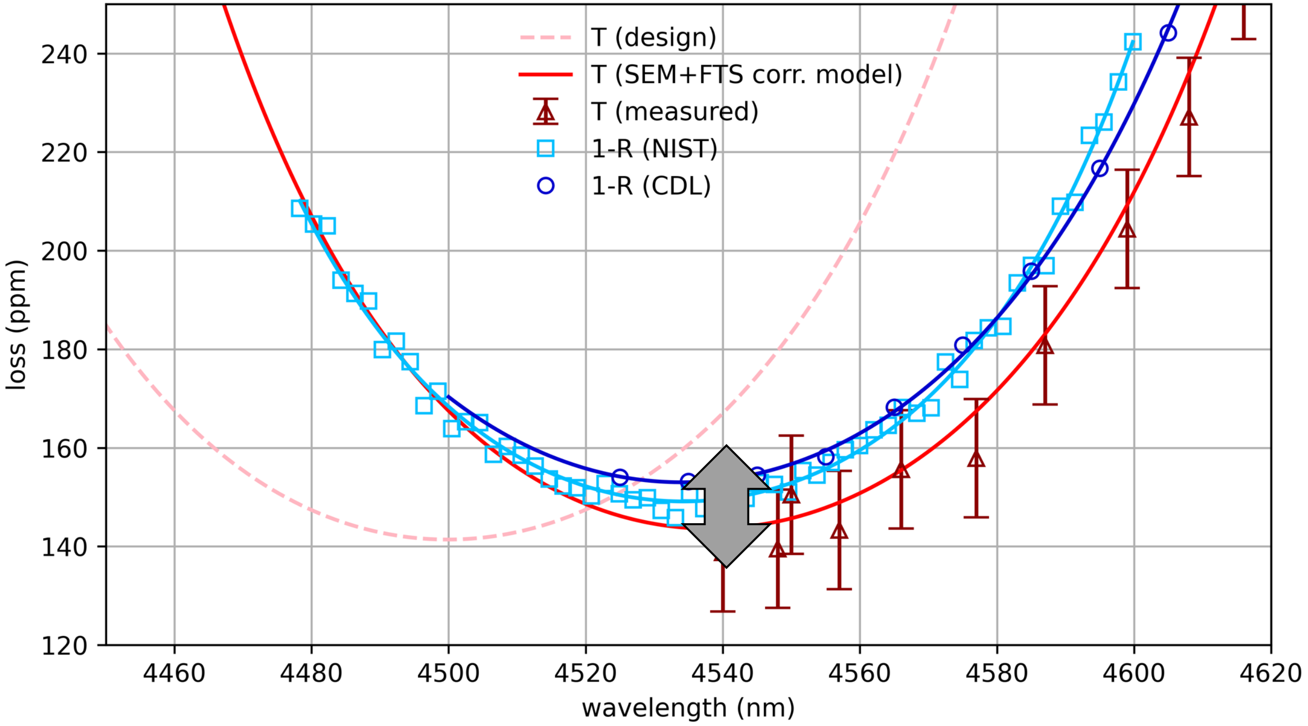

	Loss (ppm)	λ_{min} (nm)
T (measured)	143 ± 3	4536 ± 5
T+A+S (CDL)	153 ± 1	4534 ± 1
T+A+S (NIST)	149 ± 6	4533 ± 1

- Independent measurements at the CDL and NIST (team around A. Fleisher) show excellent results
  - excess optical losses (absorption + scatter) below 10 ppm!
- Potential for enhancement cavities with a finesse >100,000 @ 4.5 µm

G. Winkler, L. W. Perner, et al., "Mid-infrared interference coatings with excess optical loss below 10 ppm," Optica **8**, 686-696 (2021)
https://doi.org/10.1364/OPTICA.405938

Summary

Distributed Bragg Reflectors

- Principle
- Calculation of stob-bands

Production techniques and wavelength coverage

- E-beam evaporation
- Sputtering / IBS
- Molecular beam epitaxy

Characterization of high-finesse mirrors

- Determination of stop-band width FTS
- Direct transmission
- Absorption measurements (PCI)
- Loss measurements via CRD

Thank you for your attention!!!

???